Exploiting Alternative Cell Death Mechanisms to Overcome Drug Resistance in Leukemia

---

Dissertation

zur

Erlangung der naturwissenschaftlichen Doktorwürde
(Dr. sc. nat.)

vorgelegt der

Mathematisch-naturwissenschaftlichen Fakultät

der

Universität Zürich

Von

Júlia Aguadé Gorgorió

aus

Spanien

Promotionskommission

PD MD Dr. Jean-Pierre Bourquin (Vorsitz)
Dr. Beat Bornhauser (Leitung der Dissertation)
Prof. Dr. Christian Münz
Prof. Dr. Dr. Hans-Uwe Simon
Dr. W. Wei-Lynn Wong

Zürich, 2017

Summary

Children diagnosed with acute lymphoblastic leukemia (ALL) have nowadays a favorable prognosis, with around 80% achieving long term survival. However, around 20% of patients suffer relapse, leading to a dismal prognosis. One of the leading causes of relapse in ALL is the development of drug resistance through the dysregulation of cell death mechanisms. Impaired apoptosis is frequent in cancer and leads to a decreased response to standard chemotherapies. We and others hypothesized that inducing alternative cell death mechanisms such as necroptosis could prevent or circumvent drug resistance in such malignancies. Indeed, we identified the SMAC (second mitochondria derived activator of caspases) mimetic (SM) birinapant as a potent inducer of apoptosis and necroptosis in a subset of resistant and high risk ALL patient-derived samples. Responsive samples could be selected according to their expression of *TNFR2* (tumor necrosis factor receptor 2), which is required for SM response. Furthermore, we identified a novel role of TNFR2 in the regulation of TNFR1- and RIP1-dependent cell death in leukemia.

RIP1 is a central regulator of cell survival and cell death by both apoptosis and necroptosis. To assess whether inducing RIP1-dependent cell death could circumvent resistance, we screened a panel of B- and T-ALL patient-derived samples for their response to the SM birinapant and identified a subset of B-ALL cases which showed exquisite sensitivity. By combining the lentiCRISPR gene editing technology with *in vivo* drug selection we determined that SM induce RIP1-dependent apoptosis and necroptosis simultaneously, challenging the common concept that necroptosis is only activated in the context of apoptosis inhibition. Finally, we show that inactivation of RIP1 in ALL does not confer resistance to commonly used chemotherapeutic agents, suggesting that RIP1 targeting agents will provide therapeutic options that have not been exploited for this disease so far.

The identification of molecular markers to preselect patients with a high likelihood to respond to novel targeted therapies such as SM is required in order to translate their use to clinical practice. *TNFR2* scored among the best correlating genes associated with SM response by gene expression profiling, and its expression predicted the response to SM in an independent cohort. We discovered that TNFR2 promotes TNFR1- and RIP1-dependent cell death. Consequently, CRISPR-mediated *TNFR1* and *TNFR2* knockout patient-derived cells were resistant to birinapant. In absence of TNFR2, RIP1 is not recruited to TNFR1 upon treatment with SM, indicating that TNFR2 is an essential upstream regulator of RIP1-mediated cell death.

Overall, our work highlights the importance of developing RIP1-targeting strategies to induce necroptosis and circumvent drug resistance in ALL, and identifies SM as promising agents for the treatment of specific subsets of ALL patients. Finally, the unexpected function of TNFR2 in this context provides new leads for further investigation of this important cell death pathway.

Zusammenfassung

Kinder mit akuter lymphatischer Leukämie (ALL) haben heutzutage eine Langzeitüberlebensrate von 80% und damit eine gute Prognose. Etwa 20% der Kinder erleiden jedoch ein Rezidiv, welches meist mit einer ungünstigen Prognose einhergeht. Einer der Gründe für ein ALL-Rezidiv ist die Resistenzentwicklung gegen Chemotherapeutika durch die Dysregulation von Zelltodmechanismen. Beeinträchtigungen der Apoptose sind in verschiedensten Krebsentitäten zu finden und führen zu einer verringerten Reaktion auf Standardchemotherapeutika. Es wird angenommen, dass die Induktion alternativer Zelltodmechanismen, wie der Nekroptose, Resistenzen verhindern oder umgehen könnte. Tatsächlich konnten wir Birinapant, ein *SMAC-mimetic* (SM, *second mitochondria derived activator of caspases*), als potenten Aktivator von Apoptose und Nekroptose in einer Kohorte von resistenten und hochrisiko-klassifizierten ALL-Patientenproben identifizieren.

RIP1 ist ein zentraler Regulator von Apoptose, Nekroptose und Zellüberleben. Zum Beweis, dass Resistenzen durch die Induktion von RIP1-abhängigem Zelltod umgangen werden können, haben wir eine Kohorte von B- und T-ALL Patientenproben auf ihre Birinapant-Sensitivität getestet. Wir konnten dabei eine Subgruppe von B-ALL Fällen identifizieren, welche eine hohe Sensitivität zeigten. Durch die Kombination von Gen-Knockouts mittels CRISPR-Technologie und einer *in vivo* Selektion durch Birinapant konnten wir zeigen, dass *SMAC-mimetics* RIP1-abhängige Apoptose und Nekroptose simultan induzieren. Diese Beobachtung steht im Gegensatz zu der allgemeinen Annahme, dass Nekroptose ausschliesslich in Apoptose-inhibierten Zellen auftreten kann. Des Weiteren konnten wir zeigen, dass die Inaktivierung von RIP1 in ALL nicht direkt zur Resistenz gegen klassische Chemotherapeutika führt, wodurch RIP1 potentielle therapeutische Optionen bietet, welche bisher noch nicht für ALL validiert wurden.

Die Identifikation von molekularen Markern zur Selektion von Patienten, die mit einer hohen Wahrscheinlichkeit auf neue Therapien wie SM reagieren, ist wichtig um ihre Effektivität in der Klinik vorherzusagen. Von den hier untersuchten Genen zeigte TNFR2 (*tumor necrosis factor receptor 2*) die höchste Korrelation mit der SM-Sensitivität. TNFR2 ist für die SM-Reaktion erforderlich und wir konnten dessen Expression zur Selektion von Birinapant-sensitiven Proben in einer unabhängigen Kohorte nutzen. Des Weiteren konnten wir zeigen, dass TNFR2 den TNFR1- und RIP1-abhängigen Zelltod aktivieren kann und das TNFR1- und TNFR2-Knockouts zu einer Birinapant-Resistenz in Patientenproben führen. In Abwesenheit von TNFR2 ist die SM-abhängige RIP1 Rekrutierung durch TNFR1 inhibiert, was darauf hinweist, dass TNFR2 ein essentieller Regulator des RIP1-vermittelten Zelltodes ist.

Zusammengefasst beweist unsere Arbeit, wie wichtig die Entwicklung von RIP1-spezifischen Strategien zur Induktion von Nekroptose ist, welche die Umgehung von Resistenzen in ALL ermöglichen können. Wir konnten zeigen, dass SM vielversprechendee Wirkstoffe für einen spezifischen Subtyp der ALL sind. Schlussendlich ermöglicht auch die unerwartete Rolle von TNFR2 in diesem Kontext neue Ansätze zur Erforschung dieses wichtigen Zelltod-Signalweges.

Table of contents

1. Introduction

1.1 Acute lymphoblastic leukemia

Acute lymphoblastic leukemia (ALL) is a subtype of leukemia characterized by an overproliferation of immature white blood cells (lymphoblasts) of B, T, or mixed lineage origin. Patients with ALL present symptoms of decreased hematopoiesis in the bone marrow, including anemia (fatigue and paleness), thrombocytopenia (bleeding), and neutropenia (infections)[1]. ALL is the most common malignancy in children, with an incidence of 46.7 new cases per million children under 15 years of age per year in Europe according to the World Health Organization[2], and represents almost 30% of all pediatric cancers. It affects mostly children between the ages of 3 and 5 and it is one of the leading causes for disease mortality in childhood. However, nowadays an exceptional overall survival of 90% has been achieved[1] (Figure 1A).

Leukemogenesis follows the "two-hit" hypothesis, according to which two or more molecular changes leading to increased proliferation and arrested maturation are required to induce the malignant phenotype. This has been confirmed by the observations that the chromosomal translocations associated with leukemia are often not sufficient to cause the disease, and that some of the characteristic leukemic translocations are also found in a small percentage of healthy children. Additionally, some translocations like the one encoding for the fusion protein ETV6-RUNX1 can already be present during the fetal period, indicating the presence of a pre-leukemic cell[3].

ALL is a genetically heterogeneous polyclonal disease, characterized by the presence of chromosomal translocations, gains or losses of whole chromosomes, and other genetic aberrations such as small insertions/deletions or single nucleotide variants. The translocations and rearrangements are often considered the leukemia initiating events and often involve hematopoietic transcription factors or activated oncogenes. The most common genetic aberrations in precursor B-ALL include the translocations *ETV6-RUNX1*, *TCF3-PBX1*, and *BCR-ABL*, hyperdiploidy, hypodiploidy, and rearrangements of *MLL* (especially frequent in infant ALL), *CRLF2* or *IGH*. Frequent alterations in T-ALL include rearrangements of the T cell receptor with transcription factors. Besides these initiating events, additional alterations are found in genes involved in lymphoid development and maturation, tumor suppression, cell cycle control, or therapy resistance. Those include genes like *PAX5*, *IKZF1*, *EBF1*, or *CDKN2A.* Single nucleotide polymorphisms (SNPs) are also identified affecting genes from key signaling pathways, such as activating mutations in the Ras pathway, the p53 tumor suppression pathway, and cytokine receptor signaling[1,4].

Determining the immunophenotype and the presence of specific alterations is important for the diagnosis and is critical for risk stratification. Additionally, the quantification of minimal residual disease (MRD) after induction therapy by PCR or flow cytometry is also essential for risk stratification. An MRD of less than 0.01% at day 33 after the start of induction therapy indicates low risk of relapse,

while an MRD equal or higher that 0.01% leads to a 3-5 fold increase of treatment failure[1,5]. The standard treatment protocol consists of three phases: induction (4-6 weeks), intensification (6-8 months), and maintenance (18-30 months), with the induction phase being the same for all patients and the following phases adapted to the risk stratification. Glucocorticoids, vincristine, and L-asparaginase are used during induction therapy, methotrexate is used during the intensification and during maintenance, in the latter in combination with mercaptopurine or thioguanine. Tailoring the therapy to the risk and characteristics of each patient has contributed greatly to achieving the current 90% survival rate. Furthermore, the increased knowledge of the leading genetic lesions in ALL will allow the development of novel targeted therapies. This has been successfully demonstrated in the case of tyrosine kinase inhibitors (imatinib, dasatinib) targeting the fusion protein BCR/ABL, which have dramatically improved the prognosis of patients with this subtype of leukemia[1].

Despite the high survival rates, 15 to 20% of ALL patients suffer relapse, which is accompanied by a poor prognosis and dismal outcome (Figure 1B)[6]. The genetic features of relapse can often be traced back to minor subclones present at diagnostic, indicating a clonal ancestry of the relapsed disease from the original ALL at diagnosis[3]. Only in very rare cases of T-ALL the relapse is considered a new disease. The majority of relapse patients maintain the initial chromosomal aberrations and acquire new alterations. The most common mutations acquired at relapse involve CREBP, an important mediator of the transcriptional response to glucocorticoids, KRAS, or NT5C2, an enzyme implicated in the metabolism of mercaptopurine and thioguanine[1,7,8]. Many alterations leading to resistance to apoptosis are also involved in drug resistance, therapy failure, and relapse[9,10], and are further described in section 1.2.3.

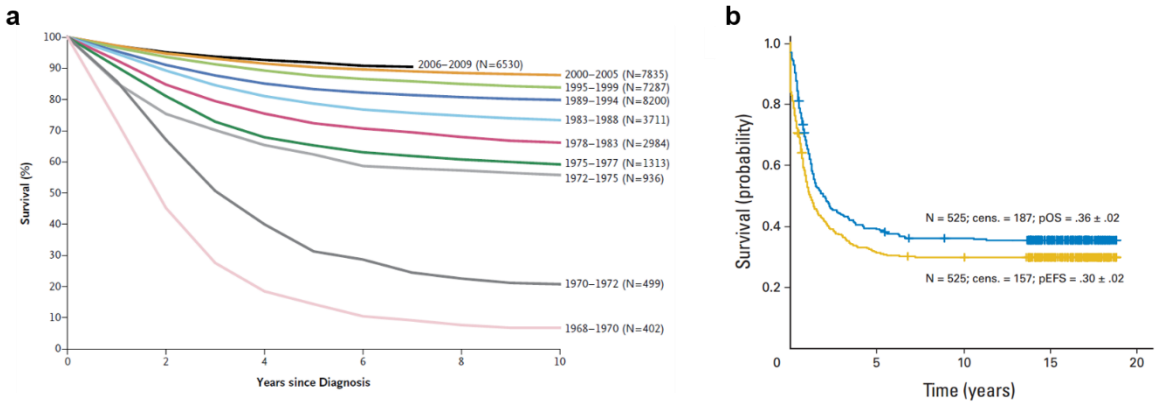

Figure 1. A Overall survival among children with ALL from 1968 to 2009[1]. **B** Overall survival (blue) and event-free survival (yellow) among children with first relapse ALL[6].

The genetic and biologic complexity of ALL requires clinically relevant models for the development of new approaches, which are needed in particular for relapsed ALL cases. Many syngeneic mouse models of ALL have been engineered based on the introduction of the characteristic translocation or rearrangement in immunocompetent mice[11–13]. This approach allows studying the interactions with the microenvironment and the behavior of the leukemia in an immunocompetent host. They present

however important disadvantages. The introduction of chromosomal translocations as leukemia initiating event is only exceptionally sufficient to induce leukemia, and the additional alterations introduced to induce ALL in transgenic mice often don't represent those present in patients. Additionally, the introduction of the common ALL chromosomal aberrations in murine cells often leads to the generation of acute myeloid leukemia (AML) or other hematologic malignancies different from the intended subtype of ALL. Thus, the models are limited and can't represent the diversity of ALL[11]. Most of the downsides of using syngeneic mouse models for the study of ALL are avoided with the use of xenogeneic models in immunocompromised mice. NSG (NOD-SCID-gamma) mice, which present a defective innate and adaptive immune system, can be engrafted with patient-derived ALL cells, which expand while maintaining the original transcriptome, phenotype, and clonal composition of the original disease[14,15]. As part of the AEIOP-BFM-ALL and the IntReALL study groups for de novo and relapsed ALL respectively, our research group has established a xenograft bank of around 200 clinically relevant cases. Those include standard risk samples as well as high risk subgroups including TCF3-HLF, MLL-AF4 and other cases with unknown genetic traits[14,15]. Xenografting patient-derived cells allows studying ALL without losing the complexity of the disease, and represents a good platform for clinically relevant *in vivo* drug testing. The biggest drawback of the xenograft model is the lack of a functional host immune system, preventing the study of its role in leukemia development and the testing of immunotherapeutic approaches[11,14].

1.2 Programmed cell death in cancer

Failure to activate cell death mechanisms is one of the main reasons for the appearance of drug resistance and relapse. Programmed cell death includes all cell death modalities which are regulated at the molecular level, and can thus be prevented by specific inhibitor compounds or genetic deletions. It encompasses anoikis, entosis, parthanatos, pyroptosis, autophagic cell death, apoptosis, and necroptosis among others (Figure 2). Furthermore, cell death can also occur in an unregulated manner, as in the case of necrosis. The study of cell death in ALL can contribute to understanding the mechanisms of therapy failure and relapse, and can help identifying new therapeutic targets.

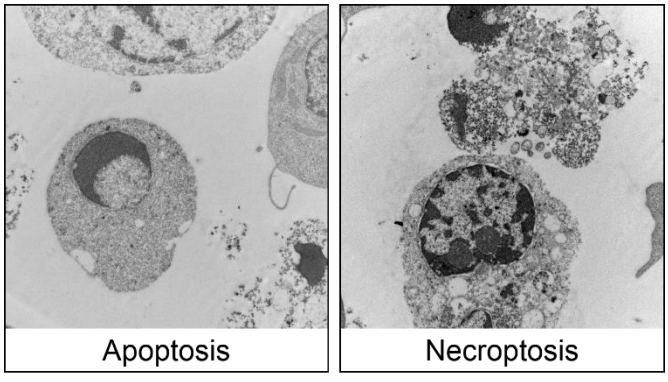

Figure 2. Electron microscopy images of apoptosis and necroptosis at 5600x magnification.

1.2.1 Apoptosis is the best characterized form of programmed cell death

The term apoptosis, "falling off" in ancient Greek, was first introduced in 1972 to define a programed mechanism of cell turnover occurring during embryonic development as well as in healthy adult tissues[16]. Since then it has been thoroughly studied and it is nowadays the best described mode of cell death. Examples of physiological roles of apoptosis during embryonic development include the removal of excessive neurons which fail to connect to muscular cells, or the removal of interdigital cells. It is also involved in the maturation of immune cells, by leading to the death of T cells which recognize self-antigens. Many pathologies are linked to defective apoptosis, such as Huntington's disease, Alzheimer, myocardial infarction, or autoimmune diseases[17].

Apoptotic cells present a characteristic morphology of decreased cellular volume, nuclear fragmentation, chromatin condensation, permeabilization of the outer mitochondrial membrane (MOMP), and membrane blebbing. Apoptotic cells are rapidly cleared by macrophages in the absence of major inflammatory reactions[18]. Mechanistically, apoptosis can be classified as intrinsic or extrinsic depending on the molecular pathway mediating it.

Intrinsic apoptosis is induced by various intracellular stress signals such as DNA damage, excitotoxicity, oxidative stress, or ER (endoplasmic reticulum) stress, which eventually converge upon BCL-2 (B cell lymphoma-2) family members [19]. The balance between the pro- and anti-apoptotic BCL-2 factors determines the integrity of the outer mitochondrial membrane (OMM) and the fate of the cell.

Anti-apoptotic BCL-2 family members are present in the OMM and are responsible for directly inhibiting the pro-apoptotic members. They include BCL-2, BCL-xL (BCL-2 related gene long isoform), BCL-w, and MCL-1 (myeloid cell leukemia 1). Anti-apoptotic BCL-2 proteins are considered oncogenes and their dysregulation plays a key role in cancer development (see section 1.2.2). The pro-apoptotic members can be further distinguished between effectors, BH3-only "sensitizers", and BH3-only "direct activators". The first group (BCL-2 family effectors) includes BAX (BCL-2 associated x protein) and BAK (BCL-2 antagonist killer 1), which oligomerize in the OMM and directly induce its permeabilization. The protein BOK is a potential member of this subgroup, although its activity is not yet fully characterized. On the other hand, BH3-only "sensitizers" are proteins with a specific binding profile to the anti-apoptotic proteins, and they don't directly cause apoptosis but lower the threshold for its induction. BH-3 only "sensitizers" include BAD (BCL-2 antagonist of cell death), Noxa, and BIK (BCL-2 interacting killer). BH3-only "direct activators" also bind to the anti-apoptotic factors, but additionally they can directly induce BAX-BAK oligomerization. This subgroup includes BID (BCL-2 interacting domain death antagonist) and BIM (BCL-2 interacting mediator of cell death) (Table 1)[20,21].

Anti-apoptotic BCL-2 family proteins	A1, BCL-2, BCL-w, BCL-xL, MCL-1
BCL-2 family effector proteins	BAK and BAX
BH3-only "direct activators"	BID and BIM
BH3-only "sensitizers"	BAD, BIK, BMF, HRK, Noxa, PUMA

Table 1. Classification of BCL-2 family proteins according to their function. Adapted from [21].

The destabilization of the BCL-2 family balance and the activation of BAX or BAK lead to MOMP and to the release to the cytosol of toxic proteins from the mitochondrial intermembrane spaces, including cytochrome C, AIF (apoptosis inducing factor), ENDOG (endonuclease G), and SMAC (Second mitochondrial-derived activator of caspases). Subsequently, cytochrome C and APAF-1 (apoptotic protease activating factor-1) form a complex (apoptosome) which binds and activates caspase-9. Caspase-9 activates then the effector caspases-3 and -7, which are responsible for the final execution of apoptosis. MOMP represents a point of no return in the induction of apoptosis, and it is therefore highly regulated (Figure 3)[19–22].

Extrinsic apoptosis is initiated by the binding of extracellular ligands to their corresponding death receptors, such as FasL to Fas, TNFα (tumor necrosis factor α) to TNFR1 (TNF receptor 1), or TRAIL (TNF-related apoptosis inducing ligand) to TRAILR (TRAIL receptor) -1 and -2. The activation of the receptor leads in turn to its internalization and the recruitment of an intracellular complex termed DISC (death inducing signaling complex). This assembly is mediated by the presence of a specific domain present both in all death receptors and in the intracellular adaptor proteins, termed death domain (DD). One of the proteins recruited to the DISC is pro-caspase-8, which can be activated and subsequently cleave and activate caspases -3 and -7 (Figure 3). In certain cell types this is sufficient to induce cell death, independently of the mitochondria. In other cell types caspase-8 can cleave BID, leading to the formation of a truncated protein (tBID) which can directly cause MOMP. This represents a point of crosstalk between the

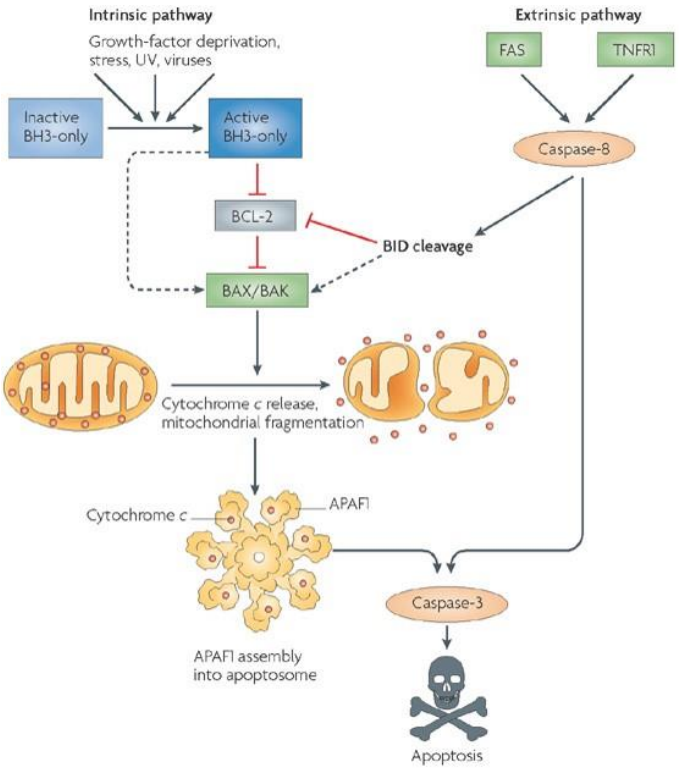

Figure 3. Overview of the intrinsic and extrinsic apoptosis pathways[20].

intrinsic and the extrinsic apoptosis pathways [19,22]. The regulation of death receptor signaling and the specific characteristics of each receptor are described in detail in section 1.3.

1.2.2 Apoptosis in cancer

The activation of apoptosis is a key mechanism in tumor suppression, and is therefore considered one of the hallmarks of cancer. BCL-2 family pro-apoptotic proteins are needed to induce cell death in response to hyperactive oncogenes such as *MYC*, or to DNA damage sensors like p53 and other key checkpoint proteins. A dysregulation of intrinsic apoptosis can therefore promote the survival of malignant cells. For instance, increased expression of BCL-2 is found to synergize with *MYC* amplifications in a subset of large B cell lymphomas, which have a worse prognosis in the presence of *MYC* and *BCL2* concurrent translocations. Furthermore, mutations in the pro-apoptotic effectors BAX and BAK can also confer survival advantage, and have been detected in some human carcinomas. Thus, dysregulation of the intrinsic apoptosis plays a key role in oncogenesis[23–27].

1.2.3 Apoptosis in cancer therapy

Evasion of apoptosis is not only involved in oncogenesis, but it also has a major role in drug resistance and therapy failure. Most chemotherapeutic drugs, as well as radiotherapy and novel targeted therapies induce apoptosis in cancer cells. Indeed the apoptotic threshold can be used in some cases to predict the response of tumors to chemotherapy[28–30]. The apoptotic threshold or apoptosis priming can be determined through BH3 profiling, a method that measures the concentration of a BH3 synthetic peptide necessary to induce MOMP in single cells *in vitro*[31].

The inability of cancer cells to undergo apoptosis in response to therapy represents a crucial clinical challenge for the treatment of most malignancies, including ALL[9,10]. The frontline agents used for the treatment of ALL (e.g. dexamethasone, vincristine, and L-asparaginase) rely on the induction of apoptosis to eliminate cancer cells, and therefore defects in the apoptotic response can confer resistance to such compounds. Dexamethasone and other glucocorticoid drugs activate apoptosis by affecting the expression of pro- and anti-apoptotic proteins hence disrupting their balance[32,33]. Decreased induction of the pro-apoptotic BIM and upregulation of the anti-apoptotic proteins BCL-2 and MCL-1 have been implicated in the clinical resistance to glucocorticoids[9,33,34]. Vincristine is a microtubule destabilizing drug that induces G_2M arrest[35]. Moreover, it has been shown to induce apoptosis independently of the mitotic arrest through the production of ROS and activation of caspases-9 and -3[35–38]. Although not completely characterized, vincristine resistance has been linked to increased anti-apoptotic BCL-2 family members as well as dysregulation of the extrinsic apoptosis pathway[9,39]. L-asparaginase depletes L-asparagine and glutamine, aminoacids essential for the growth of tumor cells, leading to cell cycle arrest and apoptosis. Resistance to L-asparaginase correlates with decreased caspase-3 activation[10] and dysregulation of the pro-apoptotic proteins BCL2L13 and HRK (activator of apoptosis, harakiri) as well

as TNFα[9], and has also been linked to the activation of compensatory cytoprotective autophagy[40]. Furthermore, the targeted BCR/ABL inhibitor imatinib induces cell death through BCL-2 regulated apoptosis. Resistance can be acquired by loss of BIM and BAD, and increased BCL-2 expression[41].

Besides dysregulation of the intrinsic apoptosis cascade, the initial steps of extrinsic apoptosis have also been found to be defective in certain tumor types. For instance, loss of death receptors is reported in a substantial proportion of lymphoma and leukemia cell lines[10,42]. The inhibitor of apoptosis proteins (IAPs) cIAP1, cIAP2, and XIAP, which control the activation of caspases and receptor interacting protein 1 (RIP1)-mediated death signaling, have been found to be overexpressed in many cancers including leukemia[43–45]. Other mechanisms involved in apoptosis resistance include induction of cytoprotective autophagy, the stabilization of anti-apoptotic factors by HSP90, or upregulation of the proteasome activity[46].

1.2.4 Targeting resistance to apoptosis

Since dysregulation of BCL-2 family proteins plays such a key part in therapy resistance, small molecule compounds that can mimic the pro-apoptotic BH3-only proteins and target one or more anti-apoptotic proteins have been developed. The BH3 mimetics ABT-737 and ABT-263 target BCL-2, BCL-xL, and BCL-w, and show potent activity against various tumor types. However, their clinical use is limited by the induction of strong thrombocytopenia. This problem is avoided by ABT-199, a highly selective BCL-2 inhibitor. ABT-199 has shown potent effects against many hematologic malignancies, including the fatal TCF3-HLF-positive ALL subset[15]. Inhibitors against Mcl-1, which lead to the liberation of BAX and BAK, have also been developed. Besides these inhibitors of the anti-apoptotic BCL-2 family members, direct agonists of BAX and BAK such as BAM7 have been reported. However, they are still in the initial stages of development. Other drugs developed to restore sensitivity to apoptosis include autophagy inhibitors, or inhibitors of the IAPs called SMAC mimetics (SM)[21,46–48]. SM are discussed further in section 1.4.

1.2.5 Necroptosis is an alternative form of programmed cell death

Necrosis was considered until recently to be a mode of spontaneous or unregulated cell death. The term necroptosis was first coined to describe a programmed form of necrosis which could be induced by Fas and TNFR activation in the absence of apoptotic signaling, and could be inhibited by the small molecule inhibitor of RIP1 kinase activity necrostatin-1 (Nec-1)[49]. Since its initial definition a decade ago, necroptosis has been increasingly studied and characterized.

Necroptosis is involved in maintaining homeostasis in adult tissues such as the intestinal epithelium. It also plays important roles in the immune system for instance by regulating T cell proliferation and macrophage survival, it serves as an antiviral backup to apoptosis in infected cells, and it modulates

emergency hematopoiesis. Excessive necroptosis is also related to many pathological situations, including neurodegeneration, ischemic brain injury, or stroke[18,49–51].

Necroptosis and necrosis exhibit the same morphological features, which differ from apoptosis. They present with an increase of cellular volume, mitochondrial swelling, intact nuclei, and rupture of the plasma membrane[18].

Many signals can trigger necroptosis, including intracellular signals such as DNA damage or oxidative stress, or extracellular signals such as ligation of death receptors (TNFR1, Fas, and TRAILR1-2), interferon (IFN) receptors, or pathogen recognition receptors (toll-like receptors, TLRs). Necroptosis has been best studied in the model of TNFR1 activation. The first stages of necroptosis after TNFR1 ligation coincide with its activation of extrinsic apoptosis (see section 1.2.1). After TNFR1 activation and internalization, the DISC is recruited, which contains FADD (Fas associated death domain), TRADD (TNF receptor associated death domain), RIP1, and RIP3, besides caspase-8. In certain contexts formation of the DISC leads to extrinsic apoptosis, then caspase-8 cleaves and inhibits RIP1 and RIP3, the key molecules mediating necroptosis. In case of caspase inhibition, a complex containing RIP1 and RIP3 (necrosome) is formed. This leads to their phosphorylation, and the subsequent phosphorylation and activation of MLKL (mixed lineage kinase-like). Active MLKL forms homo-trimers which translocate to the plasma membrane and disrupt its integrity, executing thus cell death[18,50,52–56] (Figure 4). The interplay between apoptosis and necroptosis, and the details of death receptor signaling are described further in sections 1.2.9 and 1.3 respectively.

The destruction of the plasma membrane of necroptotic cells leads to the release of inflammatory signals such as damage associated molecular patterns (DAMPS), contributing to the notion that necroptosis is more inflammatory than apoptosis. However, many confounding factors hinder answering this question. Cell death, and necroptosis in particular, is very tightly linked to inflammation. Many of the ligands and receptors involved in cell death are also potent inflammatory mediators depending on the cellular context. It has been proposed that TNFα-induced necroptosis acts as an anti-inflammatory mechanism by abrogating the production of inflammatory cytokines, which necroptosis-resistant cells would continue to produce. In some cases, necroptosis can also lead to the destruction of biological barriers, leading to the activation of the immune response by microbial agents, such as in the intestinal epithelium or the skin [57–59]. Furthermore, proteins involved in the necroptosis pathway such as RIP3 have been involved in inflammatory signaling independently of cell death[60].

1.2.6 Necroptosis in cancer

Defects in necroptosis have also been implicated in oncogenesis. Mutations and SNPs in RIP3 as well as in CYLD (cylindromatosis), a key protein implicated in the switch between TNFR1 pro-survival and pro-death signaling, have been identified in chronic lymphocytic leukemia (CLL), Non-Hodgkin's lymphoma, or epidermal cancers. Furthermore, the inflammatory environment caused by necroptosis

can also promote tumorigenesis. Necrotic cells release interleukin 1α (IL-1α), which can promote proliferation in the neighboring cells. Additionally, necrotic cells can recruit immune cells, driving increased angiogenesis, proliferation, and invasiveness[25,50,61,62].

1.2.7 Necroptosis in cancer therapy and resistance to necroptosis

Most chemotherapeutic drugs induce apoptosis, which is often dysfunctional in refractory or relapsed tumors. In that case, the tumors can become cross-resistant to structurally and functionally unrelated drugs. While many strategies have been directed at restoring apoptosis sensitivity (i.e. BH3 mimetics), some propose profiting from independent cell death mechanisms to overcome such multifactorial resistance combining inducers of different cell death modalities. Thus necroptosis represents an attractive target[63,64].

Many have confirmed this hypothesis with various small molecules and in different types of cancer. Refractory patient-derived ALL samples were sensitized to dexamethasone by the small molecule obatoclax (GX15-070) through the induction of autophagy-dependent necroptosis[65]. Obatoclax was also shown to induce autophagy-dependent TNFα-independent necroptosis in rhabdomyosarcoma cells[66] and a triple mode of cell death by apoptosis, necroptosis and autophagy in infant leukemia with MLL rearrangements[67]. Necroptosis can also be induced by the natural compound shikonin and its derivates in a wide range of apoptosis-resistant cancer cell lines harboring BCL-2 or BCL-xL overexpression[68]. Other necroptosis-inducing compounds include the sphingosine analog FTY720, a diphtheria toxin conjugate, or the combination of 5-fluorouracil with the pan-caspase inhibitor IDN-7314[69–71]. Furthermore, a recent study showed that RIP3-dependent necroptosis could also contribute to the response to standard chemotherapeutics such as DNA-damaging agents[72].

Malignancies of hematologic and colorectal origin show special sensitivity to necroptosis. However, not all cell types are competent to undergo this mode of cell death. 57% of small cell lung carcinomas and 85% of breast cancer patients show hypermethylation of the RIP3 promoter, resulting in loss of expression[72,73]. Decreased RIP3 and MLKL expression are also reported for AML and CLL, as well as many cancer cell lines[64]. This suggests that pre-treatment with hypomethylating agents could be used to restore necroptotic sensitivity[72].

1.2.8 Other cell death modalities

Anoikis is a mode of cell death induced in adherent cells by the detachment from the extracellular matrix (ECM). Its upstream activation signals lead to the activation of intrinsic apoptosis, which finally executes cell death. Entosis occurs also after loss of contact with the ECM. In this case the cell is engulfed by another cell of the same type and the final cell death is not executed by caspases. Parthanatos is a caspase-independent pathway mediated by the overactivation of PARP1 (poly ADP-

ribose polymerase 1). Pyroptosis is mediated by caspase-1 activation and is associated with the release of interleukins-1ß and -18[19].

Autophagy is a necessary process for the maintenance of the cellular homeostasis. It is characterized by the formation of double membrane vesicles (autophagosomes) that engulf cellular contents and recycle them after fusing with lysosomes. Autophagy is generally considered a cytoprotective mechanism. However, it has been found to mediate cell death in certain conditions, especially in the case of apoptosis inhibition. The term autophagic cell death is used in instances when it can be rescued by genetic ablation of at least two different autophagy genes. This is important in order to differentiate cell death mediated by autophagy from cell death accompanied by autophagy, which can be the case of necroptosis[19,74,75].

1.2.9 Crosstalk between cell death modalities

Despite being mechanistically well defined, numerous points of crosstalk exist between the various cell death modalities. Experimental inhibition of apoptosis by pan-caspase inhibitors is often necessary for the induction of necroptosis. Additionally, the embryonic lethality of either *CASPASE8* or *FADD* knockout mice is rescued by an additional *RIP3* knockout. This indicates that apoptosis exerts a negative control of necroptosis[76]. The switch between apoptosis and necroptosis downstream of RIP1 has been proposed to be controlled by the availability of the downstream effectors[77]. Besides MLKL-mediated necroptosis, RIP3 can mediate in parallel FADD-dependent apoptosis to control influenza A respiratory infection[78].

Autophagy favors the induction of necroptosis downstream of TRAILR activation by promoting the assembly of the necrosome on the autophagic membranes, which serve as a scaffold. Blocking the formation of autophagosomes causes the cells to default to apoptosis[79]. Necroptosis was found to require autophagy for the response to Obatoclax in ALL patient-derived samples[65].

Apoptosis is also linked with autophagy through the binding of BCL-2 and BCL-xL to Beclin-1, the central regulator of autophagy initiation. Beclin-1 is constitutively inhibited by BCL-2 and BCL-xL, which are displaced by BAD upon starvation to promote autophagy[21]. Additionally, autophagy can decrease TRAIL-induced apoptosis by degrading the pro-apoptotic protein PUMA (p53 upregulated modulator of apoptosis)[80].

1.3 Death receptor signaling: TNF and TNFR families

The TNF superfamily (TNFSF) is represented in Drosophila by a single gene homologue, *Eiger*, and doesn't exist in prokaryotes, yeast or nematodes. The human TNFSF comprises 19 ligands and 29 receptors, most of them with important functions in the development and activity of the immune system. For instance, TNFSF signaling can influence T cell responses by activating antigen presenting cells, or directly stimulating T cell proliferation. The best studied TNFSF ligands are TNFα, TRAIL, FasL,

RANKL (receptor activator of nuclear factor kappa-B ligand), and TWEAK (TNF-related weak inducer of apoptosis)[81,82].

TNFSF ligands are generated as type II transmembrane proteins (single-pass transmembrane with a signal-anchor sequence and the C-terminal targeted to the ER lumen) that contain a homotrimeric c-terminal TNF homology domain at the extracellular region. TNFSF ligands form homotrimers, with the only exception of lymphotoxin ß, which heterotrimerizes with lymphotoxin α. The extracellular domain is often cleaved by proteolysis, releasing the ligand into the extracellular space. Some receptors of the TNF receptor superfamily (TNFRs) respond differently to their soluble and membrane bound ligands. Generally, one trimeric ligand interacts with three monomeric receptors. TNFRs are type I (single-pass transmembrane proteins with a stop-transfer sequence and the N-terminal domain targeted to the extracellular space) or type III (single-pass transmembrane with a signal-anchor sequence and the N-terminal targeted to the ER lumen) transmembrane proteins which contain 1 to 4 cysteine rich domains (CRD) on the extracellular region. TNFRs can be structurally classified into death domain (DD)-containing receptors, decoy receptors, or TRAF-(TNF receptor associated factor) binding receptors. DD-containing TNFRs can activate cell death through the interaction with other DD-containing proteins. TRAF-binding receptors lack the DD, but enclose a sequence of 4 to 6 aminoacids to recruit TRAF proteins in the intracellular domain[81–83]. The specificity of each ligand for a particular receptor can vary. All ligands bind 1 to 5 receptors, while most receptors bind only 1 to 3 ligands[81,84].

1.3.1 TNFα is an important inflammatory cytokine

TNFα is an inflammatory cytokine produced as a transmembrane protein (mTNF) of 233 aminoacids. It is cleaved by metalloproteases such as TACE (TNF-alpha converting enzyme, also known as ADAM-17) to produce the soluble TNFα (sTNF), of 157 aminoacids. The intracellular domain produced after the cleavage migrates into the nucleus, while the extracellular domain is secreted. Both mTNF and sTNF act as homotrimers. TNFα is mostly produced and secreted by cells of the immune system and is an important player in many inflammatory diseases such as rheumatoid arthritis. mTNF is present in T cells, monocytes/macrophages, and NK cells, and it plays an important role in host defense. mTNF on T cells induces activation of monocytes, memory T cell response against intracellular pathogens, and can kill HIV infected lymphocytes through TNFR1-TNFR2 cooperative signaling. When expressed by infected T cells, mTNF can increase B cell activation. In contrast with mTNF, which acts through cell-cell contact or in an autocrine manner, sTNF can have paracrine and systemic effects[81,83,85,86].

The soluble and membrane-bound forms of TNFα signal through the receptors TNFR1 and TNFR2 differently. mTNF binds and activates TNFR1 and TNFR2, while sTNF binds both receptors but signals preferentially through TNFR1. The ability of the receptor to respond to sTNF is determined by an extracellular region proximal to the transmembrane domain termed stalk region. This region determines the local enrichment of receptors and their PLAD- (pre-ligand assembly domain) mediated homotrimer

formation in the absence of ligand. The stalk region of TNFR1 is necessary for the response to sTNF, while the stalk region of TNFR2 prevents it. This leads to important differences in the downstream signaling and outcome of m and sTNF and has consequences for the treatment of autoimmune diseases with TNFα neutralizing antibodies such as infliximab, etanercept, or adalimumab. They are all effective at neutralizing sTNF but vary in their activity against mTNF[83,84,87].

TNFα has been implicated in tumor development by its ability to induce proliferative signaling, production of angiogenic molecules such as VEGF (vascular endothelial growth factor) and IL-8 (interleukin 8), and chromosomal instability through the induction of FAT10, a ubiquitin-like protein modifier related with aberrant mitosis. It has been found to be constitutively produced by the microenvironment in several tumor types[88].

1.3.2 TNFR1 is a main inducer of pro-survival and death signaling

TNFR1 is ubiquitously expressed at low levels (300 to 10.000 receptors per cell), can be activated by both s and mTNF, and translocates to lipid rafts once activated. *TNFR1* knockout mice have a similar phenotype to *TNFα* knockout mice, showing impaired B cell development and increased susceptibility to bacterial infections among others. TNFR1 can activate both cell survival and cell death pathways, depending on the signaling induced downstream. However, in most cell types TNFα induces survival signaling by default, and the activation of TNFα-induced cell death requires downstream dysregulations[83,89,90].

1.3.2.1 TNFR1 in pro-survival signaling

TNFR1 can activate NF-κB (nuclear factor κ B) and MAPK (mitogen-activated protein kinase) signaling pathways, including JNK (c-Jun N-terminal kinase), ERK (extracellular signal-regulated kinase), and p38, thus promoting cell survival and inflammation. TNFR1 pro-survival signaling is important for the maturation and the stimulatory capacity of dendritic cells, proliferation of lymphocytes, or antibody production among others[91,92].

TNFα-induced pro-survival and pro-inflammatory signaling after TNFR1 activation is mediated by the so called complex I. Complex I is formed by the interaction of TNFR1 through its DD with other DD-containing proteins, such as TRADD. TRADD then recruits RIP1 and TRAF2, which brings cIAP1 and cIAP2 with it. cIAPs can ubiquitinate themselves and RIP1 by K11, K63 and K48 linkages, and the ubiquitination of RIP1 is required for the downstream induction of NF-κB. The addition of K63 ubiquitin chains leads to the recruitment of additional complexes essential for survival signaling. One complex recruited is the IKK complex, which is necessary for NF-κB activation and contains NEMO (NF-κB essential modulator) and IKK (IκB kinase) 1 and 2. When phosphorylated and activated by TAK1 (transforming growth factor ß-activated kinase 1), another protein recruited to complex 1, IKK2 can phosphorylate IκBα (inhibitor of κB alpha), leading to its degradation. This frees the NF-κB dimers

p50/p65, which translocate to the nucleus and initiate expression of pro-survival and pro-inflammatory genes such as *c-FLIP* (cellular FLICE inhibitory protein), *BCL2*, *TRAF2* or *cIAPs*. Another pro-survival complex recruited to complex I through K63 linkages contains TAK1, TAB2 (TAK1 binding protein 1), and TAB3. Besides activating IKK1 and 2, TAK1 can activate MAPK signaling, including JNK, ERK1/2, and p38 (Figure 4). Additionally, the linear ubiquitinating complex formed by LUBAC (linear ubiquitin chain assembly complex), HOIL (haem-oxidized IRP2 ubiquitin ligase-1), HOIP (HOIL-1 interacting protein), and Sharpin, is also recruited to complex I and adds linear ubiquitin chains (M1) to TNFR1, TRADD, RIP1 and NEMO[89,90,93,94].

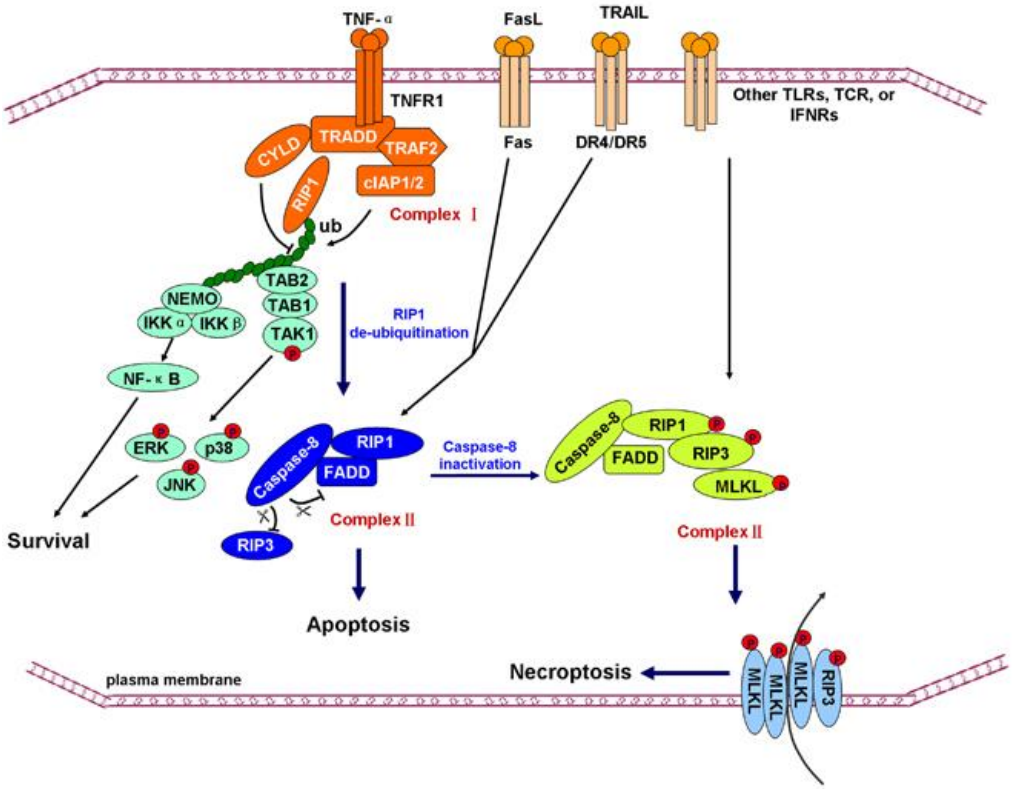

Figure 4. Overview of death receptor signaling. TNFR1 can induce cell survival, apoptosis, and necroptosis depending on the intracellular context. Adapted from [64].

Since the recruitment of pro-survival mediators to complex I relies on ubiquitin chains, deubiquitinating enzymes (DUBS) such as A20, CYLD, and OTU (ovarian tumor), are also part of the complex and are involved in its regulation. A20 can remove K48, K63, and M1 linkages, and removes K63 form RIP1 and TNFR1. It has also been found to act downstream of complex I by restricting RIP3 ubiquitination and impairing the formation of the necrosome[95]. CYLD is recruited by HOIP through SPATA2 (spermatogenesis-associated protein 2)[96] and can deubiquitinate RIP1, TRAF2, and NEMO. Additionally, OTU is recruited through LUBAC and is an M1 specific DUB[89,90,93].

1.3.2.2 TNFR1 in death signaling

TNFR1 can induce cell death through the arrangement of the cytosolic complex II, formed by TRADD, RIP1, FADD, caspase-8, caspase-10, and c-FLIP. The oligomerization of caspases in complex II can trigger their activation and induce apoptosis. On the other hand, in conditions of caspase deficiency or insufficient caspase activation, RIP1 can interact with RIP3 through the RHIM domain, form the necrosome, and lead to a series of phosphorylation events of RIP1, RIP3 and MLKL, hence activating necroptosis[89,93] (Figure 4). Apoptosis and necroptosis are described in section 1.2.

The transition from the complex I to the complex II or the necrosome occurs when complex I is destabilized (early checkpoint) or the NF-κB pathway is inhibited (late checkpoint). The deubiquitination of RIP1 caused by a loss or inhibition of cIAPs leads to its translocation to the cytosol and the formation of complex II. Similar effects take place in cases of decreased LUBAC activity (by mutations in HOIL or HOIP), or deficiency of TAK1 or NEMO. Furthermore, phosphorylation of RIP1 by IKKs keeps RIP1 in complex I. The inhibition of protein translation by cycloheximide or deletions in the NF-κB pathway also induce the formation of complex II due to the decreased expression of pro-survival proteins, however the exact mechanism is still unknown[89,90,93]. Furthermore, the outcome of TNFR1 activation is also regulated at the level of the receptor itself. K63 ubiquitination of TNFR1 by RNF8 (ring finger protein 8) promotes its internalization, the subsequent formation of complex II, and the activation of cell death[97]. TNFR1-induced cytotoxicity can also be impaired by TACE-induced shedding of the receptor as a feedback response to apoptosis and reactive oxygen species[98,99].

The activation of cell death is also regulated at the level of complex II by c-FLIP, a catalytically inactive caspase-8 homolog expressed via the NF-κB pathway. The long isoform of c-FLIP forms a slightly active complex with caspase-8, preventing its fully activation and cleaving RIP1 and RIP3 to block necroptosis. The short isoform of c-FLIP inhibits caspase-8 directly[89].

1.3.3 TNFR2 is not a death receptor but can modulate cell death

Contrary to TNFR1, the expression of TNFR2 is limited to certain cells of the immune system such as T lymphocytes, thymocytes, neurological cells such as oligodendrocytes, astrocytes, or microglia, endothelial cells, cardiac myocytes, and mesenchymal stem cells. Unlike TNFR1, which can be detected in larger clusters, TNFR2 is homogeneously distributed in the plasma membrane and is only efficiently activated by mTNF, differences which are dictated by its stalk region[83]. The intracellular domain of TNFR2 contains 5 highly conserved sequences named module I-V. Modules IV and V include TRAF2 binding sites, and module III is responsible for TRAF2 degradation. The function of modules I and II is still unknown[100] (Figure 5).

TNFR2 signaling can activate canonical and non-canonical NF-κB signaling. Unlike TNFR1, *TNFR2* knockout mice have a normal development and only mild phenotype, with a slightly decreased

sensitivity to TNFα. This indicates that the main outcomes of TNFα signaling are mediated by TNFR1, while TNFR2 can have modulatory effects[90]. In many cases, TNFR2 signaling has the opposite effects from TNFR1 signaling. For instance, TNFR1 signaling promotes tissue damage in response to heart failure, while TNFR2 is cardioprotective. Similar consequences are seen for neurological damage and tissue regeneration. TNFR2 and TNFR1 signaling pathways can also cooperate to induce both survival and cell death[101] (see section 1.3.3.3).

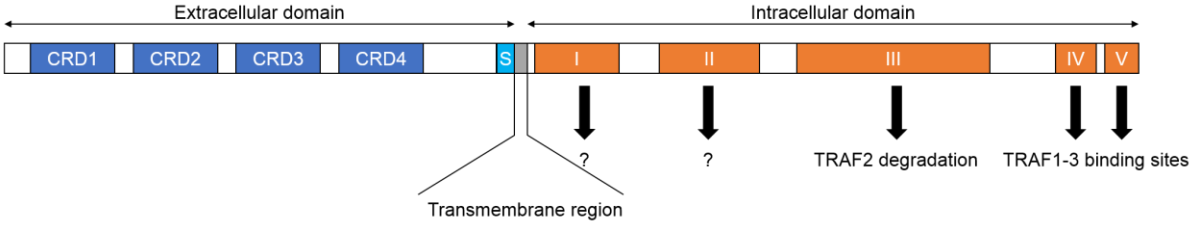

Figure 5. Structure of TNFR2. CRD1-4 are the cysteine rich domains, responsible for TNFα binding; S is the stalk region; I-V are the intracellular domains. Domain III is necessary for TRAF2 degradation, while domains IV and V are two independent TRAF binding sites.

1.3.3.1 TNFR2 in pro-survival signaling

The best characterized signaling events downstream of TNFR2 are those involved in the activation of cell survival mechanisms through the canonical and non-canonical NF-κB pathways. The ligation of mTNF induces the trimerization of TNFR2 and the subsequent recruitment of TRAF2, an event necessary for NF-κB activation. TRAF2 is constitutively bound to cIAP1 and cIAP2, and under basal conditions they can bind to the cytosolic complex formed by TRAF3 and NIK (NF-κB inducing kinase), leading to NIK ubiquitination and degradation. The recruitment the TRAF2-cIAP1-cIAP2 complex to TNFR2 prevents NIK degradation. NIK phosphorylates and activates of IKKα, which phosphorylates p100 and targets it for proteasome-mediated proteolysis, giving rise to the p52 fragment and activating the non-canonical NF-κB. TNFR2 can also activate the PI3K (phosphoinositide 3 kinase)/Akt pathway, which in turn phosphorylates IKKα. In this case IKKα phosphorylates IKKß, which phosphorylates IκBα, causing its degradation and the activation of p50/p65 canonical NF-κB (Figure 6). TNFR2 induces sustained NF-κB signaling which can last up to 24h, while NF-κB induction by TNFR1 is short-lived and lasts between 1 and 3 hours. This also indicates differential feedback regulation[88,100,102]. TNFR2-induced canonical NF-κB signaling is negatively regulated through the ubiquitination and proteasomal degradation of TRAF2, which is mediated by cIAP1 and cIAP2 and is independent of the binding site of TRAF2 in the intracellular domain of TNFR2. The exact regulation of this feedback loop is still unknown but phosphorylation events and proteins such as sphingosine-1-phosphate could be implicated[88,103,104].

Additionally, TNFR2 can activate JNK by inducing MEKK1 (MAPK kinase kinase 1) autophosphorylation. Aminopeptidase P3, a novel adaptor molecule recruited to the TNFR2 complex after ligation, has been found to play a role in this pathway[88,105]. TNFR2 can also activate Etk, a tyrosine

kinase implicated in angiogenesis, cell adhesion, migration, and survival, in a TRAF-2 independent manner[106].

TNFR2 plays important roles in immune regulation independently of TNFR1, such as inducing the activation, proliferation, and survival of T cells in response to infection[83,102]. Defects in the TNFα-mediated NF-κB signaling pathway occur in autoreactive T cells and are implicated in various autoimmune disorders[101]. Genomic alterations in *TNFRSF1B* (the gene encoding TNFR2) related to increased non-canonical NF-κB signaling have been found in a subset of cutaneous T cell lymphomas[107]. Furthermore, a promoter haplotype of TNFRSF1B that causes increased TNFR2 expression has been linked to increased TNFα release after LPS (lipopolysaccharide) treatment, leading to lower endotoxin tolerance[108].

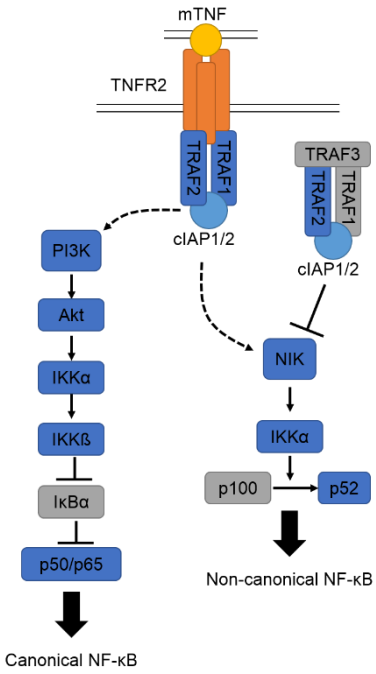

Figure 6. Overview of TNFR2-mediated pro-survival signaling.

1.3.3.2 TNFR2 in death signaling

Direct association of TNFR2 in cell death signaling has been reported in few cases, while its ability to contribute to TNFR1-mediated cell death is well established. Direct cell death signaling by TNFR2 has been found in response to TNFα, as well as to direct activation by cross-linking, in U937 and KYM-1 cell lines[109]. Overexpression of TNFR2 in T cells leads to TNF-induced cell death in the presence of RIP1, or NF-κB activation in its absence, while specific stimulation of TNFR1 in the same cells does not[110]. Additionally, TNFR2 is required for cisplatin-induced necrosis and apoptosis in the kidney[111], and TNFR2 agonism induces cell death of insulin-autoreactive T cells in diabetic patients[112]. The mentioned effects are all TNFR1-independent. The mechanisms by which TNFR2 can indirectly sensitize to cell death are discussed below, in section 1.3.3.3.

1.3.3.3 Crosstalk between TNFR2 and other death receptors in death signaling

TNFR2 can contribute to and enhance TNFR1-mediated cell death by various mechanisms, including blocking shared downstream pro-survival molecules and increasing TNFR1 activation. TRAF2 is essential for TNFR1 and TNFR2 signaling and has a main role in the interplay between both receptors[88,102]. TNFR1 induction of NF-κB and JNK pro-survival signaling requires TRAF2, which is degraded by TNFR2 activation, increasing thus TNFR1-mediated cell death. On the other hand, TNFR1 increases the levels of TRAF1, which can retain TRAF2 in the cytoplasm and restrict its degradation, preventing thus cell death[113–115]. Other studies have shown that the effect of TRAF2 depletion on

TNFR1 mediated cytotoxicity is not due to a decrease of NF-κB activation, but other mechanisms must be involved[116]. Another means by which TNFR2 and other non DD-containing TNFRs can increase TNFR1-induced cell death is via the increased production of mTNF, which can then activate TNFR1 in an auto- and paracrine manner[101,115,117]. Additionally, TNFR2 has been found to increase the concentration of TNFα at the membrane independently of any downstream events, and facilitate its binding to TNFR1, an effect known as ligand passing[118].

TNFR2 can sensitize to TNFR1-induced necroptosis by increasing the recruitment of RIP1 to TNFR1, or the recruitment of FADD to RIP1. The causes for this enhanced recruitment are still unknown, but could also be mediated by TRAF2 degradation and a decreased steric hindrance at the TNFR1 complex[101,119]. TNFR2 can also mediate TLR4-induced necroptosis via the production of mTNF in dendritic cells[120], as well as allow cell death in response to LPS in macrophages[121].

1.3.4 Other death receptors

Other well characterized TNFSF death receptors include Fas and TRAILR1-2. Similar to TNFR1, the DISC is recruited to the death domain of Fas and TRAILR1-2 after ligation. However, in this case, TRADD is not necessary for DISC assembly, and TRAF2 is not recruited. Additionally, FasL and TRAIL can only induce necroptosis in the context of caspase inhibition or FADD absence[19,122].

Besides TNFRSF members, RIP1-mediated cell survival and cell death can also be induced downstream or Toll-like receptors (TLRs) 3 and 4, which are pattern recognition receptors that respond to pathogen-derived products like viral dsRNA and lipopolysaccharide (LPS). TLRs recruit TRIF (TIR-domain-containing adapter-inducing interferon-β), leading to recruitment and ubiquitination of RIP1, TRAF6, and TAK1. This activates NF-κB or cell death depending on the context. Similarly, the interferon (IFN) pathway can activate RIP1 and RIP3 in response to bacterial infection, causing cell death of macrophages[93,120].

1.4 SMAC mimetics induce apoptosis and necroptosis

IAPs are key players in cell survival, acting both through the direct inhibition of caspases-3, -7, and -9 (XIAP), as well as through the ubiquitination of RIP1 downstream of death receptors (cIAP1 and cIAP2), preventing thus the formation of death complexes[94,123–126]. These pro-survival molecules are overexpressed in many malignancies including leukemia, have been implicated in drug resistance, and often correlate with poor prognosis, making them attractive targets for anticancer therapy[43,44,123,127].

IAP proteins are endogenously regulated by SMAC, a mitochondrial protein that translocates to the cytosol in response to apoptosis induction, and binds and inhibits cIAPs and XIAP, mediating a negative feedback loop[128]. Similarly to BH3 mimetics, small molecule peptidomimetics of SMAC (SMAC mimetics, SM) were developed with the aim of resensitizing cells to apoptosis. The binding of SM to XIAP leads to the release of caspases-3, -7, and -9, allowing the reactivation of apoptosis. At the same

time, the binding to cIAP1 and cIAP2 promotes their auto-ubiqitination and subsequent proteasomal degradation, leading to the deubiquitination of RIP1 and its switch from pro-survival to pro-death. Additionally, the loss of cIAPs leads to the stabilization of NIK and the subsequent activation of the non-canonical NF-κB pathway, which upregulates *TNF* among other genes. The production of TNFα can then potentiate the activation of cell death in an auto- or paracrine manner, and is required for SM-induced cell death in many cell lines[48].

SM mimic the N-terminal region of SMAC, responsible for the binding to the BIR (baculovirus IAP repeat) domains of IAPs, and can be structurally classified as monovalent or bivalent. Bivalent SM mimic the structure of the SMAC homodimer and are considered more potent because they bind IAPs with higher affinity[48]. The degree of specificity for one or more IAPs also depends on the chemical structure[129]. Considering the lethal phenotype of mice lacking cIAP1 together with cIAP2 or XIAP[130], a second-generation of SM compounds have been developed to have higher selectivity for cIAP1 versus cIAP2 in order to improve tolerability[131].

SM act as chemosensitizers and have been found to synergize with chemotherapy, radiotherapy, immune stimulants, and death receptor agonists such as TNFα, Fas, or TRAIL[129,132–135]. In leukemia, SM have been found to synergize with glucocorticoids in ALL[136], with the BCR/ABL inhibitor nilotinib[137], and with p38, MK2 (MAPK-activated protein kinase 2), or caspase inhibitors like emricasan in AML[138,139]. Many clinical trials for SM in combination with first-line chemotherapy are ongoing[127].

Some SM including birinapant, LCL161, and BV6, also showed activity as single agents against certain tumor types (both in cell lines and patient-derived xenografts), with the most promising results against hematologic malignancies, including various subtypes of leukemia[135,139–141]. However, the results of the clinical trials conducted so far with SM as single agents show only minor responses[127,142], indicating the need for establishing predictive biomarkers of response. The ability to respond to SM has been linked to the induction of TNFα production and autocrine positive-feedback, to the expression of TNFR1, as well as to the induction of NF-κB signaling[139,141,143]. Additionally, resistance to SM has been correlated with lower levels of XIAP[141], upregulation or stabilization of cIAP2[144,145], inability to form the ripoptosome[146], as well as drug efflux by the ABCB1 transporter[128].

1.5 CRISPR: a novel gene-editing technology

The CRISPR (clustered regularly interspaced short palindromic repeats) technology of genome editing was developed from the discovery of bacterial immune mechanisms. In bacteria such as *Streptococcus pyogenes*, foreign DNA from viruses or plasmids is incorporated into the host genome between CRISPR repeat sequences. The transcripts from those sequences (crRNAs) hybridize with a tracrRNA (transactivating CRISPR RNA), which recruits the nuclease Cas9 to cleave the invading DNA sequences. This bacterial defense mechanism has been adapted as a tool for genome engineering in cells

and whole organisms to generate knockouts for the study gene function, tag endogenous genes, or model diseases[147,148].

The generation of specific DNA double strand breaks (DSB) by the Cas9 nuclease can activate on the one hand to non-homologous end joining (NHEJ), a repair mechanism which generates insertions and deletions (indel) at the targeted site. This can lead to a change in the reading frame or change the binding site for promoters or enhancers, hence disrupting protein expression. On the other hand, DSB can be repaired by homologous recombination (HR), which can generate point mutations, or large insertions through the recombination with foreign "donor DNA". Furthermore, Cas9 mutants have been generated which cleave only one DNA strand (nickases), or which have no enzymatic activity but bind to the target DNA (dead Cas9 or dCas9)[148].

The CRISPR technology offers certain advantages compared to previous genome engineering tools like zinc finger nucleases or TALENs (transcription activator-like effector nucleases). The design of specific CRISPR sequences is simpler, because it uses RNA instead of protein to target the nuclease to a specific DNA sequence. This also allows the generation of large libraries for screening. Additionally, CRISPR can be easily adapted to generate DSB at multiple sites in parallel. However, the specificity of the system is not yet fully understood. Cas9 proteins tolerate certain amounts of mismatches and can therefore have off-target effects that need to be accounted for[148].

2. Subject of investigation and my contributions

Impaired apoptosis execution is one of the leading causes of drug resistance and relapse in ALL. Inducing alternative cell death mechanisms such as necroptosis is an attractive strategy to circumvent or overcome apoptosis blockade. Understanding the mechanisms of necroptosis induction and identifying markers of response may provide new approaches for targeted treatment in refractory and relapse ALL cases.

The main aims of my PhD project were the following:

1. Understanding the mechanisms regulating RIP1-dependent death, including the role of TNFα and death receptors.
2. Identification of biomarkers indicative of a response.
3. Validation of RIP1-targeting therapies *in vivo* in high risk disease, including evaluation of the therapeutic potential of SMAC mimetics.

I significantly contributed in:

Manuscript 1: Activation of concurrent apoptosis and necroptosis by SMAC mimetics for the treatment of refractory and relapsed ALL (shared first author). Contributions to figures 3, 4, and 5; supplementary figures 2 and 3; supplementary table 1. I contributed to the *in vivo* experiments, performed the quantitative PCR for TNFα, and the western blots for the protein levels and NFκB induction in patient-derived xenografts. I also characterized the mixed phenotype in cell lines (viability and TUNEL assays) and validated the CRISPR knockout cell lines and xenografts.

Manuscript 2: TNFR2 is essential for RIP1-dependent cell death in refractory ALL (manuscript in preparation, first author). Contributions to all figures and all supplementary figures and tables. I performed the quantitative PCR for TNFR2 and the other related genes in patient-derived samples form responders and non-responders, and validated TNFR2 at the protein level. I generated the overexpression constructs, validated the overexpression and CRISPR knockout stable cell lines, and performed the viability assays. I contributed to the *in vivo* CRISPR experiments, validated the knockouts and screened them *in vitro*, as well as the primary samples from the alternative cohort. I also performed the NFκB western blot analysis, and the immunoprecipitations in cell lines and patient-derived xenografts.

3. Results

3.1 Manuscript 1

Activation of concurrent apoptosis and necroptosis by SMAC mimetics for the treatment of refractory and relapsed ALL

Authors: Scott McComb[§], Júlia Aguadé-Gorgorió[§], Lena Harder, Blerim Marovca, Gunnar Cario, Cornelia Eckert, Martin Schrappe, Martin Stanulla, Arend von Stackelberg, Jean-Pierre Bourquin[§], Beat C. Bornhauser[§,*]

*Corresponding author

§These authors contributed equally to this manuscript

Abstract

More precise treatment strategies are urgently needed to decrease toxicity and improve outcomes for treatment-refractory leukemia. We used ex vivo drug response profiling of high risk, relapsed, or refractory acute lymphoblastic leukemia (ALL) cases and identified a subset with exquisite sensitivity to small molecule mimetics of the secondary mitochondria-derived activator of caspases protein SMAC (SMAC mimetics, SM). Potent ex vivo activity of the SM birinapant correlated with dramatic in vivo anti-leukemic effects, as indicated by delayed engraftment, decreased leukemia burden, and prolonged survival of xenografted mice. Antileukemic activity was dependent on simultaneous execution of apoptosis and necroptosis, as demonstrated by functional genomic dissection with a multi-colored lentiCRISPR approach to simultaneously disrupt multiple genes in patient-derived ALL. SM specifically targeted RIP1-dependent death, and CRISPR-mediated disruption of RIP1 completely blocked SM-induced death yet had no impact on the response to standard anti-leukemic agents. Thus, SM compounds such as birinapant circumvent escape from apoptosis in leukemia by activating a potent dual RIP1-dependent apoptotic and necroptotic cell death, which is not exploited by current therapy. Ex vivo drug activity profiling could provide important functional diagnostic information to identify patients who may benefit from targeted treatment with birinapant in early clinical trials.

For detailed information see attached manuscript 1 (pages 49-87)

3.2 Manuscript 2

TNFR2 is essential for RIP1-dependent cell death in refractory ALL

Authors: Júlia Aguadé-Gorgorió, Scott McComb, Maria Pamela Dobay, Lena Harder, Blerim Marovca, Silvia Jenni, Gunnar Cario, Cornelia Eckert, Jean-Pierre Bourquin, Beat C. Bornhauser*

*Corresponding author

Abstract

The identification of molecular determinants that regulate sensitivity to specific agents is essential for the development of new therapeutic approaches in cancer. We have earlier shown that a subset of refractory acute lymphoblastic leukaemia (ALL) samples respond to SMAC-mimetic induced IAP depletion by concurrently inducing RIP1-dependent apoptosis and necroptosis. Herein we show that this response correlates with the expression of TNF receptor 2 (TNFR2) in primary ALL. Using CRISPR/Cas9-mediated knockout of TNFR1 and 2 and in vivo selection with SMAC mimetics we show that TNFR1 and 2 are both functionally required for cell death. SMAC mimetics induced recruitment of RIP1 to TNFR1, which was abolished in cells deficient for TNFR2. Our data indicate that TNFR2 predicts sensitivity to SMAC mimetics and plays a key role in modulating a switch from RIP1-controlled cell survival to cell death.

For detailed information see attached manuscript 2 (pages 89-120)

4. Discussion

4.1 Clinical challenges in ALL therapy

The treatment of ALL has reached nowadays an exceptional rate of overall survival of 90%. However, 15 to 20% of patients still relapse and have a much worse prognosis. Relapsed ALL usually has acquired drug resistance[1]. Identifying new drugs and combinations active against resistant relapsed ALL is imperative for improving the outcome of these patients. Activating necroptosis could prevent relapse if induced in combination with standard therapies, or circumvent drug resistance in refractory cases, and represents an attractive strategy for cancer therapy. We have shown that activating RIP1-dependent cell death by SMAC mimetics effectively kills high risk and relapsed ALL[149] (manuscript 1), and we have established TNFR2 expression as a predictive marker of response, facilitating the translation to clinical practice (manuscript 2).

4.2 Xenograft mouse model: a clinically relevant setting for the study of ALL

Working with a clinically relevant system that reflects the biology of the disease is essential for target identification and drug discovery. The xenograft model of ALL allows expanding patient material while maintaining its genomic and transcriptomic characteristics as well as its subclonal composition[14]. We have observed dramatic differences between ALL cell lines and patient-derived samples, including the response to SM alone (both in potency and diversity in the response), the proportion of necroptosis or mixed-phenotype in response to birinapant, or the phenotype after TNFR2 overexpression.

We have adapted the lentiCRISPR technology to generate knockouts in patient-derived cells and used the xenograft model to evaluate if the knockouts acquire resistance to SM treatment. The introduction of a specific fluorescent gene in each of the CRISPR/Cas9 lentiviral plasmids allows the simultaneous generation of multiple knockouts from one population after sorting single, double, triple, or quadruple fluorescence-positive cells (Multi-colored lentiCRISPR, Figure 7). The expansion of knockout cells *in vivo* under treatment not only indicates survival but also the ability to proliferate, providing the combined information of viability and clonogenic assays. This is a valuable strategy which can easily be adapted

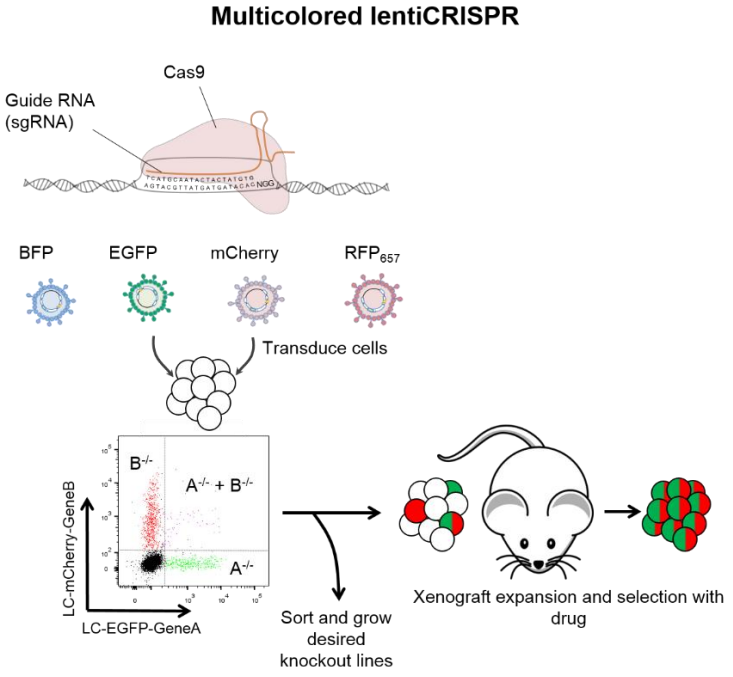

Figure 7. Scheme of multicolored lentiCRISPR approach for the generation of knockout cell lines and *in vivo* selection of knockout patient-derived cells. Figure adapted from [149].

to high throughput CRISPR screening for the identification of genes essential for drug response. However, it is limited by the low transduction efficiency of patient-derived ALL. Using CRISPR screening and *in vivo* selection to identify genes which confer resistance to a given compound would be difficult, since the population of interest would be rare at the beginning and would be lost under treatment.

Using the lentiCRISPR system we have generated *RIP3* and *FADD* knockouts form the same patient sample, which respond to birinapant exclusively by apoptosis or necroptosis respectively. These represent an ideal tool to compare the inflammatory responses induced by both cell death modalities. However, the study would be limited by the lack of a functional immune system in the NSG mouse model.

4.3 Resistance to apoptosis is a common feature of refractory and relapsed cancer

Chemotherapeutic drugs, radiotherapy, and some novel targeted therapies induce apoptosis in tumor cells, independently of their mechanism of action. However, it is important to consider that activating apoptosis doesn't necessarily mean relying on apoptosis to induce cell death. Unpublished data from our lab indicates that many classical chemotherapeutic compounds thought to induce apoptosis can still induce cell death in *CASPASE3* and *7* double knockout patient-derived ALL, showing that other cell death mechanisms could be implicated. Furthermore, there are many downstream points of crosstalk between cell death modalities, as highlighted by the fact that inducing necroptosis requires in many cases the inhibition of apoptosis.

Nevertheless, resisting apoptosis or cell death in general is one of the hallmarks of cancer[25] and many malignancies including ALL show features of apoptosis resistance. Many proteins involved in intrinsic apoptosis are altered in ALL, especially BCL-2 family proteins, as well as other players involved in the extrinsic apoptosis pathway[9,33,34]. Resistance to frontline chemotherapy correlates with a decreased execution of apoptosis[10], and the presence of apoptosis resistant (or unprimed) cells subpopulations in AML as determined by BH3 profiling correlates with drug resistance and predicts clinical response[150]. Additionally, dysfunctions in apoptosis can also confer resistance to novel targeted therapies such as imatinib[41].

This must be taken into account when designing treatment strategies aimed for relapse or resistant cases. Alternative cell death pathways which do not rely on the apoptotic machinery could be exploited, as well as strategies directly targeting the resistance mechanisms.

4.4 Identifying drugs active against resistant and relapsed ALL

Many approaches can be taken to successfully identify specific drug sensitivities in resistant and relapsed ALL. Yet they all require molecular knowledge of the disease or the identification of biomarkers of response.

4.4.1 Targeting genetic alterations

ALL is characterized by gross genetic aberrations, frequently leading to the expression of abnormal fusion proteins. Those represent attractive targets for novel therapies, since they are leukemia-specific and are often master regulators of the leukemic phenotype.

The development of tyrosine kinase inhibitors targeting the constitutively active fusion protein BCR/ABL has led to an improved prognosis of *BCR/ABL+* patients, allowing also the use of a less intensive chemotherapeutic regimen[1]. However, most of the leukemic aberrant fusion proteins don't have enzymatic activity but act as transcriptional regulators[3]. Hence targeting those proteins presents an increased difficulty. Transcriptional cofactors, modulators, epigenetic readers, or post-translational modifications necessary for the activity of the aberrant transcription factor could represent potential attractive targets as long as they can be inhibited with small molecules. Some successful examples of using such approaches for cancer treatment include bromodomain inhibitors, Notch1 inhibitors, or p53 reactivators[151]. Treatment with the small molecule JQ1, an inhibitor of bromodomain family proteins, leads to a decreased *MYC* transcription and reduces the expression of c-Myc target genes in B-ALL, decreasing leukemia viability[152]. Notch1 is a transmembrane receptor which has transcriptional activity after cleavage and liberation of its intracellular domain. The abrogation of Notch1 signaling can be achieved by allosteric antibodies or gamma secretase inhibitors, which interfere with Notch cleavage[151]. P53 reactivation can be achieved by targeting the negative modulators of p53 activity HDM2 and HMDX. The small molecule Nutlin-3 and stapled peptides mimicking the p53 transactivation domain disrupt the inhibitory p53-HDM2 and/or p53-HMDX complexes, leading to selective cytotoxicity in p53 wild type cells[153]. Altogether, targeting transcription factors for cancer treatment requires a deep understanding of their functional regulation.

4.4.2 Identifying pathway dependencies from transcriptomics

Transcriptome profiling can help establish distinct targetable pathway dependencies for subsets of ALL. This approach revealed a similar gene expression to BCR/ABL leukemia in the Philadelphia-like (ph-like) subtype, which presents a myriad of kinase-activating lesions. This suggests a dependency on kinase signaling pathways and the potential activity of tyrosine kinase inhibitors in ph-like ALL[1,154]. Transcriptomics of the fatal B-ALL subtype harboring the *TCF3-HLF* translocation revealed an overexpression of the anti-apoptotic protein BCL2. Indeed targeting apoptosis resistance with the BH3 mimetic ABT199 showed a potent activity against patient-derived TCF3-HLF positive samples *in vitro* and *in vivo*[15].

4.4.3 Unbiased drug screening identifies sensitivity patterns

An unbiased approach to detect specific drug sensitivities is high throughput *in vitro* drug screening of primary samples or patient-derived xenografts. A drug screening system of ALL in co-culture with

mesenchymal stromal cells was previously established in the lab and is routinely used to test drug response in various subsets of ALL[155]. The response *in vitro* correlates with the response *in vivo* in the xenograft model for the great majority of cases. This system has allowed identifying extraordinary drug sensitivities for specific patients or subgroups. For instance, it identified ABT199 as a potent drug against TCF-HLF[15], MLL-AF4, and T-ALL, and the SRC inhibitor dasatinib against T-ALL[156]. Additionally, a subset of cases with increased proliferation rates showed increased sensitivity to cell cycle targeting drugs. Besides target and biomarker discovery, individualized drug screening could potentially be used to personalize the treatment for high risk patients. This approach is currently being used for the Inform (individualized therapy for relapsed malignancies in childhood) study, in which samples from refractory or relapsed cases are tested *in vitro* using the mentioned drug screening platform for their response to a panel of clinical and investigational drugs. The information obtained from the screening together with the rest of the diagnostic information can then be used to make informed decisions regarding treatment options in refractory cases.

4.4.4 Targeting cell death to overcome resistance

Since apoptosis dysfunction is a general cause for resistance in primary and relapse malignancies, and many cancers depend on the higher expression of anti-apoptotic proteins for their survival, directly targeting the apoptosis blockade or lowering the apoptosis threshold represents an attractive strategy. Indeed, BH3 mimetics show a very promising activity against many malignancies, including leukemia[21,46,47]. However, many types of defects can cause decreased apoptosis execution, and they can vary between cancers or between subclones, making it more difficult to specifically target the origin of resistance.

Apoptosis was the first identified mode of regulated cell death. Since then many modalities of programmed cell death have been described, including necroptosis. Inducing alternative modes of cell death presents advantages over resensitizing to apoptosis, since they do not rely on a frequently abrogated cascade. Combining drugs to target various cell death pathways could also hinder the appearance of general resistance, since more alterations would be necessary[63].

Glucocorticoids are first line drugs for the treatment of ALL. Resistance to glucocorticoids is indicative of poor prognosis and can occur through dysregulation of intrinsic apoptosis. Resensitization to glucocorticoids could be obtained by combining them with arsenic trioxide, which lead to increased BAD and decreased XIAP levels, and resensitization to apoptosis[157]. Glucocorticoids could also be effectively combined with obatoclax, which led to the induction of necroptosis in an autophagy-dependent manner[65]. This indication that necroptosis could be induced and have a potential clinical benefit in refractory ALL was the starting point of this project.

4.5 Circumventing drug resistance in ALL through RIP1-directed strategies

cIAPs are highly expressed in ALL and regulate both apoptosis and necroptosis, making them attractive targets to circumvent resistance. SMAC mimetics (SM) induce the degradation of cIAP1 and cIAP2, and inhibit XIAP, leading to a pro-death state of RIP1 on the one side, and to the liberation of caspases on the other[43,44]. Using the mentioned drug screening platform we screened a heterogeneous cohort of B- and T-ALL patient-derived samples for their response to the SM birinapant and LCL161. We observed exquisite responses to birinapant *in vitro* for a subset of B-ALL samples and we confirmed the responses *in vivo*. The IC_{50} in response to birinapant had no correlation with the diagnostic genomic characteristics nor the clinical risk stratification, and many refractory and relapse cases were among the most sensitive. Additionally, potent activity of birinapant was detected *in vivo* in xenografts which relapsed after treatment with vincristine, dexamethasone, and L-asparaginase[141]. Thus, exploiting RIP1-dependent cell death is a promising approach against high risk and relapse cases, which have few therapeutic options.

We screened a panel of drugs, including the most common drugs used in ALL, in *RIP1* knockout patient-derived cells generated by lentiCRISPR. None of them relied on RIP1 for its activity, indicating that RIP1 will not be selected against during previous chemotherapy. Therefore, RIP1-targeting strategies could have encouraging results against drug-resistant cancers. A high-throughput small molecule screen comparing wild type and *RIP1* knockout patient-derived ALL could reveal novel interesting compounds. However, RIP1 is not essential for ALL survival, since *RIP1* knockout patient-derived cells do not show a growth disadvantage *in vivo*, and acquired resistance could eventually develop.

The strong single-agent activity of birinapant could not be observed in leukemia cell lines, which require the combination of SM with TNFα for cell death. This highlights the importance of working with a representative and clinically relevant model such as patient-derived xenografts.

We used chemical inhibitors and lentiCRISPR gene knockout to assess the cell death phenotype induced by birinapant, and saw that in most samples apoptosis and necroptosis were induced simultaneously, always in a RIP1-dependent way. In cell lines, this mixed phenotype was only observed in Jurkat. The rest were exclusively apoptotic and did not represent our observations from patient-derived samples. The presence of a mixed phenotype is novel, since necroptosis is mostly described in the context of inhibited apoptosis[18,50,139], and makes SM attractive for the treatment of resistant disease (Figure 8).

Apoptosis and necroptosis were jointly induced at the single cell level, as revealed by the fact that only cells with a double apoptotic and necroptotic knockout could expand under treatment. However, it is not yet clear if apoptosis and necroptosis are simultaneously activated in each cell, or if both pathways are available but one is the default and the other serves as a backup only if the first is blocked. The staining for TUNEL and live/dead cells by flow cytometry showed a majority of cells with intermediate TUNEL signal, indicating that there could be simultaneous apoptosis and necroptosis in each cell. However, single cell analysis of an apoptotic and a necroptotic marker, for instance active caspase-3 and phosphorylated MLKL, should be performed to answer this question.

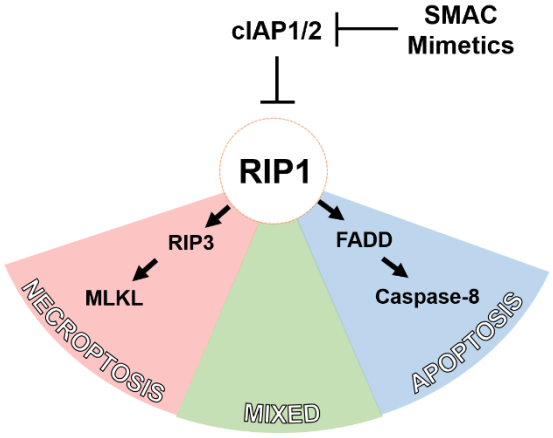

Figure 8. Model of RIP1-mediated necroptosis, apoptosis, and mixed phenotype. Adapted from [149].

Other interesting observations arise from analyzing the death phenotype in patient-derived ALL in response to SM. A subgroup of samples showed sensitivity to necrostatin-1 (nec) alone, indicating a dependence on RIP1 kinase activity for survival or a particular sensitivity to the off-target effects of nec. Another subgroup was not rescued by either nec, zVAD, or the combination, but was rescued by *RIP1* knockout. This suggests that RIP1 could be implicated in other cell death mechanisms besides apoptosis and necroptosis, or that it could be mediating cell death through indirect effects. Additionally, none of the samples had a purely apoptotic phenotype.

4.6 Identifying mechanisms of resistance to SM

Potent activity of SM and birinapant in particular has been detected against other types of leukemia, including MLL rearranged and ph-like AML[135,139,141]. However, activity of SM as single agents seems to be particularly high against hematologic malignancies compared to other solid tumors, and the clinical trials have had modest success so far[127,142]. In agreement, cancers of hematologic origin and colorectal tumors are distinctively sensitive to necroptosis. This could be determined in part by the expression of *RIP3* and *MLKL*, which are usually downregulated or silenced in cancer[72,73]. Our results in cell lines corroborate this hypothesis, since only Jurkat cells, which respond to birinapant and TNFα with a mixed phenotype, have detectable RIP3 protein expression. RIP3 was undetectable for the other cell lines tested, 658, Nalm6, and CEM-C7, which showed an exclusively apoptotic phenotype.

Birinapant targets cIAPs and indirectly targets RIP1. The levels of cIAP1/2 and RIP1 were homogeneous among all B-ALL samples, regardless of their response to birinapant. We couldn't observe any consistent differences among patient samples for the other players involved in RIP1-mediated cell death. Additionally, we couldn't detect differences in *TNFα* expression between

responders and non-responders and neutralizing TNFα didn't prevent cell death. TNFα-independent responses to SM have been previously observed by others[132,136,158,159]. Further experiments would be required to confirm if TNFα is required, since there is still the possibility that mTNF or intracellular TNFα are involved. We are currently generating lentiCRISPR *TNFα* knockouts in patient-derived cells to answer this question.

Other mechanisms of resistance to SM have been proposed. Those include the stabilization or upregulation of cIAP2[144,160], or the activity of caspases -8 and -10[161,162], which we could not detect in our cohort. Moreover, the inability to form the ripoptosome was described as the cause for SM resistance in CLL[146]. However, the formation of the ripoptosome is a downstream event and a consequence of RIP1 activation, and likely not the cause of resistance *per se*.

4.7 TNFR2 expression predicts the response to SM

Diverse resistance mechanisms can coexist within a cohort or even within a single patient, making its clinical application for patient selection more difficult. The word biomarker is usually used for molecular indicators of a process, such as cIAP1 degradation in response to SM, or caspase-3 cleavage after apoptosis induction. However, we considered that finding molecular markers of responsive patients which can be identified without needing to treat the patient would be beneficial and could facilitate its integration in the diagnostic pipeline. Therefore we focused on detecting markers which could predict SM response.

Using gene expression profiles we detected *TNFRSF1B* (encoding TNFR2) as one of the best indicators of responsiveness, which we validated by quantitative PCR (qPCR) in two independent cohorts. This is essential for assessing its predictive value. However, the detection of TNFR2 protein levels by flow cytometry, a technique routinely used in the diagnostic of ALL, is very low and setting a threshold is practically impossible. Another option would be to standardize the qPCR, which is also often used in the diagnostic lab. This method allows a clear separation between TNFR2-high and -low, but the cutoff to what is considered high would have to be established according to clinical data of SM response. Determining the cause for the differential expression of TNFR2 could be helpful, since it could be used as a surrogate readout. Some SNPs with a role in *TNFR2* expression have been reported, for instance rs522807, a SNP at the *TNFR2* promoter which correlates with increased expression[108]. We could not detect this SNP in any of the samples (data not shown), but additional SNPs could be tested. Additionally, *TNFR2* gene expression varies during the different stages of B cell development according to the Differentiation Map[163] (Figure 9A), suggesting that ALL blocked at distinct stages of differentiation could have different response to SM.

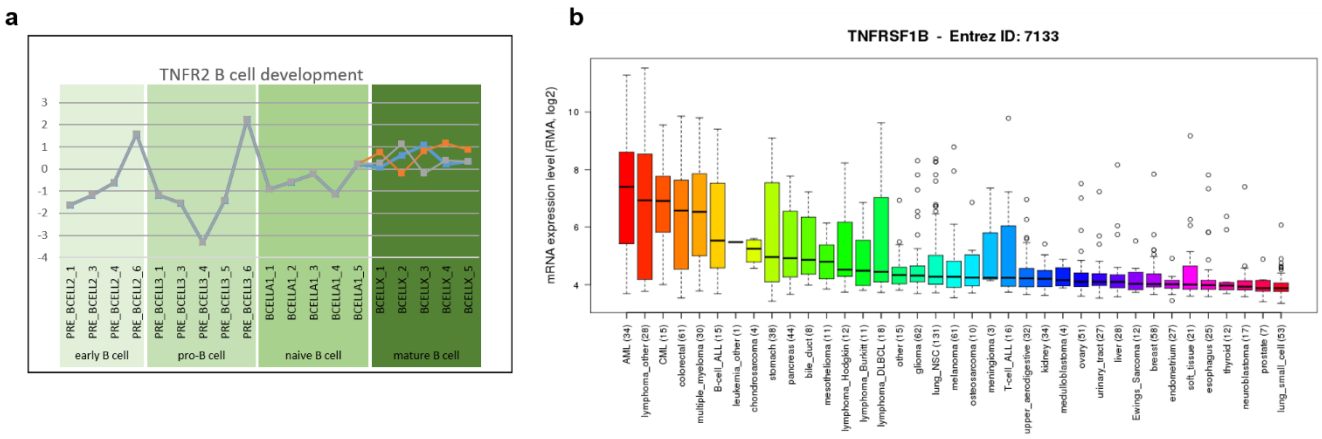

Figure 9A TNFR2 expression during B cell development. In the mature B cell stage, the colors indicate the following: in blue mature B cells able to switch, in orange mature B cells, and in grey class switched mature B cells (data extracted from the Differentiation Map[163]). **B** TNFR2 expression in cancer cell lines (data obtained from the Cancer Cell Line Encyclopedia[164]).

The predictive value of *TNFR2* expression for the response to SM in other subtypes of leukemia or other cancers has not been established yet. According to the Cancer Cell Line Encyclopedia[164], lymphomas or colorectal cancers show high TNFR2 expression and could be good candidates to further explore this avenue. Interestingly, AML cell lines show the highest expression and AML primary samples have been reported to be responsive to SM[139,141] (Figure 9B).

Using the gene expression profiles we also identified *TRAF6* and *ADAM17* as genes correlating with a lack of response. TRAF6 is involved in NF-κB induction downstream of TNFRs and TLRs[165], and *TRAF6* knockout increased response to birinapant in the partially sensitive 658 cell line (data not shown). *ADAM17* encodes TACE, the enzyme responsible for the processing of mTNF to sTNF, as well as for the shedding of TNFRs[85,99]. This could indicate that non-responders have higher TACE levels and therefore more sTNF while responders have more mTNF. Considering that TNFR2 signals preferentially after mTNF binding, TACE levels could play a role in the responsiveness to birinapant.

4.8 TNFR2 is mechanistically involved in the response to SM

TNFR2 is not only a predictive marker but is also mechanistically necessary for SM response in patient-derived B-ALL. Both *TNFR1* and *TNFR2* knockouts expanded *in vivo* under treatment with birinapant and showed a dramatically increased resistance to birinapant *ex vivo*, although the resistance is not complete and the expansion kinetics are slower than RIP1ko. This indicates that TNFR1 and TNFR2 cooperate to induce RIP1-dependent cell death in response to SM. Interestingly, *TNFR1* and *TNFR2* knockouts showed no growth disadvantage *in vivo* compared to the wild type cells before treatment, indicating that the cells are not dependent on TNFR1/2 signaling for proliferation and survival, and the same was observed for *TNFα* knockouts (data not shown). If the response is confirmed to be TNFα-independent, this would indicate a receptor-dependent but ligand-independent role of TNFRs in RIP1-mediated death, where TNFR1 and 2 could be necessary for their scaffold function.

To understand the mechanism of crosstalk between TNFR2 and TNFR1 in RIP1-dependent cell death we overexpressed TNFR2 in ALL cell lines. We observed a RIP1-dependent sensitization to TNFα in cell lines, which reflected the birinapant response in TNFR2-high patient-derived samples, but had no effect on the response to birinapant. However, TNFR2-high patient-derived cells don't show an increased sensitivity to TNFα (data not shown), stressing again differences between patient samples and cell lines. We attempted to overexpress TNFR2 in non-responders but the positive population didn't expand, suggesting that samples with low TNFR2 basal levels might be sensitive to its overexpression. Additionally, the transduction levels were low, making it difficult to monitor the population.

Some mechanisms of crosstalk between TNFR1 and TNFR2 have been described, including ligand passing effect[118], and the abrogation of NF-kB pro-survival signaling after TNFR2-induced TRAF2 degradation[88,102]. However, we could not observe any of the previous mechanisms in the SM-responders compared to non-responders or to TNFR2 knockouts. We observed a decreased recruitment of RIP1 to TNFR1 in non-responders and *TNFR2* knockout patient-derived samples compared to responders after birinapant treatment, indicating that TNFR2 facilitates the recruitment of RIP1 to TNFR1 and promotes cell death. A similar observation was reported in TNFR2 pre-stimulated cells, which showed increased TNFR1-dependent necroptosis and RIP1 recruitment in response to TNFα. The effect was proposed to be mediated by TRAF2 degradation, leading to a decreased steric hindrance at the TNFR1[119]. We propose that TNFR2 might exert a comparable role in the response to birinapant by displacing TRAF2 or other shared interactors from TNFR1 (Figure 10).

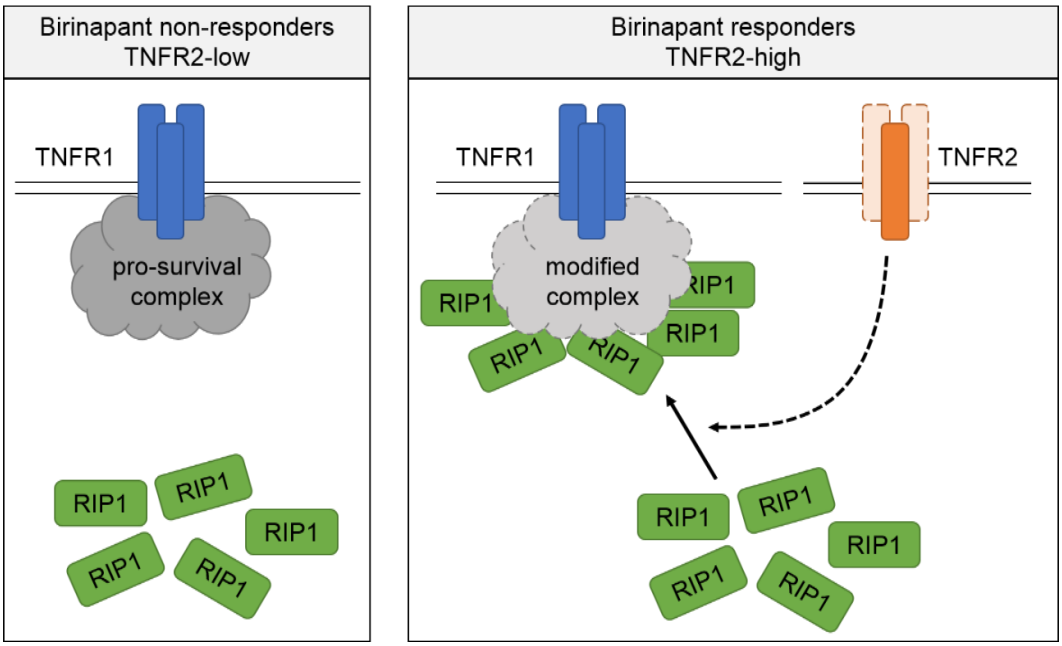

Figure 10. Proposed model for the regulation of the TNFR1-RIP1 death axis by TNFR2 in response to birinapant (model from manuscript 2).

To test this hypothesis we are adapting the TNFR1 co-immunoprecipitation method shown in manuscript 2 for mass spectrometry, and we will compare the TNFR1 complex in the presence or absence of TNFR2 and birinapant treatment. By understanding which of the changes that occur at the TNFR1 complex are regulated by TNFR2, we aim to identify the role of TNFR2 in SM response (Figure 10). Additionally, *TNFR2* knockout patient-derived cells could be reconstituted with various mutants of TNFR2, for instance unable to bind TRAFs or unable to induce TRAF2 degradation[116]. Understanding the mechanisms by which TNFR2 promotes RIP1-dependent cell death will help propose rational drug combination approaches. It could also contribute to the treatment of autoimmune diseases, which show elevated TNFR2 expression. TNFR2 agonism has been described to selectively induce cell death of autoreactive T cells in type 1 diabetes among others[101,112], indicating a potential use of SM.

In conclusion, we propose inducing alternative cell death mechanisms such as necroptosis as means to target the clinical challenges of drug resistance and relapse in cancer. Using the clinically relevant xenograft model and unbiased drug screening allowed the identification of SM as promising drugs for the treatment of ALL, as well as TNFR2 as a regulator of the cell death response. Overall, our work contributes to the clinical translation of necroptosis-inducing strategies.

5. References

1. Hunger, S. P. & Mullighan, C. G. Acute Lymphoblastic Leukemia in Children. *New England Journal of Medicine* **373,** 1541–1552 (2015).
2. World Health Organization. Incidence of childhood leukaemia. (2009). Available at: http://www.euro.who.int/__data/assets/pdf_file/0005/97016/4.1.-Incidence-of-childhood-leukaemia-EDITED_layouted.pdf. (Accessed: 30th September 2016)
3. Lo Nigro, L. Biology of childhood acute lymphoblastic leukemia. *J. Pediatr. Hematol. Oncol.* **35,** 245–252 (2013).
4. Mullighan, C. G. Genomic Characterization of Childhood Acute Lymphoblastic Leukemia. *Seminars in hematology* **50,** 314–324 (2013).
5. Eckert, C. *et al.* Monitoring minimal residual disease in children with high-risk relapses of acute lymphoblastic leukemia: prognostic relevance of early and late assessment. *Leukemia* **29,** 1648–1655 (2015).
6. Tallen, G. *et al.* Long-term outcome in children with relapsed acute lymphoblastic leukemia after time-point and site-of-relapse stratification and intensified short-course multidrug chemotherapy: results of trial ALL-REZ BFM 90. *J. Clin. Oncol.* **28,** 2339–2347 (2010).
7. Tasian, S. K., Loh, M. L. & Hunger, S. P. Childhood acute lymphoblastic leukemia: Integrating genomics into therapy. *Cancer* n/a–n/a (2015). doi:10.1002/cncr.29573
8. Mullighan, C. G. & Downing, J. R. Genome-wide profiling of genetic alterations in acute lymphoblastic leukemia: recent insights and future directions. *Leukemia* **23,** 1209–1218 (2009).
9. Holleman, A. The expression of 70 apoptosis genes in relation to lineage, genetic subtype, cellular drug resistance, and outcome in childhood acute lymphoblastic leukemia. *Blood* **107,** 769–776 (2006).
10. Holleman, A., den Boer, M. L., Kazemier, K. M., Janka-Schaub, G. E. & Pieters, R. Resistance to different classes of drugs is associated with impaired apoptosis in childhood acute lymphoblastic leukemia. *Blood* **102,** 4541–4546 (2003).
11. Jacoby, E., Chien, C. D. & Fry, T. J. Murine Models of Acute Leukemia: Important Tools in Current Pediatric Leukemia Research. *Front Oncol* **4,** (2014).
12. Hauer, J., Borkhardt, A., Sánchez-García, I. & Cobaleda, C. Genetically engineered mouse models of human B-cell precursor leukemias. *Cell Cycle* **13,** 2836–2846 (2014).
13. Bhatia, S., Daschkey, S., Lang, F., Borkhardt, A. & Hauer, J. Mouse models for pre-clinical drug testing in leukemia. *Expert Opin Drug Discov* **11,** 1081–1091 (2016).
14. Schmitz, M. *et al.* Xenografts of highly resistant leukemia recapitulate the clonal composition of the leukemogenic compartment. *Blood* **118,** 1854–1864 (2011).
15. Fischer, U. *et al.* Genomics and drug profiling of fatal TCF3-HLF-positive acute lymphoblastic leukemia identifies recurrent mutation patterns and therapeutic options. *Nat Genet* **47,** 1020–1029 (2015).
16. Kerr, J. F. R., Wyllie, A. H. & Currie, A. R. Apoptosis: A Basic Biological Phenomenon with Wide-ranging Implications in Tissue Kinetics. *Br J Cancer* **26,** 239–257 (1972).
17. Strachan, T. & Read, A. *Human Molecular Genetics*. (Garland Science, 2011).
18. Vandenabeele, P., Galluzzi, L., Vanden Berghe, T. & Kroemer, G. Molecular mechanisms of necroptosis: an ordered cellular explosion. *Nature Reviews Molecular Cell Biology* **11,** 700–714 (2010).
19. Galluzzi, L. *et al.* Molecular definitions of cell death subroutines: recommendations of the Nomenclature Committee on Cell Death 2012. *Cell Death Differ* **19,** 107–120 (2012).
20. Youle, R. J. & Strasser, A. The BCL-2 protein family: opposing activities that mediate cell death. *Nat Rev Mol Cell Biol* **9,** 47–59 (2008).
21. Chipuk, J. E., Moldoveanu, T., Llambi, F., Parsons, M. J. & Green, D. R. The BCL-2 Family Reunion. *Molecular Cell* **37,** 299–310 (2010).
22. Tait, S. W. G. & Green, D. R. Mitochondria and cell death: outer membrane permeabilization and beyond. *Nature Reviews Molecular Cell Biology* **11,** 621–632 (2010).
23. Adams, J. M. & Cory, S. The Bcl-2 apoptotic switch in cancer development and therapy. *Oncogene* **26,** 1324–1337 (2007).

24. Brown, J. M. & Attardi, L. D. The role of apoptosis in cancer development and treatment response. *Nat Rev Cancer* **5,** 231–237 (2005).
25. Hanahan, D. & Weinberg, R. A. Hallmarks of cancer: the next generation. *Cell* **144,** 646–674 (2011).
26. Johnson, N. A. *et al.* Concurrent Expression of MYC and BCL2 in Diffuse Large B-Cell Lymphoma Treated With Rituximab Plus Cyclophosphamide, Doxorubicin, Vincristine, and Prednisone. *JCO* **30,** 3452–3459 (2012).
27. Lowe, S. W., Cepero, E. & Evan, G. Intrinsic tumour suppression. *Nature* **432,** 307–315 (2004).
28. Kracikova, M., Akiri, G., George, A., Sachidanandam, R. & Aaronson, S. A. A threshold mechanism mediates p53 cell fate decision between growth arrest and apoptosis. *Cell Death Differ* **20,** 576–588 (2013).
29. Laurent, A. & Blasi, F. Differential DNA damage signalling and apoptotic threshold correlate with mouse epiblast-specific hypersensitivity to radiation. *Development* **142,** 3675–3685 (2015).
30. Weyhenmeyer, B. C. *et al.* Predicting the cell death responsiveness and sensitization of glioma cells to TRAIL and temozolomide. *Oncotarget* **5,** (2016).
31. Vo, T.-T. *et al.* Relative Mitochondrial Priming of Myeloblasts and Normal HSCs Determines Chemotherapeutic Success in AML. *Cell* **151,** 344–355 (2012).
32. Laane, E. *et al.* Dexamethasone-induced apoptosis in acute lymphoblastic leukemia involves differential regulation of Bcl-2 family members. *Haematologica* **92,** 1460–1469 (2007).
33. Ploner, C. *et al.* Glucocorticoid-induced apoptosis and glucocorticoid resistance in acute lymphoblastic leukemia. *The Journal of Steroid Biochemistry and Molecular Biology* **93,** 153–160 (2005).
34. Lugthart, S. *et al.* Identification of genes associated with chemotherapy crossresistance and treatment response in childhood acute lymphoblastic leukemia. *Cancer Cell* **7,** 375–386 (2005).
35. Kavallaris, M. Microtubules and resistance to tubulin-binding agents. *Nat Rev Cancer* **10,** 194–204 (2010).
36. Groninger, E., de Graaf, S. S. N., Meeuwsen-de Boer, G. J., Sluiter, W. J. & Poppema, S. Vincristine-induced apoptosis in vivo in peripheral blood mononuclear cells of children with acute lymphoblastic leukaemia (ALL). *British Journal of Haematology* **111,** 875–878 (2000).
37. Groninger, E., Meeuwsen-De Boer, G. J., De Graaf, S. S. N., Kamps, W. A. & De Bont, E. S. J. M. Vincristine induced apoptosis in acute lymphoblastic leukaemia cells: a mitochondrial controlled pathway regulated by reactive oxygen species? *Int. J. Oncol.* **21,** 1339–1345 (2002).
38. Huschtscha, L. I., Bartier, W. A., Ross, C. E. & Tattersall, M. H. N. Characteristics of cancer cell death after exposure to cytotoxic drugs in vitro. *Br J Cancer* **73,** 54–60 (1996).
39. Kang, M. H. *et al.* Activity of vincristine, L-ASP, and dexamethasone against acute lymphoblastic leukemia is enhanced by the BH3-mimetic ABT-737 in vitro and in vivo. *Blood* **110,** 2057–2066 (2007).
40. Song, P. *et al.* Asparaginase induces apoptosis and cytoprotective autophagy in chronic myeloid leukemia cells. *Oncotarget* **6,** 3861–3873 (2015).
41. Kuroda, J. *et al.* Bim and Bad mediate imatinib-induced killing of Bcr/Abl+ leukemic cells, and resistance due to their loss is overcome by a BH3 mimetic. *PNAS* **103,** 14907–14912 (2006).
42. Braun, F. K. *et al.* Blockade of Death Receptor-Mediated Pathways Early in the Signaling Cascade Coincides with Distinct Apoptosis Resistance in Cutaneous T-Cell Lymphoma Cells. *Journal of Investigative Dermatology* **127,** 2425–2437 (2007).
43. Notarbartolo, M. *et al.* Expression of the IAPs in multidrug resistant tumor cells. *Oncology Reports* **11,** 133–136 (2004).
44. Fulda, S. Inhibitor of Apoptosis (IAP) proteins in hematological malignancies: molecular mechanisms and therapeutic opportunities. *Leukemia* **28,** 1414–1422 (2014).
45. Tamm, I. *et al.* Expression and prognostic significance of IAP-family genes in human cancers and myeloid leukemias. *Clin. Cancer Res.* **6,** 1796–1803 (2000).
46. Mohammad, R. M. *et al.* Broad targeting of resistance to apoptosis in cancer. *Seminars in Cancer Biology* **35, Supplement,** S78–S103 (2015).
47. Ke, B., Tian, M., Li, J., Liu, B. & He, G. Targeting Programmed Cell Death Using Small-Molecule Compounds to Improve Potential Cancer Therapy. *Medicinal Research Reviews* (2016). doi:10.1002/med.21398

48. Fulda, S. Smac mimetics as IAP antagonists. *Seminars in Cell & Developmental Biology* **39,** 132–138 (2014).
49. Degterev, A. *et al.* Chemical inhibitor of nonapoptotic cell death with therapeutic potential for ischemic brain injury. *Nat Chem Biol* **1,** 112–119 (2005).
50. Wu, W., Liu, P. & Li, J. Necroptosis: An emerging form of programmed cell death. *Critical Reviews in Oncology/Hematology* **82,** 249–258 (2012).
51. Croker, B., John|Gerlic,Motti. Fight or flight: regulation of emergency hematopoiesis by pyroptosis and necroptosis. *Current opinion in hematology* **22,** 293–301 (2015).
52. Sun, L. *et al.* Mixed Lineage Kinase Domain-like Protein Mediates Necrosis Signaling Downstream of RIP3 Kinase. *Cell* **148,** 213–227 (2012).
53. Zhao, J. *et al.* Mixed lineage kinase domain-like is a key receptor interacting protein 3 downstream component of TNF-induced necrosis. *PNAS* **109,** 5322–5327 (2012).
54. Cai, Z. *et al.* Plasma membrane translocation of trimerized MLKL protein is required for TNF-induced necroptosis. *Nat Cell Biol* **16,** 55–65 (2014).
55. Murphy, J. M. *et al.* The pseudokinase MLKL mediates necroptosis via a molecular switch mechanism. *Immunity* **39,** 443–453 (2013).
56. Biton, S. & Ashkenazi, A. NEMO and RIP1 Control Cell Fate in Response to Extensive DNA Damage via TNF-α Feedforward Signaling. *Cell* **145,** 92–103 (2011).
57. Pasparakis, M. & Vandenabeele, P. Necroptosis and its role in inflammation. *Nature* **517,** 311–320 (2015).
58. Kaczmarek, A., Vandenabeele, P. & Krysko, D. V. Necroptosis: The Release of Damage-Associated Molecular Patterns and Its Physiological Relevance. *Immunity* **38,** 209–223 (2013).
59. Kearney, C. J. *et al.* Necroptosis suppresses inflammation via termination of TNF- or LPS-induced cytokine and chemokine production. *Cell Death Differ* (2015). doi:10.1038/cdd.2014.222
60. Lawlor, K. E. *et al.* RIPK3 promotes cell death and NLRP3 inflammasome activation in the absence of MLKL. *Nat Commun* **6,** 6282 (2015).
61. Grivennikov, S. I., Greten, F. R. & Karin, M. Immunity, Inflammation, and Cancer. *Cell* **140,** 883–899 (2010).
62. Fulda, S. The mechanism of necroptosis in normal and cancer cells. *Cancer Biology & Therapy* **14,** 999–1004 (2013).
63. Hu, X. & Xuan, Y. Bypassing cancer drug resistance by activating multiple death pathways – A proposal from the study of circumventing cancer drug resistance by induction of necroptosis. *Cancer letters* **259,** 127–137 (2008).
64. Su, Z., Yang, Z., Xie, L., DeWitt, J. P. & Chen, Y. Cancer therapy in the necroptosis era. *Cell Death Differ* **23,** 748–756 (2016).
65. Bonapace, L. *et al.* Induction of autophagy-dependent necroptosis is required for childhood acute lymphoblastic leukemia cells to overcome glucocorticoid resistance. *Journal of Clinical Investigation* **120,** 1310–1323 (2010).
66. Basit, F., Cristofanon, S. & Fulda, S. Obatoclax (GX15-070) triggers necroptosis by promoting the assembly of the necrosome on autophagosomal membranes. *Cell Death Differ* **20,** 1161–1173 (2013).
67. Urtishak, K. A. *et al.* Potent obatoclax cytotoxicity and activation of triple death mode killing across infant acute lymphoblastic leukemia. *Blood* **121,** 2689–2703 (2013).
68. Han, W. *et al.* Shikonin circumvents cancer drug resistance by induction of a necroptotic death. *Mol Cancer Ther* **6,** 1641–1649 (2007).
69. Oliver Metzig, M. *et al.* Inhibition of caspases primes colon cancer cells for 5-fluorouracil-induced TNF-α-dependent necroptosis driven by RIP1 kinase and NF-κB. *Oncogene* (2015). doi:10.1038/onc.2015.398
70. Saddoughi, S. A. *et al.* Sphingosine analogue drug FTY720 targets I2PP2A/SET and mediates lung tumour suppression via activation of PP2A-RIPK1-dependent necroptosis: Tumour necroptosis by FTY720-I2PP2A/SET binding. *EMBO Molecular Medicine* **5,** 105–121 (2013).
71. Horita, H., Frankel, A. E. & Thorburn, A. Acute Myeloid Leukemia-Targeted Toxin Activates Both Apoptotic and Necroptotic Death Mechanisms. *PLOS ONE* **3,** e3909 (2008).

72. Koo, G.-B. *et al.* Methylation-dependent loss of RIP3 expression in cancer represses programmed necrosis in response to chemotherapeutics. *Cell Res* **25,** 707–725 (2015).
73. Fukasawa, M. *et al.* Microarray analysis of promoter methylation in lung cancers. *J Hum Genet* **51,** 368–374 (2006).
74. Liu, Y. & Levine, B. Autosis and autophagic cell death: the dark side of autophagy. *Cell Death Differ* **22,** 367–376 (2015).
75. Muñoz-Pinedo, C. & Martin, S. J. Autosis: a new addition to the cell death tower of babel. *Cell Death Dis* **5,** e1319 (2014).
76. Oberst, A. *et al.* Catalytic activity of the caspase-8-FLIPL complex inhibits RIPK3-dependent necrosis. *Nature* **471,** 363–367 (2011).
77. Cook, W. D. *et al.* RIPK1- and RIPK3-induced cell death mode is determined by target availability. *Cell Death Differ* **21,** 1600–1612 (2014).
78. Nogusa, S. *et al.* RIPK3 Activates Parallel Pathways of MLKL-Driven Necroptosis and FADD-Mediated Apoptosis to Protect against Influenza A Virus. *Cell Host & Microbe* **20,** 13–24 (2016).
79. Goodall, M. L. *et al.* The Autophagy Machinery Controls Cell Death Switching between Apoptosis and Necroptosis. *Developmental Cell* **37,** 337–349 (2016).
80. Fitzwalter, B. E. & Thorburn, A. Recent insights into cell death and autophagy. *FEBS J* **282,** 4279–4288 (2015).
81. Bossen, C. *et al.* Interactions of Tumor Necrosis Factor (TNF) and TNF Receptor Family Members in the Mouse and Human. *J. Biol. Chem.* **281,** 13964–13971 (2006).
82. Watts, T. H. TNF/TNFR family members in costimulation of T cell responses. *Annu. Rev. Immunol.* **23,** 23–68 (2005).
83. Richter, C. *et al.* The Tumor Necrosis Factor Receptor Stalk Regions Define Responsiveness to Soluble versus Membrane-Bound Ligand. *Mol. Cell. Biol.* **32,** 2515–2529 (2012).
84. Lang, I. *et al.* Binding studies of TNF receptor superfamily (TNFRSF) receptors on intact cells. *J. Biol. Chem.* jbc.M115.683946 (2015). doi:10.1074/jbc.M115.683946
85. Horiuchi, T., Mitoma, H., Harashima, S., Tsukamoto, H. & Shimoda, T. Transmembrane TNF-α: structure, function and interaction with anti-TNF agents. *Rheumatology (Oxford)* **49,** 1215–1228 (2010).
86. Rossol, M. *et al.* Interaction between Transmembrane TNF and TNFR1/2 Mediates the Activation of Monocytes by Contact with T Cells. *J Immunol* **179,** 4239–4248 (2007).
87. Nguyen, D. X. & Ehrenstein, M. R. Anti-TNF drives regulatory T cell expansion by paradoxically promoting membrane TNF–TNF-RII binding in rheumatoid arthritis. *J Exp Med* **213,** 1241–1253 (2016).
88. Cabal-Hierro, L. & Lazo, P. S. Signal transduction by tumor necrosis factor receptors. *Cellular Signalling* **24,** 1297–1305 (2012).
89. Varfolomeev, E. & Vucic, D. Intracellular regulation of TNF activity in health and disease. *Cytokine* (2016). doi:10.1016/j.cyto.2016.08.035
90. Ting, A. T. & Bertrand, M. J. M. More to Life than NF-κB in TNFR1 Signaling. *Trends in Immunology* **37,** 535–545 (2016).
91. Maney, N. J., Reynolds, G., Krippner-Heidenreich, A. & Hilkens, C. M. U. Dendritic cell maturation and survival are differentially regulated by TNFR1 and TNFR2. *J. Immunol.* **193,** 4914–4923 (2014).
92. Hayden, M. S. & Ghosh, S. Signaling to NF-kappaB. *Genes Dev.* **18,** 2195–2224 (2004).
93. Christofferson, D. E., Li, Y. & Yuan, J. Control of Life-or-Death Decisions by RIP1 Kinase. *Annual Review of Physiology* **76,** 129–150 (2013).
94. Li, H., Kobayashi, M., Blonska, M., You, Y. & Lin, X. Ubiquitination of RIP is required for tumor necrosis factor alpha-induced NF-kappaB activation. *J. Biol. Chem.* **281,** 13636–13643 (2006).
95. Onizawa, M. *et al.* The ubiquitin-modifying enzyme A20 restricts ubiquitination of the kinase RIPK3 and protects cells from necroptosis. *Nat Immunol* **16,** 618–627 (2015).
96. Wagner, S. A., Satpathy, S., Beli, P. & Choudhary, C. SPATA2 links CYLD to the TNF-α receptor signaling complex and modulates the receptor signaling outcomes. *EMBO J* **35,** 1868–1884 (2016).
97. Fritsch, J. *et al.* Cell Fate Decisions Regulated by K63 Ubiquitination of Tumor Necrosis Factor Receptor 1. *Mol. Cell. Biol.* **34,** 3214–3228 (2014).

98. Yu, M., Lam, J., Rada, B., Leto, T. L. & Levine, S. J. Double-stranded RNA Induces Shedding of the Soluble 34-kDa TNFR1 from Human Airway Epithelial Cells via TLR3-TRIF-RIP1-dependent Signaling: Roles for Duox2- and Caspase-dependent Pathways. *J Immunol* **186,** 1180–1188 (2011).
99. Rowlands, D. J. *et al.* Activation of TNFR1 ectodomain shedding by mitochondrial Ca2+ determines the severity of inflammation in mouse lung microvessels. *Journal of Clinical Investigation* **121,** 1986–1999 (2011).
100. Cabal-Hierro, L. *et al.* TRAF-mediated modulation of NF-kB AND JNK Activation by TNFR2. *Cellular Signalling* **26,** 2658–2666 (2014).
101. Faustman, D. & Davis, M. TNF receptor 2 pathway: drug target for autoimmune diseases. *Nat Rev Drug Discov* **9,** 482–493 (2010).
102. Naudé, P. J. W., den Boer, J. A., Luiten, P. G. M. & Eisel, U. L. M. Tumor necrosis factor receptor cross-talk. *FEBS J.* **278,** 888–898 (2011).
103. Alvarez, S. E. *et al.* Sphingosine-1-phosphate is a missing cofactor for the E3 ubiquitin ligase TRAF2. *Nature* **465,** 1084–1088 (2010).
104. Park, E.-S. *et al.* Tumor necrosis factor (TNF) receptor-associated factor (TRAF)-interacting protein (TRIP) negatively regulates the TRAF2 ubiquitin-dependent pathway by suppressing the TRAF2-sphingosine 1-phosphate (S1P) interaction. *J. Biol. Chem.* **290,** 9660–9673 (2015).
105. Inoue, M. *et al.* Aminopeptidase P3, a new member of the TNF-TNFR2 signaling complex, induces phosphorylation of JNK1 and JNK2. *J. Cell. Sci.* **128,** 656–669 (2015).
106. Pan, S. *et al.* Etk/Bmx as a tumor necrosis factor receptor type 2-specific kinase: role in endothelial cell migration and angiogenesis. *Mol. Cell. Biol.* **22,** 7512–7523 (2002).
107. Ungewickell, A. *et al.* Genomic analysis of mycosis fungoides and Sézary syndrome identifies recurrent alterations in TNFR2. *Nat. Genet.* **47,** 1056–1060 (2015).
108. Fairfax, B. P. *et al.* A common haplotype of the TNF receptor 2 gene modulates endotoxin tolerance. *J Immunol* **186,** 3058–3065 (2011).
109. Grell, M., Zimmermann, G., Hülser, D., Pfizenmaier, K. & Scheurich, P. TNF receptors TR60 and TR80 can mediate apoptosis via induction of distinct signal pathways. *J Immunol* **153,** 1963–1972 (1994).
110. Pimentel-Muiños, F. X. & Seed, B. Regulated Commitment of TNF Receptor Signaling: A Molecular Switch for Death or Activation. *Immunity* **11,** 783–793 (1999).
111. Ramesh, G. & Reeves, W. B. TNFR2-mediated apoptosis and necrosis in cisplatin-induced acute renal failure. *American Journal of Physiology - Renal Physiology* **285,** F610–F618 (2003).
112. Ban, L. *et al.* Selective death of autoreactive T cells in human diabetes by TNF or TNF receptor 2 agonism. *PNAS* **105,** 13644–13649 (2008).
113. Weiss, T. *et al.* TNFR80-dependent enhancement of TNFR60-induced cell death is mediated by TNFR-associated factor 2 and is specific for TNFR60. *J. Immunol.* **161,** 3136–3142 (1998).
114. Weiss, T. *et al.* Enhancement of TNF receptor p60-mediated cytotoxicity by TNF receptor p80: requirement of the TNF receptor-associated factor-2 binding site. *J Immunol* **158,** 2398–2404 (1997).
115. Siegmund, D., Kums, J., Ehrenschwender, M. & Wajant, H. Activation of TNFR2 sensitizes macrophages for TNFR1-mediated necroptosis. *Cell Death Dis* **7,** e2375 (2016).
116. Cabal-Hierro, L. *et al.* A TRAF2 binding independent region of TNFR2 is responsible for TRAF2 depletion and enhancement of cytotoxicity driven by TNFR1. *Oncotarget* **5,** 224–236 (2014).
117. Grell, M. *et al.* Induction of cell death by tumour necrosis factor (TNF) receptor 2, CD40 and CD30: a role for TNF-R1 activation by endogenous membrane-anchored TNF. *EMBO J.* **18,** 3034–3043 (1999).
118. Tartaglia, L. A., Pennica, D. & Goeddel, D. V. Ligand passing: the 75-kDa tumor necrosis factor (TNF) receptor recruits TNF for signaling by the 55-kDa TNF receptor. *J. Biol. Chem.* **268,** 18542–18548 (1993).
119. Chan, F. K.-M. *et al.* A Role for Tumor Necrosis Factor Receptor-2 and Receptor-interacting Protein in Programmed Necrosis and Antiviral Responses. *J. Biol. Chem.* **278,** 51613–51621 (2003).
120. Biragyn, A. *et al.* Murine beta-defensin 2 promotes TLR-4/MyD88-mediated and NF-kappaB-dependent atypical death of APCs via activation of TNFR2. *J. Leukoc. Biol.* **83,** 998–1008 (2008).
121. Legarda, D. *et al.* CYLD Proteolysis Protects Macrophages from TNF-Mediated Auto-necroptosis Induced by LPS and Licensed by Type I IFN. *Cell Rep* **15,** 2449–2461 (2016).

122. Vanlangenakker, N., Vanden Berghe, T. & Vandenabeele, P. Many stimuli pull the necrotic trigger, an overview. *Cell Death Differ.* **19,** 75–86 (2012).
123. Bertrand, M. J. M. *et al.* cIAP1 and cIAP2 Facilitate Cancer Cell Survival by Functioning as E3 Ligases that Promote RIP1 Ubiquitination. *Molecular Cell* **30,** 689–700 (2008).
124. Riedl, S. J. *et al.* Structural Basis for the Inhibition of Caspase-3 by XIAP. *Cell* **104,** 791–800 (2001).
125. Srinivasula, S. M. *et al.* A conserved XIAP-interaction motif in caspase-9 and Smac/DIABLO regulates caspase activity and apoptosis. *Nature* **410,** 112–116 (2001).
126. Chai, J. *et al.* Structural Basis of Caspase-7 Inhibition by XIAP. *Cell* **104,** 769–780 (2001).
127. Fulda, S. Promises and Challenges of Smac Mimetics as Cancer Therapeutics. *Clin. Cancer Res.* **21,** 5030–5036 (2015).
128. Talbott, R. L. *et al.* Pharmacology of smac mimetics; chemotype differentiation based on physical association with caspase regulators and cellular transport. *Experimental Cell Research* doi:10.1016/j.yexcr.2015.08.011
129. Fulda, S. & Vucic, D. Targeting IAP proteins for therapeutic intervention in cancer. *Nat Rev Drug Discov* **11,** 109–124 (2012).
130. Silke, J. & Vaux, D. L. IAP gene deletion and conditional knockout models. *Seminars in Cell & Developmental Biology* doi:10.1016/j.semcdb.2014.12.004
131. Condon, S. M. *et al.* Birinapant, a Smac-Mimetic with Improved Tolerability for the Treatment of Solid Tumors and Hematological Malignancies. *J. Med. Chem.* **57,** 3666–3677 (2014).
132. Allensworth, J. L., Sauer, S. J., Lyerly, H. K., Morse, M. A. & Devi, G. R. Smac mimetic Birinapant induces apoptosis and enhances TRAIL potency in inflammatory breast cancer cells in an IAP-dependent and TNF-α-independent mechanism. *Breast Cancer Res. Treat.* **137,** 359–371 (2013).
133. Vince, J. E. *et al.* IAP Antagonists Target cIAP1 to Induce TNFα-Dependent Apoptosis. *Cell* **131,** 682–693 (2007).
134. Roesler, S., Eckhardt, I., Wolf, S. & Fulda, S. Cooperative TRAIL production mediates IFNα/Smac mimetic-induced cell death in TNFα-resistant solid cancer cells. *Oncotarget* (2016). doi:10.18632/oncotarget.6915
135. Benetatos, C. A. *et al.* Birinapant (TL32711), a Bivalent SMAC Mimetic, Targets TRAF2-Associated cIAPs, Abrogates TNF-Induced NF- B Activation, and Is Active in Patient-Derived Xenograft Models. *Molecular Cancer Therapeutics* **13,** 867–879 (2014).
136. Belz, K. *et al.* Smac mimetic and glucocorticoids synergize to induce apoptosis in childhood ALL by promoting ripoptosome assembly. *Blood* **124,** 240–250 (2014).
137. Weisberg, E. *et al.* Smac mimetics: implications for enhancement of targeted therapies in leukemia. *Leukemia* **24,** 2100–2109 (2010).
138. Lalaoui, N. *et al.* Targeting p38 or MK2 Enhances the Anti-Leukemic Activity of Smac-Mimetics. *Cancer Cell* **29,** 145–158 (2016).
139. Brumatti, G. *et al.* The caspase-8 inhibitor emricasan combines with the SMAC mimetic birinapant to induce necroptosis and treat acute myeloid leukemia. *Science Translational Medicine* **8,** 339ra69–339ra69 (2016).
140. Varfolomeev, E. *et al.* IAP Antagonists Induce Autoubiquitination of c-IAPs, NF-κB Activation, and TNFα-Dependent Apoptosis. *Cell* **131,** 669–681 (2007).
141. Lueck, S. C. *et al.* Smac mimetic induces cell death in a large proportion of primary acute myeloid leukemia samples, which correlates with defined molecular markers. *Oncotarget* (2016). doi:10.18632/oncotarget.10390
142. Noonan, A. M. *et al.* Pharmacodynamic markers and clinical results from the phase 2 study of the SMAC mimetic birinapant in women with relapsed platinum-resistant or -refractory epithelial ovarian cancer. *Cancer* **122,** 588–597 (2015).
143. Petersen, S. L. *et al.* Autocrine TNFα Signaling Renders Human Cancer Cells Susceptible to Smac-Mimetic-Induced Apoptosis. *Cancer Cell* **12,** 445–456 (2007).
144. Lee, E.-W. *et al.* USP11-dependent selective cIAP2 deubiquitylation and stabilization determine sensitivity to Smac mimetics. *Cell Death Differ* **22,** 1463–1476 (2015).

145. Petersen, S. L., Peyton, M., Minna, J. D. & Wang, X. Overcoming cancer cell resistance to Smac mimetic induced apoptosis by modulating cIAP-2 expression. *PNAS* **107,** 11936–11941 (2010).
146. Maas, C. *et al.* CLL cells are resistant to smac mimetics because of an inability to form a ripoptosome complex. *Cell Death Dis* **4,** e782 (2013).
147. Jansen, R., Embden, J. D. A. van, Gaastra, W. & Schouls, L. M. Identification of genes that are associated with DNA repeats in prokaryotes. *Mol. Microbiol.* **43,** 1565–1575 (2002).
148. Sander, J. D. & Joung, J. K. CRISPR-Cas systems for editing, regulating and targeting genomes. *Nat. Biotechnol.* **32,** 347–355 (2014).
149. McComb, S. *et al.* Activation of concurrent apoptosis and necroptosis by SMAC mimetics for the treatment of refractory and relapsed ALL. *Science Translational Medicine* **8,** 339ra70 (2016).
150. Bhola, P. D. *et al.* Functionally identifiable apoptosis-insensitive subpopulations determine chemoresistance in acute myeloid leukemia. *J. Clin. Invest.* **126,** 3827–3836 (2016).
151. Yeh, J. E., Toniolo, P. A. & Frank, D. A. Targeting transcription factors: promising new strategies for cancer therapy. *Curr Opin Oncol* **25,** 652–658 (2013).
152. Ott, C. J. *et al.* BET bromodomain inhibition targets both c-Myc and IL7R in high-risk acute lymphoblastic leukemia. *Blood* **120,** 2843–2852 (2012).
153. Wachter, F. *et al.* Mechanistic validation of a clinical lead stapled peptide that reactivates p53 by dual HDM2 and HDMX targeting. *Oncogene* (2016). doi:10.1038/onc.2016.361
154. Roberts, K. G. *et al.* Targetable kinase-activating lesions in Ph-like acute lymphoblastic leukemia. *N. Engl. J. Med.* **371,** 1005–1015 (2014).
155. Boutter, J. *et al.* Image-based RNA interference screening reveals an individual dependence of acute lymphoblastic leukemia on stromal cysteine support. *Oncotarget* **5,** 11501–11512 (2014).
156. Viktoras Frismantas *et al.* Ex vivo drug response profiling detects extraordinary drug activity in resistant ALL. *Submited*
157. Bornhauser, B. C. *et al.* Low-dose arsenic trioxide sensitizes glucocorticoid-resistant acute lymphoblastic leukemia cells to dexamethasone via an Akt-dependent pathway. *Blood* **110,** 2084–2091 (2007).
158. Greer, R. M. *et al.* SMAC Mimetic (JP1201) Sensitizes Non–Small Cell Lung Cancers to Multiple Chemotherapy Agents in an IAP-Dependent but TNF-α–Independent Manner. *Cancer Research* **71,** 7640–7648 (2011).
159. Eckhardt, I., Roesler, S. & Fulda, S. Identification of DR5 as a critical, NF-κB-regulated mediator of Smac-induced apoptosis. *Cell Death Dis* **4,** e936 (2013).
160. Petersen, S. L., Peyton, M., Minna, J. D. & Wang, X. Overcoming cancer cell resistance to Smac mimetic induced apoptosis by modulating cIAP-2 expression. *PNAS* **107,** 11936–11941 (2010).
161. Raulf, N. *et al.* Differential response of head and neck cancer cell lines to TRAIL or Smac mimetics is associated with the cellular levels and activity of caspase-8 and caspase-10. *Br. J. Cancer* **111,** 1955–1964 (2014).
162. Polanski, R., Vincent, J., Polanska, U. M., Petreus, T. & Tang, E. K. Y. Caspase-8 activation by TRAIL monotherapy predicts responses to IAPi and TRAIL combination treatment in breast cancer cell lines. *Cell Death Dis* **6,** e1893 (2015).
163. Differentiation Map Portal. Available at: http://portals.broadinstitute.org/dmap/home. (Accessed: 3rd October 2016)
164. Cancer Cell Line Encyclopedia. Available at: https://portals.broadinstitute.org/ccle/home. (Accessed: 3rd October 2016)
165. Kobayashi, T., Walsh, M. C. & Choi, Y. The role of TRAF6 in signal transduction and the immune response. *Microbes and Infection* **6,** 1333–1338 (2004).

Acknowledgements

The past years have been an adventure of constant learning, western blots, skiing, friendships, and political debates. I have deeply enjoyed working on this exciting project surrounded by incredible and smart people, and I have learned from every one of you.

I want to thank:

Beat, for your support and for always asking the questions I wasn't prepared for.

Jean-Pierre, for challenging me and always thinking big.

Lynn Wong, Hans-Uwe Simon, and Christian Münz, for the great discussions during the Committee meetings. Lynn, thank you for the good advice on both science and life.

Scott, for being a great teacher and for great freerides in the deep powder.

Lena, for always being there and being so cheerful; you are so wise.

Anna, for making me feel welcome since the first day and helping me through the bad times.

Yun, for always always always taking the time to help. You are the most patient person I know.

Brice, Hofy, Caterina, Blerim, Pikki, Danaëlle, Vik, Virginia, and Silvia, you make the leukemia group the best. Joana, Chiara, Dimitra, Eva, Patricia, and the rest of the people from August-Forelstrasse 1, for being great friends.

Many people have supported me and made me happy during this time (or my whole life). Nothing would be the same without you. I want to thank specially:

Albert, for coming with me to the rainiest place and for everything else. You make the funniest necroptosis jokes!

Jaume and Núria, for everything. For raising me, for teaching me to live unafraid, for taking us on so many adventures, and for never buying a tv. You are funny, smart, caring, interesting, patient, and amazing parents.

Guim, for all the fun we've had and for always putting up with my sarcasm.

Paolo, for funding a band with me, and Laura, for being such a good friend.

CURRICULUM VITAE - JÚLIA AGUADÉ GORGORIÓ

Phone: (+41) 789568446
Julia.aguade@kispi.uzh.ch
julia.aguade@gmail.com

Birthdate: August 9th 1989
Nationality: Spanish

EDUCATION

2013-2016 **Life Sciences Zurich Graduate School/Children's Hospital Zurich**, Cancer Biology PhD program, PhD Student.

2010-2011 **Eidgenössische Technische Hochschule Zürich**, Erasmus semester.

2007-2013 **University of Barcelona**, Pharmaceutical Sciences, specializing in industrial pharmacy and research. Grade point average 88%

2005-2007 **Institut d'Educació Secundària Pere Calders**, Batxillerat Científic. Grade point average 92%

2001-2002 **Velma Hamilton Middle School**, Madison (WI, USA), semester abroad.

2001-2005 **Institut d'Educació Secundària Pere Calders**, ESO.

1995-2001 **Centre d'Educació Infantil i Primària Escola Bellaterra.**

PUBLICATIONS

2016 McComb S[§], Aguadé-Gorgorió J[§], et al. Activation of concurrent apoptosis and necroptosis by SMAC mimetics for the treatment of refractory and relapsed ALL. *Science Translational Medicine*. 2016;8(339):339ra70. (Shared first author)

2016 Aguadé-Gorgorió J and Bornhauser BC. Activation of necroptosis to overcome drug resistance in leukemia. *Receptors and clinical investigation.* (In press).

2016 Dafflon C, et al. Complementary activities of DOT1L and Menin inhibitors in MLL-rearranged leukemia. *Leukemia*. (In press).

Aguadé-Gorgorió J, et al. TNFR2 is essential for RIP1-dependent cell death in refractory ALL (Manuscript in preparation)

HONORS AND AWARDS

2016 Poster prize at the 9th Swiss Apoptosis meeting.

2016 Prize for best laboratory research talk at the SPOG (Swiss Pediatric Oncology Group) Scientific Meeting

2015 Poster prize at the 6th Cancer Network Zurich Retreat.

2014 Prize for best oral presentation at the Children's Research Center Retreat.

GRANTS AND SCHOLARSHIPS

CNZ Travel Grant, February 2016. Grant given by the Cancer Network Zurich to participate in the AACR meeting 2016.

Forschungskredit, October 2014 – August 2015. Grant given by the University of Zurich to fund the doctoral studies for 11 months to perform research on the project *Exploiting alternative cell death mechanisms to overcome drug resistance in leukemia.*

Collaboration Scholarship, academic year 2011-2012. Scholarship awarded by AGAUR to collaborate with the research group Apoptosis and Cancer under tutelage of Dr. Tauler.

Student's International Mobility Scholarship, academic year 2010-2011. Scholarship awarded by AGAUR to take part of the Pharmacy studies in the ETH Zurich.

Erasmus Scholarship, academic year 2010-2011. Scholarship awarded by the Swiss Government to take part of the pharmacy studies in the ETH Zurich.

International Scholarship "Beca Internacional Bancaja", academic year 2010-2011. Scholarship awarded by banking institution 'Bancaja' to take part of the pharmacy studies in the ETH Zurich.

Ajut universitari Caixa Manresa, 2008. Award given by banking institution Caixa Manresa to the students with the best university access grades.

RESEARCH EXPERIENCE

Currently 3rd year PhD student in Dr. Bourquin's and Dr.Bornhauser's group at the Children's Hospital in Zurich. Projects: Exploiting alternative cell death mechanisms to overcome drug resistance in leukemia. Experience with xenograft mouse models, primary samples, molecular biology, and CRISPR/cas9.

Research project directed by Dr. Tauler in the department of Biochemistry and Molecular Biology (Faculty of Pharmacy, University of Barcelona) and IDIBELL (Hospitalet de Llobregat) 2011-2012. Projects: Effect of E2F1 activation on the transcription of various PP2A subunits, effect of E2F1 activation on autophagy.

LANGUAGES

Catalan: native language
Spanish: native language
English: TOEFL score 111
German: holds a CEFR B2 certificate. First year of C1 level course passed.

OTHER

Animal experimentation permit: FELASA category B for mice and rats.

Musical studies of violin and double bass.

Manuscripts

Manuscript 1

Activation of concurrent apoptosis and necroptosis by SMAC mimetics for the treatment of refractory and relapsed ALL

Manuscript 2

TNFR2 is essential for RIP1-dependent cell death in refractory ALL

Title: Activation of concurrent apoptosis and necroptosis by SMAC mimetics for the treatment of refractory and relapsed ALL

Authors: Scott McComb[1,§], Júlia Aguadé-Gorgorió[1,§], Lena Harder[1], Blerim Marovca[1], Gunnar Cario[2], Cornelia Eckert[3], Martin Schrappe[2], Martin Stanulla[4], Arend von Stackelberg[3], Jean-Pierre Bourquin[1,§], Beat C. Bornhauser[1,§,*]

Affiliations:

[1]Department of Oncology and Children's Research Centre, University Children's Hospital Zürich, 8032 Zürich, Switzerland

[2]Department of General Pediatrics, University Hospital Schleswig-Holstein, 24105 Kiel, Germany

[3]Department of Pediatric Oncology/Hematology, Charité Medical University Berlin, 13353 Berlin, Germany

[4]Pediatric Hematology and Oncology, Hannover Medical School, 30625 Hannover, Germany

*Correspondence to: Beat Bornhauser, University Children's Hospital Zurich, August-Forelstrasse 1, CH-8008 Zurich, beat.bornhauser@kispi.uzh.ch, Phone, +41 44 634 8817; Fax, +41 44 634 88 59

[§]These authors contributed equally to this manuscript

One Sentence Summary: *Ex vivo* drug profiling identifies strong anti-leukemic activity of SMAC mimetics through simultaneous activation of two different cell death pathways, apoptosis and necroptosis, in resistant ALL.

Abstract: More precise treatment strategies are urgently needed to decrease toxicity and improve outcomes for treatment-refractory leukemia. We used ex vivo drug response profiling of high risk, relapsed, or refractory acute lymphoblastic leukemia (ALL) cases and identified a subset with exquisite sensitivity to small molecule mimetics of the mitochondrial protein SMAC (SMAC mimetics, SM). Potent ex vivo activity of the SM birinapant correlated with dramatic in vivo anti-leukemic effects, as indicated by delayed engraftment, decreased leukemia burden, and prolonged survival of xenografted mice. Anti-leukemic activity was dependent on simultaneous execution of apoptosis and necroptosis, as demonstrated by functional genomic dissection with a multi-colored lentiCRISPR approach to simultaneously disrupt multiple genes in patient-derived ALL. SM specifically targeted RIP1-dependent death, and CRISPR-mediated disruption of RIP1 completely blocked SM-induced death yet had no impact on the response to standard anti-leukemic agents. Thus, SM compounds such as birinapant circumvent escape from apoptosis in leukemia by activating a potent dual RIP1-dependent apoptotic and necroptotic cell death, which is not exploited by current therapy. Ex vivo drug activity profiling could provide important functional diagnostic information to identify patients who may benefit from targeted treatment with birinapant in early clinical trials.

Main Text:

Introduction

Despite aggressive application of targeted chemotherapy, acute lymphoblastic leukemia (ALL) patients with persistent minimal residual disease (MRD), drug refractory, and/or relapsed disease still have a poor prognosis *(1, 2)* . With increasing knowledge of the genomic landscape of ALL, disease-specific oncogenic lesions amenable to personalized treatment approaches are increasingly identifiable *(3)*. Nonetheless, the efficacy of such targeted agents can be undermined by general deregulation of cell death pathways. Indeed, failure to undergo chemotherapy-induced apoptosis constitutes a key mechanism for drug resistance and clonal escape *(4)*. Thus, alternative strategies to reactivate cell death pathways are being actively pursued, but as of yet none have reached wide clinical application *(5, 6)*.

The cellular inhibitor of apoptosis proteins (IAPs: cIAP1, cIAP2, and XIAP) are often overexpressed in cancer and contribute to drug resistance *(7, 8)*. IAPs inhibit programmed cell death through a number of mechanisms, including direct inhibition of caspases *(9)* and ubiquitination of receptor-interacting protein kinase 1 (RIP1) *(10)*. Whereas RIP1 can act as a potent activator of multiple forms of programmed cell death *(11)*, its ubiquitination by cIAPs mediates pro-inflammatory signaling via NF-κB *(10, 12)*, and RIP1 can flip roles to become an inhibitor of apoptotic and necroptotic cell death *(13–15)*. Thus, RIP1 acts as a key convergence point between pro-death, pro-survival, and pro-inflammatory signals, as detailed in a number of recent reviews *(16–18)*. To short-circuit the ability of cIAPs to rewire pro-death into pro-survival signals, small molecule peptidomimetics of the secondary mitochondria-derived activator of caspases (SMAC) have been developed. These SMAC mimetics (SM) promote cell death through inhibition of IAP proteins *(19, 20)*. SM compounds have been demonstrated to induce degradation and direct inhibition of IAP proteins and drive cell death as single agents in a number of cancer cell lines *(21, 22)*. The potential for application of promising SM compounds in leukemia has yet to be fully examined.

Herein we show that a subset of ALL samples exhibits high sensitivity to SM-induced cell death in vitro and in vivo, with IC50 values below 100 nM. We use CRISPR-based genetic disruptions and pharmacologic interference to show that SM induces simultaneous activation of RIP1-mediated apoptosis and necroptosis in a manner not similarly exploited by current chemotherapeutic drugs. Our data provide strong evidence for high anti-leukemic activity of SM in relapsed ALL and suggest functional drug response profiling as a tool to identify those patients who are most likely to benefit from SM treatment. Such ex vivo drug profiling could be applied to improve personalized treatment decisions for individual patients as we recently showed for the BCL-2 inhibitor venetoclax in TCF3-HLF positive ALL *(23)*.

Results

Drug profiling identifies ALL with high sensitivity to SMAC mimetics

Given our previous identification of RIP1-dependent necroptosis as a mechanism to overcome drug resistance in ALL *(24)*, we were interested in investigating additional drugs that could activate RIP1-dependent cell death. On the basis of promising SM activity in a large scale ALL drug-screening platform previously described *(23, 25)*, we performed focused testing of SM response on a set of 51 patient-derived B cell precursor ALL xenografts enriched for samples from relapsed and drug-resistant disease (table S1A,B). ALL xenografts retain important genotypic, clonotypic, and phenotypic characteristics of primary patient samples and thus constitute a logical model to investigate refractory disease *(26, 27)*. Response to the bivalent SM compound birinapant varied greatly, with IC50 values in the low nanomolar range (<250 nM) in 17 of 51 cases (**Fig. 1**A). No toxicity was observed towards non-tumorigenic mesenchymal stromal support cells used in this co-culture assay, suggesting the existence of a therapeutic window (fig. S1A, B).Samples from high-risk or relapsed patients (labeled as very high risk, VHR; high risk, HR, or relapse, R) were among highly birinapant-sensitive cases. Similar response profiles were found for the monovalent SM compound, LCL-161 *(6)*, although with reduced potency (fig. S1C). In addition, cases with moderate sensitivity to SM were also detected in T-cell ALL (fig. S1D).

We next evaluated the anti-leukemic activity of SM in vivo using xenografted mice. Birinapant treatment initiated shortly after ALL transplantation delayed disease progression in three cases identified as highly SM-sensitive (**Fig. 1**B-D). Complete responses, as defined by the absence of leukemic cells within the blood detectable by flow cytometry, could also be achieved in these three cases when birinapant treatment was initiated after more than 30% leukemic engraftment (**Fig. 1**E-G), which corresponds to extensive extramedullary and complete bone marrow involvement. Treatment rapidly decreased the leukemic load in peripheral blood (**Fig. 1**E-G) and significantly delayed disease progression to experimental endpoints (**Fig. 1**H-J). In vivo efficacy of birinapant in delaying progression was less pronounced in two samples with lower SM sensitivity in vitro (**Fig. 1**K-P). Of note, we did not detect in vivo activity of LCL161 in 2 highly sensitive patient samples, perhaps because of the lower potency of LCL161 (fig. S1E-J). Thus, our in vitro drug profiling identified a subset of primary ALL samples with high ex vivo SM sensitivity (IC50<250 nM for 17 of 51 primary ALL samples tested), which predicted anti-leukemic efficacy in vivo in the xenograft model.

SM treatment induces varying activation of both apoptosis and necroptosis

To analyze the mechanism by which SM compounds induce cell death, we examined SM dose response curves of SM-sensitive patient samples in the presence of pharmacological inhibitors of apoptosis (pan-caspase inhibitor zVAD) and/or necroptosis (RIP1- kinase inhibitor necrostatin-1, nec). Initial experiments in two highly birinapant-sensitive leukemic samples showed that rescue from

SM-induced cell death varied greatly between patient samples. Specifically, R-03 cells required simultaneous application of zVAD and necrostatin for rescue from birinapant (**Fig. 2**A) whereas VHR-10 cells showed no significant rescue with the addition of both death inhibitors (**Fig. 2**B). To further investigate the heterogeneity of birinapant response, we screened a larger cohort of patient samples using these death inhibitors. The contribution of apoptosis and/or necroptosis varied greatly among patient samples (**Fig. 2**A-J), revealing the following death phenotypes: necroptotic samples were rescued by nec alone (**Fig. 2**C,D), mixed death phenotype samples were rescued only by a combination of zVAD and nec (**Fig. 2**E), and some samples were not rescued by any combination of inhibitors (**Fig. 2**F). None of the samples tested showed a purely apoptotic phenotype, and inhibition of RIP1 kinase with necrostatin alone actually decreased cell viability in a small number of cases, which was not subsequently rescued by zVAD (**Fig. 2**F). Similar cell death patterns were detected for birinapant and LCL161 (**Fig. 2**G-J). Taken together, these data indicate that SM treatment induces variable activation of apoptotic and necroptotic cell death in SM-sensitive patient samples.

Differential expression of TNFα, RIP1, RIP3, or IAPs does not predict SM response

SM treatment-induced expression of TNFα is an important driver of SM-induced cell death. To investigate the role of TNFα expression in the response to SM, we performed a qPCR analysis of *TNFα* mRNA with and without birinapant treatment in 16 patient samples. There was no significant difference in the expression of TNFα in samples with high or low sensitivity to birinapant, and an increase in TNFα expression upon birinapant treatment for 6 h could only be detected in two out of the 16 cases tested (**Fig. 3**A, median increase of 1.156 fold and 0.9475 fold, respectively). We also did not observe significant phosphorylation of p65, a marker for canonical NF-κB activation by TNFα, after SM treatment in SM-sensitive cells (**Fig. 3**B). Blocking TNFα signaling with a specific blocking antibody only partially decreased the response to SM in sensitive cells (**Fig. 3**C). In contrast, TNFα blockade was highly effective in a control experiment using a patient sample that only became SM-responsive when exogenous TNFα ligand was added (fig. S2A). Overall, these data indicate that ALL responsiveness to SM is not determined by differential TNFα expression, and seems only partly dependent on ligand signaling.

We next tested whether varying expression of key players of the apoptotic and necroptotic response might explain differential response to SM in patient samples. By western blot, we observed no consistent correlation of cIAP1, cIAP2, XIAP, caspase-8, FADD, RIP3, MLKL, or RIP1 protein expression with sensitivity to SM (**Fig. 3**D). Furthermore, SM treatment induced efficient degradation of cIAP1 in both sensitive and non-sensitive samples (fig. S2B). These data indicate that neither differential expression of mediators of the apoptotic and/or necroptotic death programs nor SM-induced degradation of cIAP1 correlate with response to SM in primary ALL.

RIP1 drives concurrent SM-induced apoptosis and necroptosis

In leukemic cell lines, only moderate response to single agent birinapant was detected in 2 of 5 cell lines tested (**Fig. 4**A). Consistent with previous observations in other cell lines *(21, 28)*, addition of TNFα greatly sensitized the majority of ALL cell lines to SM (**Fig. 4**B). In contrast to patient-derived cells, apoptotic responses predominated in cell lines, with only Jurkat cells recapitulating a mixed death phenotype (**Fig. 4**C). This mixed cell death phenotype does not appear to be driven by underlying clonal differences within the population, because a single cell clone line of Jurkat cells responded with similarly mixed cell death (fig. S3A). Thus, rather than consisting of different populations that respond by either necroptosis or apoptosis, we observe Jurkat cells to activate apoptosis and necroptosis simultaneously (fig S3B,C).

To explore the genetic pathways involved in the response to SM we have adapted a lentiCRISPR gene disruption approach *(29, 30)*. Using FACS sorting of cells transduced with fluorescently labelled lentiCRISPR vectors, we were able to disrupt single or multiple genes simultaneously without single cell cloning steps (fig. S3D). To assess the role of RIP1 in the response to SM, we first targeted RIP1 for genetic disruption in four leukemic cell lines (**Fig. 4**D). Loss of RIP1 resulted in a potent rescue from SM-induced cell death in both partially SM-sensitive (**Fig. 4**E,F), and SM/TNFα-sensitive cell lines independently of the mode of cell death (**Fig. 4**G-J). Consistent with previous reports *(31)*, loss of RIP1 did not inhibit moderate cell killing by TNFα alone (**Fig. 4**H,J). These results show that SM-induced death is strictly dependent on RIP1 function.

To dissect the mediators of apoptosis and necroptosis downstream of RIP1, we disrupted apoptotic mediators (FADD or Casp8), necroptotic mediators (RIP3 or MLKL), or a combination thereof in Jurkat cells. Sorting of multi-color lentiCRISPR cell subsets yielded single and double knockout cell lines with no need for single cell cloning (**Fig. 4**K). Targeted disruption of apoptotic (**Fig. 4**L) or necroptotic mediators (**Fig. 4**M) resulted in little or no rescue of cell death. Only combined disruption of both apoptosis and necroptosis significantly blocked response to SM treatment (**Fig. 4**N,O). Combined pharmacological inhibition and genetic disruption also confirmed that cells fully switch to the alternative pathway when a single pathway is inhibited (**Fig. 4**P and fig. S3E). In the leukemic cell lines observed above to be apoptotic (658w, Nalm6, and CEM-C7), SM-induced death was rescued completely by disruption of a single apoptosis gene (fig. S3F). Western blotting shows that these apoptotic leukemia cell lines lack RIP3 expression, whereas the amounts of RIP1, CASP8, FADD, and MLKL were similar compared to the mixed phenotype Jurkat cells, explaining the lack of necroptosis observed within these cells (fig. S3G). Thus, functional dissection using lentiCRISPR reveals genetic requirements for distinct death phenotypes in ALL and supports the notion that SM can drive activation of RIP1-dependent apoptotic and necroptotic cell death.

To validate RIP1 as the mediator of SM-induced cell death in vivo, we next transduced primary SM-sensitive ALL samples with lentiCRISPR targeting RIP1 (LC-EGFP-RIP1). After engraftment, we detected a consistent subpopulation of LC-EGFP-RIP1+ cells not present in untransduced controls

(**Fig. 5**A). Western blotting shows that EGFP$^+$ cells have a clear decrease of RIP1 expression relative to EGFP$^-$ and untransduced control cells after sorting (**Fig. 5**B *left*). The proportion of EGFP$^+$/RIP1-disrupted cells remained stable during engraftment, indicating that similar to leukemic cell lines, RIP1 loss does not confer a growth disadvantage for these leukemia subtypes (**Fig.** 5A-C and fig. S4A). This is in contrast to previous observations in normal bone marrow, where RIP1 deficiency can cause bone marrow failure *(32)*.

As hypothesized, birinapant treatment resulted in a selective expansion of the EGFP$^+$/RIP1-deficient hCD19$^+$ leukemic cells (**Fig. 5**A-C). Similar expansion of EGFP$^+$/RIP1-deficient cells after SM treatment was observed in 7 SM-sensitive patient samples (**Fig. 5**A-K). After birinapant treatment, both EGFP-positive and EGFP-negative subpopulations exhibited loss of RIP1 (**Fig. 5**B,E), likely because of the low EGFP expression in some cells, and we were able to detect integrated RIP1-specific sgRNA in EGFP$^-$ cells after birinapant treatment (fig. S4B). We also confirmed that there was no loss of RIP1 after treatment of untransduced patient cells (fig. S4C). Overall, these results show that RIP1 expression is not required for leukemic propagation and is essential for SM-induced death in vivo.

We next recapitulated our double knockout experiments to demonstrate parallel induction of apoptosis and necroptosis in vivo. Colored lentiCRISPR constructs targeting key mediators of both pathways (LC-EGFP-RIP3, LC-mCherry-MLKL, LC-BFP-FADD, LC-RFP657-Casp8) were transduced into an SM-sensitive ALL xenograft (R-03). At 39 days after injection of transduced cells, we detected subpopulations of all expected cell types, with the curious exception of LC-RFP657-Casp8 (**Fig. 5**L,M and S4D,E). Double-positive cells bearing lentiCRISPRs targeting apoptotic and necroptotic genes (RIP3/FADD or MLKL/FADD) were initially extremely rare, but expanded after SM treatment (**Fig. 5**L-N). In contrast, cells with single knockout or double knockout for two necroptosis genes (LC-EGFP-RIP3$^+$/LC-mCherry-MLKL$^+$) showed marginal or no outgrowth after treatment (**Fig. 5**L-N). Control cells with non-targeted lentiCRISPRs also exhibited no selection after treatment (fig. S4F). To confirm genetic disruption in double and quadruple knockout cells, we isolated cells from the spleen, sorted and expanded them by xenografting, and found that the cells showed the expected loss of protein expression and presence of sgRNA sequences (**Fig. 5**O and fig. S4G). In addition, xenografts with targeted disruption of MLKL/FADD, RIP3/FADD or MLKL/RIP3/FADD/CASP8 showed significantly decreased responses to birinapant in vitro, whereas sorted WT cells showed a response similar to untransduced control cells (**Fig.** 5P). These results provide a proof of concept that multi-colored lentiCRISPR gene targeting can be used for focused in vivo dissection of signaling pathways directly in primary patient cells, and offer an alternative to established functional genomic strategies *(33)*.

RIP1 cell death pathways are not exploited by standard anti-leukemic therapies

Having generated RIP1-deficient patient-derived ALL samples (fig. S5A), we next compared the in vitro drug response in WT and RIP1-deficient cells derived from two steroid-resistant high-risk samples and one steroid-sensitive standard risk sample. In a panel of 14 anti-leukemic drugs we observed a more than 50 fold increase in the IC50 of RIP1-deficient cells for birinapant and LCL161 (**Fig. 6**A), but not for front-line anti-leukemic drugs dexamethasone, cytarabine, bortezomib, or preclinical compounds ABT-199 or JQ-1 (**Fig. 6**B-D and fig. S5B,C). In contrast to reports implicating RIP1-dependent signaling in the response to DNA-damaging agents such as vincristine, doxorubicin, or etoposide *(34)*, loss of RIP1 in primary ALL samples did not affect response to these drugs (**Fig. 6**B). We also observed mostly unchanged sensitivity to a wider panel of chemotherapeutic drugs in the 658w-LC-EGFP-RIP1 patient-derived leukemic cell line that we generated as above (fig. S5D). RIP1-deficient 658w cells showed a somewhat attenuated response to some drugs, in particular to obatoclax, but this was not seen in primary patient cells. Overall, these data indicate that RIP1-dependent death is not exploited by standard chemotherapeutics, identifying a distinct vulnerability targeted by SM in refractory and relapsed ALL.

Discussion

There is an urgent need for the development of new treatment approaches for patients with relapsed ALL who do not respond to current therapy *(35)*. To date, only a few second-line drugs are available for salvage treatment of chemoresistant disease. Herein, we have shown that birinapant, a SMAC mimetic compound currently in phase II clinical trials for application in various solid and hematological malignancies *(20)*, induces potent leukemic cell death through parallel activation of RIP1-dependent apoptosis and necroptosis (**Fig. 5**D), and has strong anti-leukemic efficacy in vivo in a subset of primary ALL, including cases with relapsed and refractory disease.

To dissect the signaling pathway underlying the anti-leukemic potency of birinapant, we have adapted a lentiCRISPR gene disruption approach previously used for large-scale screening of knockout cell lines and tumor modelling in mice *(29, 30)*. We provide proof of concept that multi-colored lentiCRISPRs can be applied for genetic dissection in vitro and in vivo directly in primary human cancer. Given recent improvements in humanized mouse models for studying human disease *(36)*, the development of multi-colored CRISPR-Cas9 lentiviral constructs provides an alternative to previously established in vivo functional genomic strategies *(33, 37, 38)* with specific focus on dissecting the complex interaction of several genes which contribute to a specific phenotype. Our demonstration that simultaneous disruption of two distinct cell death pathways downstream of RIP1 is necessary to block SMAC mimetic response underlines the power of this approach for disentangling genetic redundancy.

The ability of SM-treated ALL cells to switch between apoptotic and necroptotic programmed cell death is reminiscent of parallel pathways of death previously observed in T cell expansion and

contraction *(39)*, suggesting that engaging both death pathways could represent a distinct vulnerability in lymphoid malignancies. Indeed, such dual death activation could circumvent clonal escape, a driver of drug resistance *(8, 40)* from either death mechanism. We consistently detected a contribution of the necroptotic pathway to SM-induced cell death in primary patient material, with no sample undergoing a purely apoptotic cell death, supporting the notion that the necroptotic pathway may constitute a particular Achilles' heel for targeted therapy in refractory disease *(24)*. Upstream of this dual death activation, our data pinpoint RIP1 as the critical target of SM-induced cell death. RIP1-deficient ALL displayed no defect in the response to several front line chemotherapeutic agents, providing a strong argument that RIP1 deficiency is unlikely to be selected for in resistant cases that have been subjected to multiple rounds of chemotherapy. Consistent with this, we observed no consistent variation in the expression of RIP1 within patient-derived samples. Our finding that RIP1-deficient cells show normal sensitivity to DNA-damaging agents (doxorubicin and etoposide) is in stark contrast to a number of reports detailing activation of the cytosolic RIP1-dependent ripoptosome complex in response to DNA damage in other cancer cell line models *(34, 41, 42)*. The reason for this discrepancy is not readily clear, but could perhaps be ascribed to cell type differences, because previous studies used cell lines derived from solid tumor models. Strategies to combine SM with RIP1-activating immunostimulatory agents such as IFN *(43, 44)* or PAMPs *(45)* may be highly effective, as has recently been demonstrated using oncolytic viruses or immunostimulatory agents in breast cancer xenografts *(46)*.

Immunodeficient mice used for xenografts of primary human ALL lack a functional immune system. In this setting, the influence of functional immune cells cannot be studied. At this point in time, there are no syngeneic mouse models available to model drug-resistant or relapsed ALL. As for many other preclinical studies of this kind, the potential of new agents can ultimately only be assessed in appropriately planned clinical trials. The importance of the IAPs as chemotherapeutic targets has long been recognized *(47)*, but potential toxicity and low single-agent efficacy of monovalent SM compounds have so far hindered their clinical application *(19, 48)*.

Our data imply that strong anti-leukemic activity of SM will depend on adequate selection of SM-sensitive ALL patients. Despite the clear implication of RIP1 and its downstream mediators in the leukemic response to SM, expression of these proteins is not predictive of SM sensitivity. Although extended genetic and functional screening may yet reveal predictive markers of SM response, our results thus far highlight the need for alternative means to identify sensitive patients. Ex vivo drug response profiling could provide an important functional layer of information for clinical application of SM treatment. Similar approaches are increasingly being incorporated into diagnostic work-flows to identify candidate drugs for the treatment of relevant patient groups *(23, 49, 50)*.

Taken together, our results provide a rationale for the further development of birinapant and other SM compounds for experimental therapy in high-risk and relapsed ALL. The fact that these agents trigger

a potent dual activation of both apoptosis and necroptosis, which is not exploited by contemporary chemotherapy, provides a strong argument to evaluate SM compounds for personalized treatment of refractory and relapsed ALL patients.

Materials and Methods

Study design:

The goal of this study was to assess the anti-leukemic potential of SMAC mimetics in drug-resistant and relapsed ALL ex vivo and in vivo, based on the initial finding of specific anti-leukemic activity of SMAC mimetics against primary ALL samples. Furthermore, we aimed to delineate the mode of action on a molecular level, and to identify the key players that control and mediate SM-induced cell death. To achieve this, we used in vivo anti-leukemic activity assays in xenograft models and developed a CRISPR-based genome editing methodology that allowed simultaneous disruption of several candidate genes in primary human tumor samples. Sample sizes were chosen based on previous experience that included statistical evaluation.

Human samples:

Xenografts were obtained from primary human ALL samples recovered from cryopreserved bone marrow aspirates of patients enrolled in the ALL-BFM 2000, 2009, and ALL-REZ-BFM 2002 studies. Informed consent was given in accordance with the Declaration of Helsinki, and approval was granted by the ethics commission of the Kanton Zurich (approval number 2014-0383). Samples were classified as standard risk (SR), medium risk (MR), high risk (HR), very high risk (VHR), morphological non-responders (MNR), or relapse samples (R) according to the clinical criteria used in the ALL-BFM 2000 study *(24, 26)*.

LentiCRISPR:

Multi-colored LentiCRISPR plasmids were derived from the LentiCRISPR v1 plasmid (Addgene Cat# 49535) *(29)*. Puromycin resistance cassette was removed using NheI and MluI restriction enzymes, and plasmids were cloned with fluorescent EGFP, TagBFP (Addgene Cat#44247), mCherry, or RFP657 (Addgene Cat#31959) sequences by standard restriction cloning technique.

Cloning of sgRNA into lentiCRISPR plasmids was performed with a single-tube restriction and ligation protocol (see Supplementary Methods).

A number of sgRNA sequences were screened for gene disruption activity in cell lines using western blotting, and the most effective were chosen for further experiments. The specific sgRNAs used are listed in supplementary table 2.

Drugs and chemicals:

Recombinant human TNFα was purchased from Gibco/Life Technologies (Cat# PHC3011), TNFα neutralizing antibody was purchased from Cell Signaling (Cat# 7321), birinapant (TL32711) was purchased from Selleckchem (Cat# S7015) for in vitro studies and from ChemieTek (Cat# CT-Biri) for in vivo studies, Z-VAD-FMK was purchased from Apex BIO (Cat# A1902), Necrostatin-1s was purchased from BioVision (Cat# 2263-1), and LCL-161 from Novartis.

For live cell microscopy, Jurkat cells were treated as indicated and stained directly with propidium iodide and CellEvent Caspase-3/7 substrate (Life Technologies, Cat# C10423) for 30 min. Live microscopy was then performed using Zeiss Axio Observer fluorescence microscope under cell culture conditions (37°C and 0.5% CO_2) to track changes in cell viability over time.

Biochemical assays:

Complete methods for in vitro viability measurement, western blotting, and FACS staining are provided in the supplementary methods section.

In vivo experiments:

10^6 patient-derived ALL cells were transplanted intravenously into immunodeficient NOD/SCID/IL2rγ^{null} (NSG) mice. For in vivo experiments, birinapant was dissolved in 12% Captisol (Ligand Pharmaceuticals) with 0.1% Tris at pH 6.8. Birinapant was given daily by intraperitoneal injection at 30 mg/kg during the indicated periods. The leukemic engraftment was measured weekly by FACS quantification of human leukemic cells in peripheral blood after red blood cell lysis and staining with hCD19-PE-Cy7 (Biolegend, Cat# 302208), hCD45-Alexa Fluor 647 (Biolegend, Cat# 304018), and mCD45-eFluor 450 (eBioscience, Cat# 48-0451-82). Age and sex matched animals were assigned randomly to the treatment or vehicle groups. Results were derived from direct analysis of leukemic engraftment in blood and thus no blinding was necessary. Animal sample sizes were chosen to minimize the number of animals used, because inter-animal variation in leukemic engraftment was generally low. No animals were excluded from analysis. In vivo experiments were approved by the veterinary office of the Canton of Zurich.

For LentiCRISPR gene disruption in patient-derived xenografts, cells were placed in monoculture in RPMI + 10% FBS and incubated at 37 ºC for 24 hours. Cells were then exposed to high titer LentiCRISPR vector (MOI≥1) in the presence of 10 ng/mL polybrene. After 24-48 hours, cells were washed 3 times with PBS and injected directly into NSG mice. Mice were then bled and the blood examined at varying time points for expression of hCD19 and appropriate fluorescent markers.

Statistics: For in vivo birinapant treatment experiments, the significance of divergence of survival curves was determined by Kaplan-Meier survival analysis and Mantel-Cox test. For in vitro analyses,

we used student's t test to detect significant divergence between test conditions. Statistical analysis was performed using GraphPad Prism 5 software package.

Supplementary materials

Supplementary Materials and Methods

Fig. S1. ALL patient samples are sensitive to LCL161 in vitro but not in vivo.

Fig. S2. TNF blocking effectively rescues TNF-dependent sensitization to birinapant.

Fig. S3. Birinapant induces dual activation of apoptosis and necroptosis in ALL cell lines.

Fig. S4. In vivo birinapant treatment selects strongly for CRISPR driven RIP1-deficient cells. Fig. S5. RIP1 is not required for response to a wide range of chemotherapeutic agents.

Table S1. Patient characteristics

Table S2. sgRNA targeting sequences utilized for gene disruptions

References and Notes:

1. F. Locatelli, M. Schrappe, M. E. Bernardo, S. Rutella, How I treat relapsed childhood acute lymphoblastic leukemia, *Blood* **120**, 2807–2816 (2012).

2. E. Curran, W. Stock, How I Treat: Acute Lymphoblastic Leukemia in Older Adolescents and Young Adults (AYAs), *Blood* , blood–2014–11–551481 (2015).

3. C. G. Mullighan, Genomic Characterization of Childhood Acute Lymphoblastic Leukemia, *Semin. Hematol.* **50**, 314–324 (2013).

4. S. Fulda, Tumor resistance to apoptosis, *Int. J. Cancer* **124**, 511–515 (2009).

5. P. E. Czabotar, G. Lessene, A. Strasser, J. M. Adams, Control of apoptosis by the BCL-2 protein family: implications for physiology and therapy, *Nat. Rev. Mol. Cell Biol.* **15**, 49–63 (2014).

6. S. Fulda, D. Vucic, Targeting IAP proteins for therapeutic intervention in cancer, *Nat. Rev. Drug Discov.* **11**, 109–124 (2012).

7. E. C. LaCasse, D. J. Mahoney, H. H. Cheung, S. Plenchette, S. Baird, R. G. Korneluk, IAP-targeted therapies for cancer, *Oncogene* **27**, 6252–6275 (2008).

8. C. Holohan, S. Van Schaeybroeck, D. B. Longley, P. G. Johnston, Cancer drug resistance: an evolving paradigm, *Nat. Rev. Cancer* **13**, 714–726 (2013).

9. Y. Suzuki, Y. Nakabayashi, K. Nakata, J. C. Reed, R. Takahashi, X-linked Inhibitor of Apoptosis Protein (XIAP) Inhibits Caspase-3 and -7 in Distinct Modes, *J. Biol. Chem.* **276**, 27058 –27063 (2001).

10. M. J. M. Bertrand, S. Milutinovic, K. M. Dickson, W. C. Ho, A. Boudreault, J. Durkin, J. W. Gillard, J. B. Jaquith, S. J. Morris, P. A. Barker, cIAP1 and cIAP2 Facilitate Cancer Cell Survival by Functioning as E3 Ligases that Promote RIP1 Ubiquitination, *Mol. Cell* **30**, 689–700 (2008).

11. J. Silke, J. A. Rickard, M. Gerlic, The diverse role of RIP kinases in necroptosis and inflammation, *Nat. Immunol.* **16**, 689–697 (2015).

12. D. J. Mahoney, H. H. Cheung, R. L. Mrad, S. Plenchette, C. Simard, E. Enwere, V. Arora, T. W. Mak, E. C. Lacasse, J. Waring, R. G. Korneluk, Both cIAP1 and cIAP2 regulate TNFα-mediated NF-κB activation, *Proc. Natl. Acad. Sci.* **105**, 11778–11783 (2008).

13. R. Weinlich, D. R. Green, The Two Faces of Receptor Interacting Protein Kinase-1, *Mol. Cell* **56**, 469–480 (2014).

14. C. P. Dillon, R. Weinlich, D. A. Rodriguez, J. G. Cripps, G. Quarato, P. Gurung, K. C. Verbist, T. L. Brewer, F. Llambi, Y.-N. Gong, L. J. Janke, M. A. Kelliher, T.-D. Kanneganti, D. R. Green, RIPK1 blocks early postnatal lethality mediated by caspase-8 and RIPK3, *Cell* **157**, 1189–1202 (2014).

15. W. J. Kaiser, L. P. Daley-Bauer, R. J. Thapa, P. Mandal, S. B. Berger, C. Huang, A. Sundararajan, H. Guo, L. Roback, S. H. Speck, J. Bertin, P. J. Gough, S. Balachandran, E. S. Mocarski, RIP1

suppresses innate immune necrotic as well as apoptotic cell death during mammalian parturition, *Proc. Natl. Acad. Sci.* **111**, 7753–7758 (2014).

16. D. Ofengeim, J. Yuan, Regulation of RIP1 kinase signaling at the crossroads of inflammation and cell death, *Nat. Rev. Mol. Cell Biol.* **14**, 727–736 (2013).

17. D. E. Christofferson, Y. Li, J. Yuan, Control of Life-or-Death Decisions by RIP1 Kinase, *Annu. Rev. Physiol.* **76**, 129–150 (2014).

18. M. Pasparakis, P. Vandenabeele, Necroptosis and its role in inflammation, *Nature* **517**, 311–320 (2015).

19. L. Bai, D. C. Smith, S. Wang, Small-molecule SMAC mimetics as new cancer therapeutics, *Pharmacol. Ther.* **144**, 82–95 (2014).

20. S. Fulda, Promises and Challenges of Smac Mimetics as Cancer Therapeutics, *Clin. Cancer Res. Off. J. Am. Assoc. Cancer Res.* **21**, 5030–5036 (2015).

21. J. E. Vince, W. W.-L. Wong, N. Khan, R. Feltham, D. Chau, A. U. Ahmed, C. A. Benetatos, S. K. Chunduru, S. M. Condon, M. McKinlay, R. Brink, M. Leverkus, V. Tergaonkar, P. Schneider, B. A. Callus, F. Koentgen, D. L. Vaux, J. Silke, IAP Antagonists Target cIAP1 to Induce TNFα-Dependent Apoptosis, *Cell* **131**, 682–693 (2007).

22. E. Varfolomeev, J. W. Blankenship, S. M. Wayson, A. V. Fedorova, N. Kayagaki, P. Garg, K. Zobel, J. N. Dynek, L. O. Elliott, H. J. A. Wallweber, J. A. Flygare, W. J. Fairbrother, K. Deshayes, V. M. Dixit, D. Vucic, IAP Antagonists Induce Autoubiquitination of c-IAPs, NF-[kappa]B Activation, and TNF[alpha]-Dependent Apoptosis, *Cell* **131**, 669–681 (2007).

23. U. Fischer, M. Forster, A. Rinaldi, T. Risch, S. Sungalee, H.-J. Warnatz, B. Bornhauser, M. Gombert, C. Kratsch, A. M. Stütz, M. Sultan, J. Tchinda, C. L. Worth, V. Amstislavskiy, N. Badarinarayan, A. Baruchel, T. Bartram, G. Basso, C. Canpolat, G. Cario, H. Cavé, D. Dakaj, M. Delorenzi, M. P. Dobay, C. Eckert, E. Ellinghaus, S. Eugster, V. Frismantas, S. Ginzel, O. A. Haas, O. Heidenreich, G. Hemmrich-Stanisak, K. Hezaveh, J. I. Höll, S. Hornhardt, P. Husemann, P. Kachroo, C. P. Kratz, G. te Kronnie, B. Marovca, F. Niggli, A. C. McHardy, A. V. Moorman, R. Panzer-Grümayer, B. S. Petersen, B. Raeder, M. Ralser, P. Rosenstiel, D. Schäfer, M. Schrappe, S. Schreiber, M. Schütte, B. Stade, R. Thiele, N. von der Weid, A. Vora, M. Zaliova, L. Zhang, T. Zichner, M. Zimmermann, H. Lehrach, A. Borkhardt, J.-P. Bourquin, A. Franke, J. O. Korbel, M. Stanulla, M.-L. Yaspo, Genomics and drug profiling of fatal TCF3-HLF-positive acute lymphoblastic leukemia identifies recurrent mutation patterns and therapeutic options, *Nat. Genet.* **47**, 1020–1029 (2015).

24. L. Bonapace, B. C. Bornhauser, M. Schmitz, G. Cario, U. Ziegler, F. K. Niggli, B. W. Schäfer, M. Schrappe, M. Stanulla, J.-P. Bourquin, Induction of autophagy-dependent necroptosis is required for childhood acute lymphoblastic leukemia cells to overcome glucocorticoid resistance, *J. Clin. Invest.* **120**, 1310–1323 (2010).

25. J. Boutter, Y. Huang, B. Marovca, A. Vonderheit, M. A. Grotzer, C. Eckert, G. Cario, B. Wollscheid, P. Horvath, B. C. Bornhauser, J.-P. Bourquin, Image-based RNA interference screening reveals an individual dependence of acute lymphoblastic leukemia on stromal cysteine support, *Oncotarget* **5**, 11501–11512 (2014).

26. M. Schmitz, P. Breithaupt, N. Scheidegger, G. Cario, L. Bonapace, B. Meissner, P. Mirkowska, J. Tchinda, F. K. Niggli, M. Stanulla, M. Schrappe, A. Schrauder, B. C. Bornhauser, J.-P. Bourquin, Xenografts of highly resistant leukemia recapitulate the clonal composition of the leukemogenic compartment, *Blood* **118**, 1854–1864 (2011).

27. E. Clappier, B. Gerby, F. Sigaux, M. Delord, F. Touzri, L. Hernandez, P. Ballerini, A. Baruchel, F. Pflumio, J. Soulier, Clonal selection in xenografted human T cell acute lymphoblastic leukemia recapitulates gain of malignancy at relapse, *J. Exp. Med.* **208**, 653–661 (2011).

28. H. Wu, J. Tschopp, S.-C. Lin, Smac Mimetics and TNFÎ±: A Dangerous Liaison?, *Cell* **131**, 655–658 (2007).

29. O. Shalem, N. E. Sanjana, E. Hartenian, X. Shi, D. A. Scott, T. S. Mikkelsen, D. Heckl, B. L. Ebert, D. E. Root, J. G. Doench, F. Zhang, Genome-scale CRISPR-Cas9 knockout screening in human cells, *Science* **343**, 84–87 (2014).

30. S. Chen, N. E. Sanjana, K. Zheng, O. Shalem, K. Lee, X. Shi, D. A. Scott, J. Song, J. Q. Pan, R. Weissleder, H. Lee, F. Zhang, P. A. Sharp, Genome-wide CRISPR Screen in a Mouse Model of Tumor Growth and Metastasis, *Cell* **160**, 1246–1260 (2015).

31. L. Zheng, N. Bidere, D. Staudt, A. Cubre, J. Orenstein, F. K. Chan, M. Lenardo, Competitive Control of Independent Programs of Tumor Necrosis Factor Receptor-Induced Cell Death by TRADD and RIP1, *Mol. Cell. Biol.* **26**, 3505–3513 (2006).

32. J. E. Roderick, N. Hermance, M. Zelic, M. J. Simmons, A. Polykratis, M. Pasparakis, M. A. Kelliher, Hematopoietic RIPK1 deficiency results in bone marrow failure caused by apoptosis and RIPK3-mediated necroptosis, *Proc. Natl. Acad. Sci.* **111**, 14436–14441 (2014).

33. L. Zender, W. Xue, J. Zuber, C. P. Semighini, A. Krasnitz, B. Ma, P. Zender, S. Kubicka, J. M. Luk, P. Schirmacher, W. Richard McCombie, M. Wigler, J. Hicks, G. J. Hannon, S. Powers, S. W. Lowe, An Oncogenomics-Based In Vivo RNAi Screen Identifies Tumor Suppressors in Liver Cancer, *Cell* **135**, 852–864 (2008).

34. T. Tenev, K. Bianchi, M. Darding, M. Broemer, C. Langlais, F. Wallberg, A. Zachariou, J. Lopez, M. MacFarlane, K. Cain, P. Meier, The Ripoptosome, a Signaling Platform that Assembles in Response to Genotoxic Stress and Loss of IAPs, *Mol. Cell* **43**, 432–448 (2011).

35. C. Eckert, N. Hagedorn, L. Sramkova, G. Mann, R. Panzer-Grümayer, C. Peters, J.-P. Bourquin, T. Klingebiel, A. Borkhardt, G. Cario, J. Alten, G. Escherich, K. Astrahantseff, K. Seeger, G. Henze, A. von Stackelberg, Monitoring minimal residual disease in children with high-risk relapses of acute lymphoblastic leukemia: prognostic relevance of early and late assessment, *Leukemia* **29**, 1648–1655 (2015).

36. A. Rongvaux, T. Willinger, J. Martinek, T. Strowig, S. V. Gearty, L. L. Teichmann, Y. Saito, F. Marches, S. Halene, A. K. Palucka, M. G. Manz, R. A. Flavell, Development and function of human innate immune cells in a humanized mouse model, *Nat. Biotechnol.* **32**, 364–372 (2014).

37. J. Zuber, K. McJunkin, C. Fellmann, L. E. Dow, M. J. Taylor, G. J. Hannon, S. W. Lowe, Toolkit for evaluating genes required for proliferation and survival using tetracycline-regulated RNAi, *Nat. Biotechnol.* **29**, 79–83 (2011).

38. R. Rudalska, D. Dauch, T. Longerich, K. McJunkin, T. Wuestefeld, T.-W. Kang, A. Hohmeyer, M. Pesic, J. Leibold, A. von Thun, P. Schirmacher, J. Zuber, K.-H. Weiss, S. Powers, N. P. Malek, M. Eilers, B. Sipos, S. W. Lowe, R. Geffers, S. Laufer, L. Zender, In vivo RNAi screening identifies a mechanism of sorafenib resistance in liver cancer, *Nat. Med.* **20**, 1138–1146 (2014).

39. I. L. Ch'en, D. R. Beisner, A. Degterev, C. Lynch, J. Yuan, A. Hoffmann, S. M. Hedrick, Antigen-mediated T cell expansion regulated by parallel pathways of death, *Proc. Natl. Acad. Sci. U. S. A.* **105**, 17463–17468 (2008).

40. F. H. Igney, P. H. Krammer, Death and anti-death: Tumour resistance to apoptosis, *Nat. Rev. Cancer* **2**, 277–288 (2002).

41. S. Biton, A. Ashkenazi, NEMO and RIP1 control cell fate in response to extensive DNA damage via TNF-α feedforward signaling, *Cell* **145**, 92–103 (2011).

42. Y. Yang, F. Xia, N. Hermance, A. Mabb, S. Simonson, S. Morrissey, P. Gandhi, M. Munson, S. Miyamoto, M. A. Kelliher, A Cytosolic ATM/NEMO/RIP1 Complex Recruits TAK1 To Mediate the NF-κB and p38 Mitogen-Activated Protein Kinase (MAPK)/MAPK-Activated Protein 2 Responses to DNA Damage, *Mol. Cell. Biol.* **31**, 2774–2786 (2011).

43. S. McComb, E. Cessford, N. A. Alturki, J. Joseph, B. Shutinoski, J. B. Startek, A. M. Gamero, K. L. Mossman, S. Sad, Type-I interferon signaling through ISGF3 complex is required for sustained Rip3 activation and necroptosis in macrophages, *Proc. Natl. Acad. Sci.* **111**, E3206–E3213 (2014).

44. R. J. Thapa, S. Nogusa, P. Chen, J. L. Maki, A. Lerro, M. Andrake, G. F. Rall, A. Degterev, S. Balachandran, Interferon-induced RIP1/RIP3-mediated necrosis requires PKR and is licensed by FADD and caspases, *Proc. Natl. Acad. Sci.* **110**, E3109–E3118 (2013).

45. W. J. Kaiser, H. Sridharan, C. Huang, P. Mandal, J. W. Upton, P. J. Gough, C. A. Sehon, R. W. Marquis, J. Bertin, E. S. Mocarski, Toll-like receptor 3-mediated necrosis via TRIF, RIP3, and MLKL, *J. Biol. Chem.* **288**, 31268–31279 (2013).

46. S. T. Beug, V. A. Tang, E. C. LaCasse, H. H. Cheung, C. E. Beauregard, J. Brun, J. P. Nuyens, N. Earl, M. St-Jean, J. Holbrook, H. Dastidar, D. J. Mahoney, C. Ilkow, F. Le Boeuf, J. C. Bell, R. G. Korneluk, Smac mimetics and innate immune stimuli synergize to promote tumor death, *Nat. Biotechnol.* **32**, 182–190 (2014).

47. I. Tamm, S. M. Kornblau, H. Segall, S. Krajewski, K. Welsh, S. Kitada, D. A. Scudiero, G. Tudor, Y. H. Qui, A. Monks, M. Andreeff, J. C. Reed, Expression and Prognostic Significance of IAP-Family Genes in Human Cancers and Myeloid Leukemias, *Clin. Cancer Res.* **6**, 1796–1803 (2000).

48. J. A. Flygare, W. J. Fairbrother, Small-molecule pan-IAP antagonists: A patent review, *Expert Opin. Ther. Pat.* **20**, 251–267 (2010).

49. J. W. Tyner, W. F. Yang, A. Bankhead, G. Fan, L. B. Fletcher, J. Bryant, J. M. Glover, B. H. Chang, S. E. Spurgeon, W. H. Fleming, T. Kovacsovics, J. R. Gotlib, S. T. Oh, M. W. Deininger, C. M. Zwaan, M. L. D. Boer, M. M. van den Heuvel-Eibrink, T. O'Hare, B. J. Druker, M. M. Loriaux, Kinase Pathway Dependence in Primary Human Leukemias Determined by Rapid Inhibitor Screening, *Cancer Res.* **73**, 285–296 (2013).

50. T. Pemovska, M. Kontro, B. Yadav, H. Edgren, S. Eldfors, A. Szwajda, H. Almusa, M. M. Bespalov, P. Ellonen, E. Elonen, B. T. Gjertsen, R. Karjalainen, E. Kulesskiy, S. Lagström, A. Lehto, M. Lepistö, T. Lundán, M. M. Majumder, J. M. L. Marti, P. Mattila, A. Murumägi, S. Mustjoki, A. Palva, A. Parsons, T. Pirttinen, M. E. Rämet, M. Suvela, L. Turunen, I. Västrik, M. Wolf, J. Knowles, T. Aittokallio, C. A. Heckman, K. Porkka, O. Kallioniemi, K. Wennerberg, Individualized systems medicine strategy to tailor treatments for patients with chemorefractory acute myeloid leukemia, *Cancer Discov.* **3**, 1416–1429 (2013).

Acknowledgments: We thank Thomas Radimerski, Novartis, for providing LCL-161.

Funding: This work was supported by the "Stiftung Kinderkrebsforschung Schweiz", the MAM-Fonds of the Children's Research Centre of the University Children's Hospital Zurich, the Empiris foundation, the clinical research focus program "human hemato-lymphatic diseases" of the University of Zurich, the Swiss Cancer League (KFS 3609-02-2015), the Novartis Foundation for Biomedical Research, the Swiss national Science Foundation SNF (310030-133108), the Canadian institutes for health research CIHR, the Forschungskredit of the University of Zurich (FK-14-016) and the Fondation Panacée.

Author contributions: S.M., J.A.-G., B.M., L.H. performed experiments and analyzed data, G.C., M.S., A.vS. and C.E. provided samples and clinical data, S.M., J.A.-G., JP.B. and B.C.B. wrote the manuscript, JP.B. and B.C.B. conceived and supervised the study.

Competing interests: JP.B. served on a pediatric advisory board for Roche. All other authors declare that they have no competing interests.

Figure legends

Fig. 1. Drug profiling identifies a cohort of ALL highly sensitive to SMAC mimetics. (**A**) ALL xenografts derived from standard risk (SR), high risk (HR), very high risk (VHR), and relapse (R) patients were treated with varying doses of birinapant for 48 hours. IC50 values were calculated based on viability staining and automated microscopy. (**B-D**) NSG mice were injected i.v. with 10^6 SM-sensitive leukemic cells and treated starting on day 2 after injection with 30 mg/kg of birinapant daily for two 2-week blocks separated by a 2-week recovery. Graphs show the proportion of human CD45+ cells within the nucleated blood cell fraction of vehicle (red lines) and birinapant treated (blue lines) animals as measured by flow cytometry. (**E-G**) Leukemic mice were treated as above with a single 2-week block of birinapant treatment starting at engraftment of >30% hCD45+ cells as determined by flow cytometry (treated group in green). (**H-J**) Survival plots for vehicle controls or mice with treated before or after engraftment for 3 different SM-sensitive patients-derived xenografts. $n \geq 3$ mice per group. (**K-P**) Experiments were performed similarly to the ones above, but using patient samples with low in vitro SM sensitivity. $n \geq 2$ mice per group.

Fig. 2. SMAC mimetics induce both apoptosis and necroptosis. (**A,B**) Patient-derived ALL cells in co-culture with MSCs were treated with varying doses of birinapant alone (black) or in combination with 25 μM zVAD (blue), 25 μM necrostatin (red), or both zVAD and necrostatin (green). Curves were calculated from the mean ± SEM of three experiments and show the relative number of live cells compared to DMSO controls. (C-F) Experiments were performed as above with a larger number of patient samples. Curves show the number of live cells at the indicated concentrations in a single experiment performed in duplicate for each patient sample. (**G**) The viability of patient samples at the birinapant IC50 in the presence or absence of death inhibitors is shown. Patients are grouped based on the pattern of rescue achieved with the death inhibitors. (**H**) Pie chart shows the proportion of patient cells grouped as necroptotic (red), mixed cell death (green), no rescue (gray), or nec sensitive (orange). (**I-J**) Patient samples were screened as above, using LCL161 instead of birinapant. (n=1 experiment in duplicate × 15 patient samples).

Fig. 3. Differential expression of TNFα, RIP1, apoptotic, or necroptotic mediators cannot explain ALL response to SM. (**A**) SM-sensitive xenograft cells were placed in monoculture with or without birinapant treatment and examined after 6 hours, after which cells were lysed and examined for TNFα expression by RT-PCR. (**B**) Xenograft cells were examined by western blotting for p65 phosphorylation at the indicated time points of birinapant incubation as shown. (**C**) SM-sensitive xenograft cells were co-cultured with MSCs and treated with varying doses of birinapant in the presence (red lines) or absence (black lines) of 1 μg/mL TNFα blocking antibody. After 48 hours, cells were stained for viability and examined via automated microscopy. Graphs show the mean ±SEM from 3 experiments performed in duplicate. (**D**) A panel of 12 patient-derived xenografts with varying SM sensitivity was examined by western blotting to assess expression of various apoptotic or necroptotic mediators.

Fig. 4. RIP1 drives SM-induced apoptosis and necroptosis. (**A**) Leukemic cell lines were treated with varying doses of birinapant as shown for 48 hours. Viability was assessed using CCK-8 colorimetric cell viability assay. (**B**) Leukemic cells were similarly treated with varying doses of birinapant in the presence of 10 ng/mL human TNFα. (**C**) Leukemic cell lines were treated with birinapant (500 nM) and TNFα (10 ng/mL) in the presence or absence of zVAD (blue), nec (red), or both (green). Viability was assessed as above and normalized to untreated control. (**D**) Four different leukemic cell lines were transduced with LentiCRISPR-EGFP targeting RIP1. Cells were subjected to 2 rounds of sorting to generate cell lines with ≥90% disrupted RIP1 expression as assessed by western blot. (**E-F**) RIP1-WT and RIP1-CRISPR cells from partially SM-sensitive cell lines were treated with

varying doses of SM as shown for 48 hours. Cell viability was assessed using CCK-8 colorimetric viability assay. (**G-J**) RIP1-WT (dashed red line) and RIP1-CRISPR (solid black line) cell lines were treated as above with varying doses of birinapant in the presence of 50 ng/mL TNFα. (**K**) Jurkat cells were transduced with LentiCRISPR carrying varying fluorescent tags and sgRNA sequences targeting Casp8, FADD, RIP3, and/or MLKL. Various single and double knockout lines were purified through at least 2 rounds of sorting to generate cell lines with disrupted expression as shown in the western blot. (**L**) Apoptotic CRISPR, (**M**) necroptotic CRISPR, or (**N,O**) apoptotic/necroptotic CRISPR cells were treated with varying doses of birinapant in the presence of 50 ng/mL TNFα. Viability was assessed at 48 hours after treatment using CCK-8. (**P**) Various CRISPR cell lines were treated with birinapant and TNFα alone (black) or in combination with zVAD (blue), nec (red), or both (green) as shown. All graphs show the mean ± SEM of at least 3 experiments performed in duplicate.

Fig. 5. RIP1 is required for SM-induced apoptosis and necroptosis in leukemia xenografts in vivo. (**A**) 10^6 highly SM-sensitive patient-derived xenograft cells (R-03) were transduced with LentiCRISPR-EGFP targeting RIP1 for 2 days and then injected into NSG mice. At weekly intervals after transplantation, the proportions of hCD45+ and GFP+ cells were assessed by flow cytometry. Treatment with 30 mg/kg of birinapant was initiated at day 14 and continued until the end of the experiment. (**B**) Cells from mice sacrificed before treatment with birinapant (left) and after treatment with birinapant (right) were sorted by EGFP expression and examined for RIP1 expression by western blot. Control cells (con) were untransduced xenograft cells derived from the same patient sample. (**C**) The proportion of EGFP+ among gated hCD45+ cells over the course of the experiment is shown; n=2 mice. (**D-F**) Targeted RIP1 disruption was performed in additional patient-derived xenograft cells (VHR-10) as above. Mice were examined for engraftment and EGFP expression in hCD45+ cells and RIP1 expression as described above; n=2 mice. (**G-K**) Additional patient samples were treated as above and examined for outgrowth of EGFP+ cells, n=1 mouse per patient. (**L-M**) Highly SM-sensitive primary cells (R-03) were transduced with LentiCRISPRs targeted against CASP8, FADD, RIP3, and/or MLKL for 2 days and then injected into NSG mice. Treatment with birinapant was initiated at day 46 and continued until the end of the experiment. Mouse peripheral blood was examined for engraftment and fluorescent markers at varying time points. Graphs show pre-gated populations to exclude triple and quadruple positive cells. (**N**) Fold change in proportion of exclusive single and double positive populations from initial detection over the course of the experiment (graph shows the mean result from 2 mice of each type). Populations of WT, double knockout, and, quadruple knockout cells from above were expanded via xenograft and examined by **(O)** western blot and **(P)** in vitro response to birinapant (graph shows the mean from 3 experiments performed in duplicate).

Fig. 6. RIP1 cell death pathways are not exploited by standard anti-leukemic therapies. (**A-C**) WT and RIP1-CRISPR cells generated as described in Figure 5 from primary samples R-03, VHR-10, and SR-03 were co-cultured with mesenchymal stromal cells and challenged with increasing doses of various chemotherapeutic drugs for 48 hours. Cell viability was assessed by viability staining and automated microscopy, and the curves were calculated from the mean ± SEM of 3 experiments. (**D**) The IC50 for the response of WT (open symbols) and RIP1-CRISPR (filled green symbols) cells from 3 primary samples (VHR-10, R-03, SR-03) to various drugs is shown. Experiments show the mean from 3 independent experiments performed in duplicate. Inset shows the mean fold change in IC50 for RIP1 deficient cells +/- SEM (**E**) Model showing the central role of RIP1 in mediating the induction of apoptosis and necroptosis in response to SMAC mimetics.

Figures

Figure 1

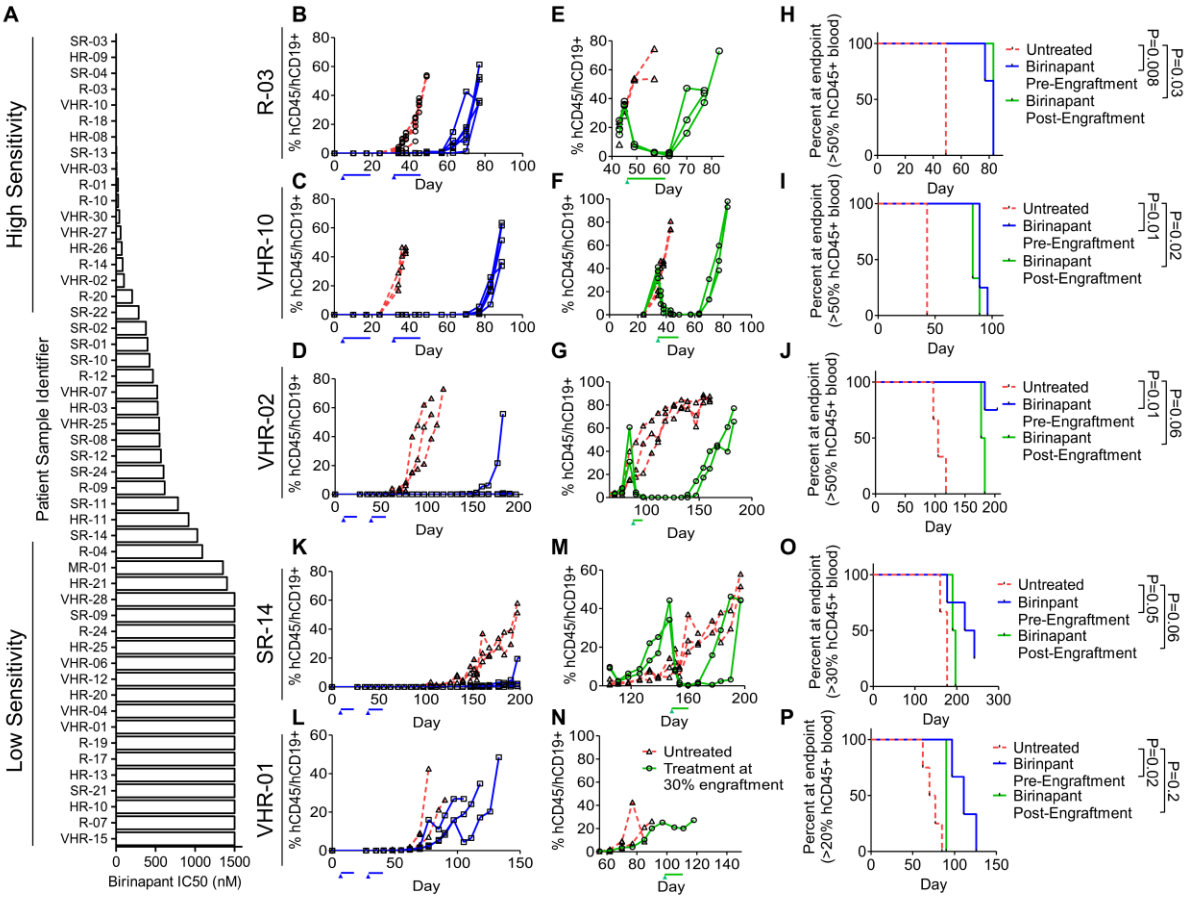

Figure 2

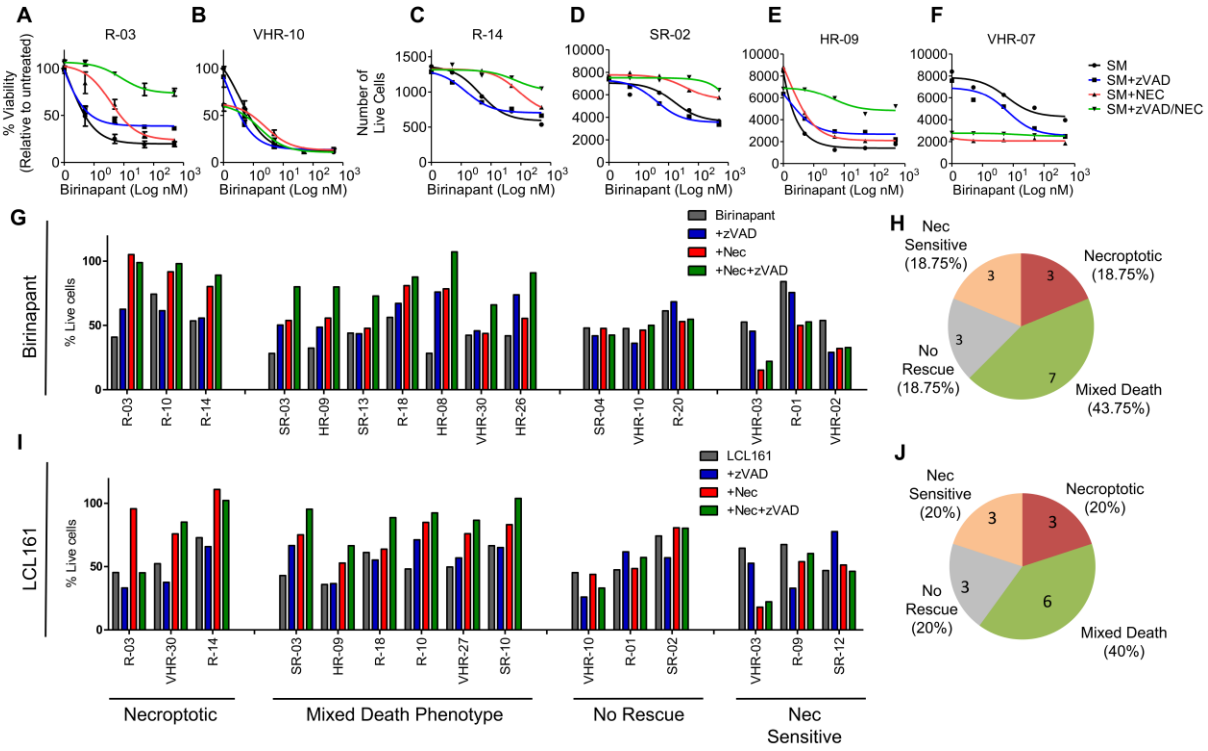
A
R-03
B
VHR-10
C
R-14
D
SR-02
E
HR-09
F
VHR-07
% Viability (Relative to untreated)
Number of Live Cells
Birinapant (Log nM)
SM
SM+zVAD
SM+NEC
SM+zVAD/NEC
G
Birinapant
% Live cells
Birinapant
+zVAD
+Nec
+Nec+zVAD
R-03
R-10
R-14
SR-03
HR-09
SR-13
R-18
HR-08
VHR-30
HR-26
SR-04
VHR-10
R-20
VHR-03
R-01
VHR-02
H
Nec Sensitive (18.75%)
Necroptotic (18.75%)
No Rescue (18.75%)
Mixed Death (43.75%)
3
3
3
7
I
LCL161
% Live cells
LCL161
+zVAD
+Nec
+Nec+zVAD
R-03
VHR-30
R-14
SR-03
HR-09
R-18
R-10
VHR-27
SR-10
VHR-10
R-01
SR-02
VHR-03
R-09
SR-12
Necroptotic
Mixed Death Phenotype
No Rescue
Nec Sensitive
J
Nec Sensitive (20%)
Necroptotic (20%)
No Rescue (20%)
Mixed Death (40%)
3
3
3
6

Figure 3

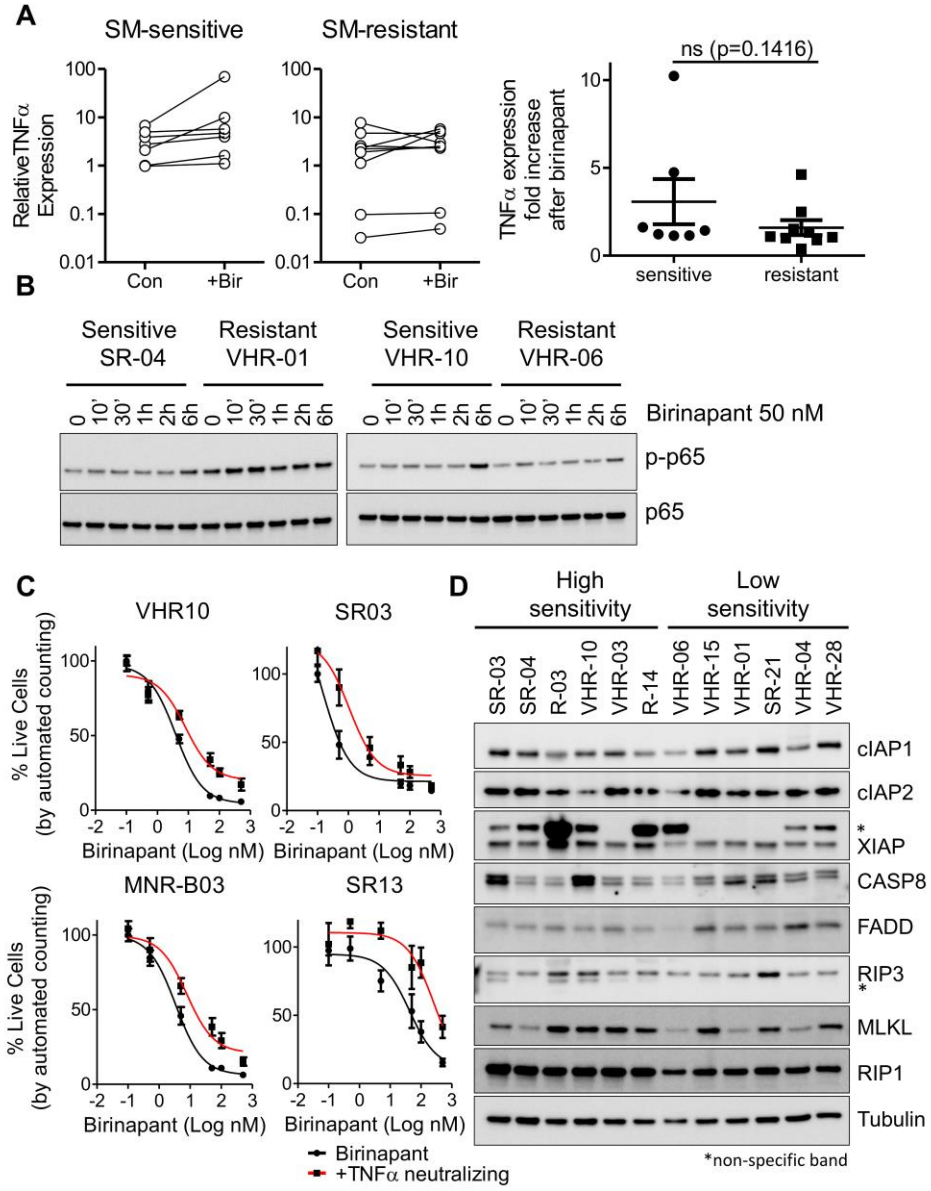
A
SM-sensitive
SM-resistant
Relative TNFα Expression
Con
+Bir
ns (p=0.1416)
TNFα expression fold increase after birinapant
sensitive
resistant
B
Sensitive SR-04
Resistant VHR-01
Sensitive VHR-10
Resistant VHR-06
Birinapant 50 nM
p-p65
p65
C
VHR10
SR03
MNR-B03
SR13
% Live Cells (by automated counting)
Birinapant (Log nM)
Birinapant
+TNFα neutralizing
D
High sensitivity
Low sensitivity
SR-03
SR-04
R-03
VHR-10
VHR-03
R-14
VHR-06
VHR-15
VHR-01
SR-21
VHR-04
VHR-28
cIAP1
cIAP2
XIAP
CASP8
FADD
RIP3
MLKL
RIP1
Tubulin
*non-specific band

Figure 4

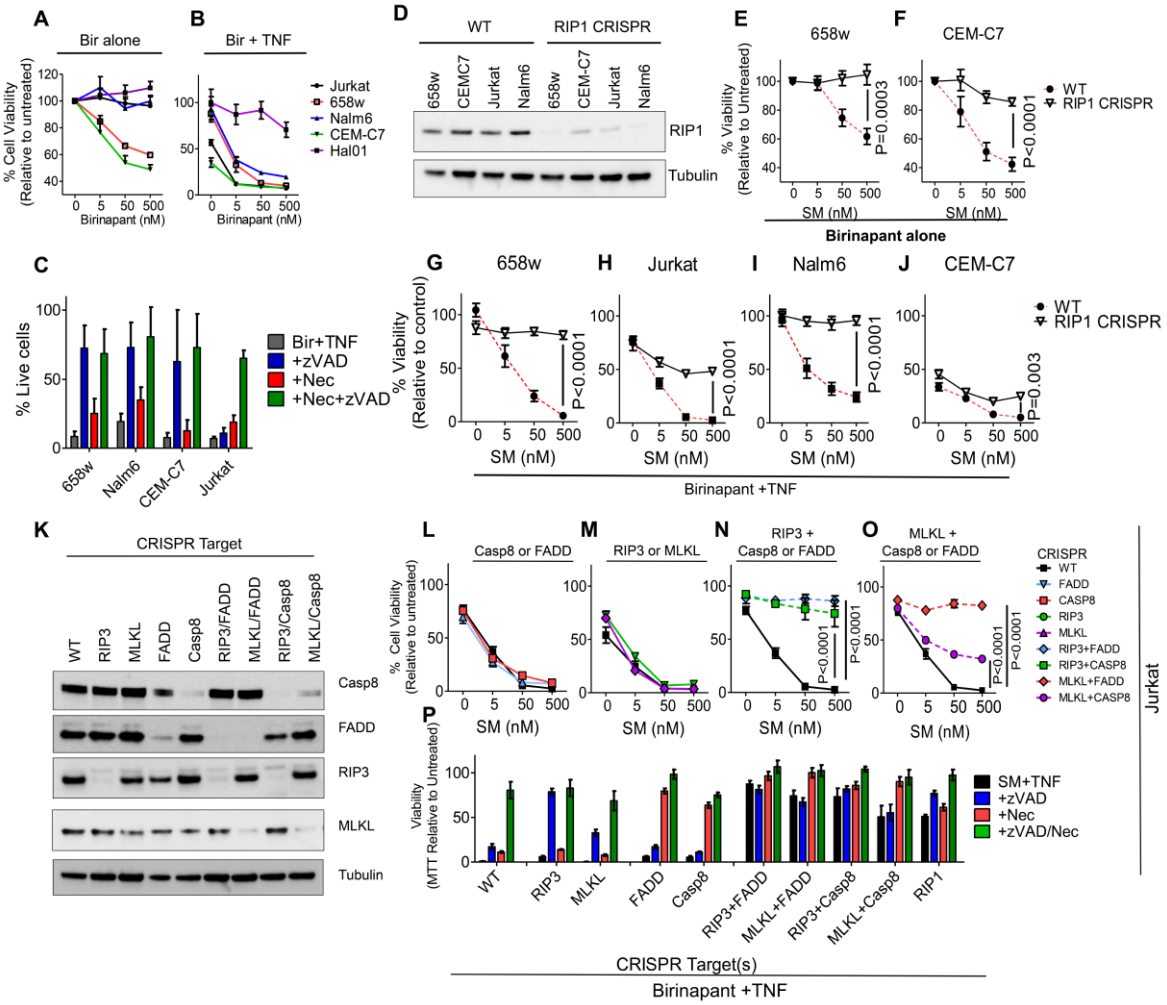
A
Bir alone
B
Bir + TNF
% Cell Viability (Relative to untreated)
Birinapant (nM)
Jurkat
658w
Nalm6
CEM-C7
Hal01
D
WT
RIP1 CRISPR
658w
CEMC7
Jurkat
Nalm6
CEM-C7
RIP1
Tubulin
E
658w
F
CEM-C7
% Viability (Relative to Untreated)
P=0.0003
P<0.0001
SM (nM)
WT
RIP1 CRISPR
Birinapant alone
C
% Live cells
Bir+TNF
+zVAD
+Nec
+Nec+zVAD
658w
Nalm6
CEM-C7
Jurkat
G
658w
H
Jurkat
I
Nalm6
J
CEM-C7
% Viability (Relative to control)
P<0.0001
P=0.003
Birinapant +TNF
K
CRISPR Target
WT
RIP3
MLKL
FADD
Casp8
RIP3/FADD
MLKL/FADD
RIP3/Casp8
MLKL/Casp8
Casp8
FADD
RIP3
MLKL
Tubulin
L
Casp8 or FADD
M
RIP3 or MLKL
N
RIP3 + Casp8 or FADD
O
MLKL + Casp8 or FADD
% Cell Viability (Relative to untreated)
CRISPR
WT
FADD
CASP8
RIP3
MLKL
RIP3+FADD
RIP3+CASP8
MLKL+FADD
MLKL+CASP8
Jurkat
P
Viability (MTT Relative to Untreated)
SM+TNF
+zVAD
+Nec
+zVAD/Nec
WT
RIP3
MLKL
FADD
Casp8
RIP3+FADD
MLKL+FADD
RIP3+Casp8
MLKL+Casp8
RIP1
CRISPR Target(s)
Birinapant +TNF

Figure 5

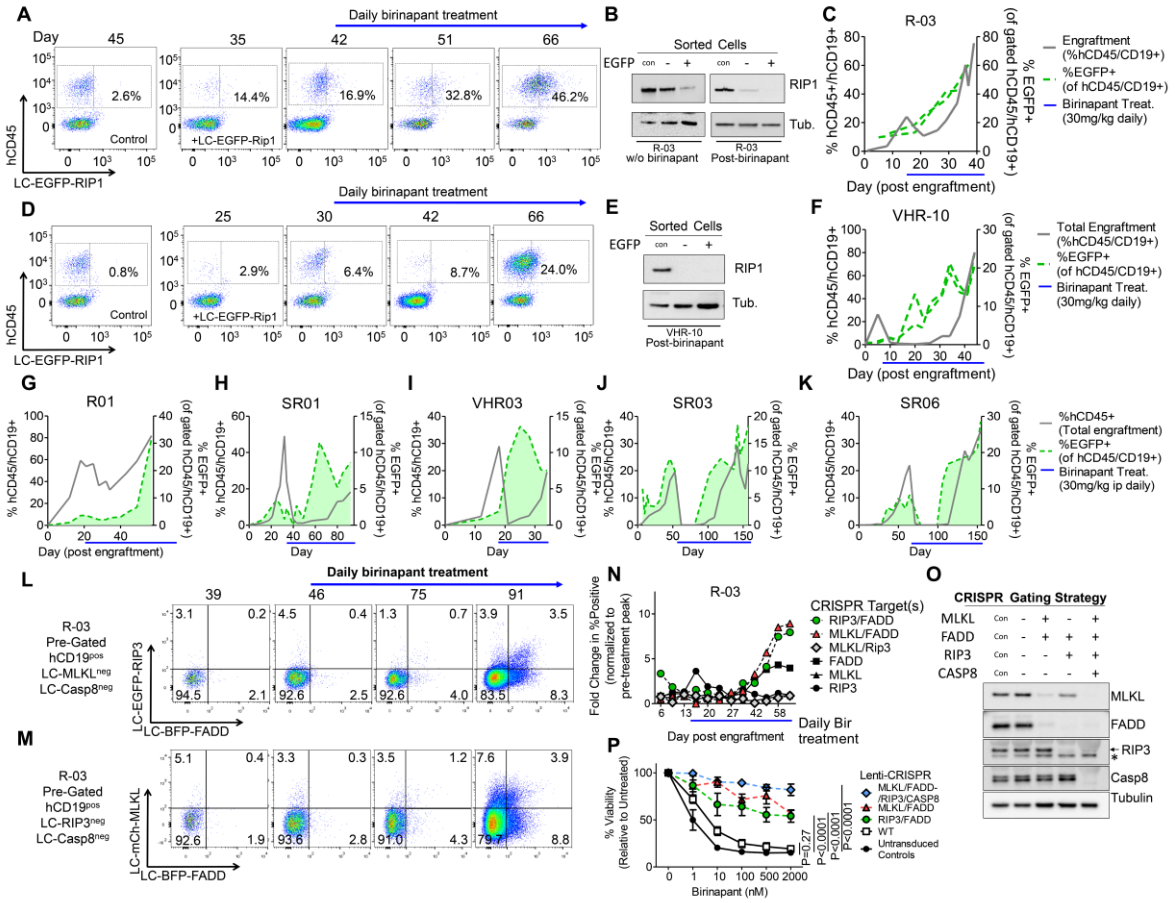

Figure 6

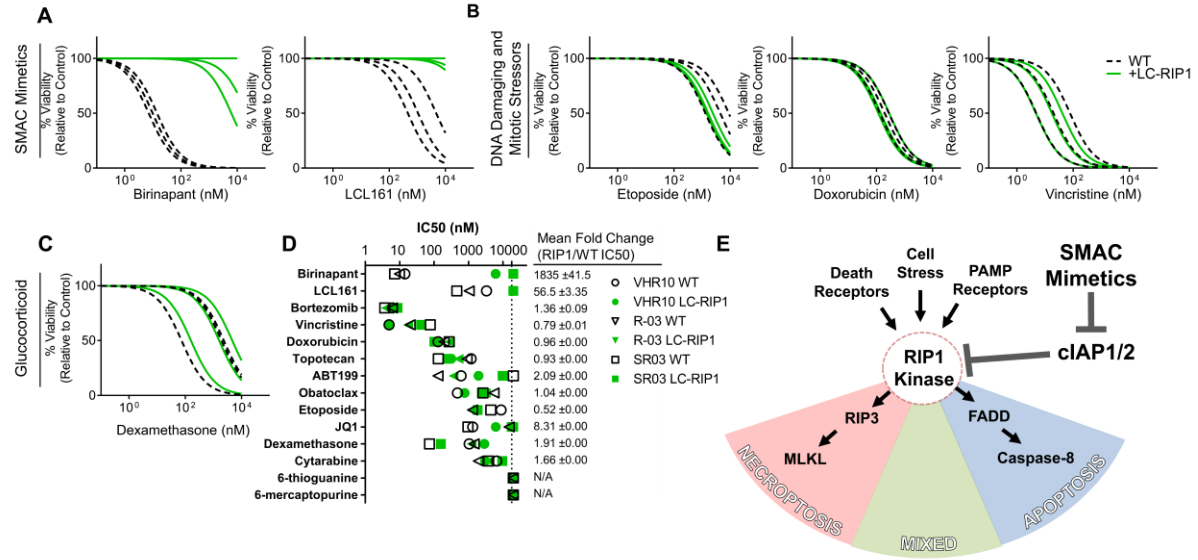

Supplemental Materials and Methods

Cell culture:

Jurkat, CEM-C7, Nalm6, patient-derived 658w cells, and hTERT-immortalized primary bone marrow mesenchymal stromal cells (hTERT-MSC) were cultured in RPMI-1640 (Sigma-Aldrich, Cat# R0883) supplemented with 10% fetal bovine serum (Sigma-Aldrich), 0.5% L-glutamine (Bioconcept), and 0.5% penicillin-streptomycin (Life Technologies). The medium was also supplemented with 1 µM hydrocortisone (Sigma-Aldrich, Cat# H0888) for hTERT-MSCs. Cells were incubated at 37 ºC and 5% CO_2. Co-culture experiments with xenograft-derived primary cells were performed in serum-free conditions in AIM-V (Life Technologies, Cat# 12055-091).
PCR-based mycoplasma testing was performed on all cell lines used. Mycoplasma-positive cells were treated with mycoplasma removal agent (Bio-Rad BUF035).

Lentiviral vectors:

Cloning of sgRNA into LentiCRISPR vectors was accomplished as follows in brief: vector, annealed sgRNA primers, Esp3I restriction enzyme (Life Technologies Cat# ER0451), and T4 DNA ligase (Life Technologies, Cat# EL0011) were combined in a single tube and subjected to 10 cycles of 37 °C for 5 minutes and 16 °C for 10 minutes for restriction and ligation respectively. Colony PCR was performed to identify clones with positive sgRNA insertion.

Production of lentiviral vectors was performed according to standard protocol. In brief, 293T cells were transfected using polyethylenimine (Polysciences, Cat# 24765-2) with LentiCRISPR, pVSV.G plasmid (Addgene Cat# 8454), and psPAX (Addgene Cat# 12260) in a ratio of 4:1:1. Medium was changed after 4 hours, and virus was collected at 24, 48, and 72 hours after transfection of plasmids. Virus was concentrated for in vivo studies using ultracentrifugation at 25000 g for 2 hours. Viral transductions were performed using hexadimethrine bromide (Sigma-Aldrich, Cat# H9268) and viral vectors at low MOI (0.1-0.2).

Western blot analysis:

3×10^5 cells were lysed in 1x SDS loading buffer (62.5 nM Tris pH 6.8, 1% SDS, 0.005% bromophenol blue, 4% glycerol, 1% (v/v) ß-mercaptoethanol). Cell lysates were separated by SDS-PAGE (Criterion XT Precast Gels, BIO-RAD, 4-12% Bis-Tris, Cat# 345-0125) and transferred onto nitrocellulose membranes (Trans-Blot Turbo transfer pack, BIO-RAD, Cat# 170-4159). Membranes were blocked with 5% non-fat milk, and the following antibodies were used: mouse anti-RIP1 form BD Biosciences (Cat# 51-6559), mouse anti-caspase 8 (Cat# 9746), rabbit anti-FADD (Cat# 2782), rabbit anti-phospho-NF-κB p65 (Cat# 3033), and rabbit anti-NF-κB p65 (Cat# 4764) from Cell Signaling, mouse anti-tubulin (Sigma-Aldrich, Cat# 081M4861), rabbit anti-RIP3 from Abnova (Cat# PAB0287), and rat anti-MLKL from Millipore (Cat# MABC604). Horseradish peroxidase-conjugated goat anti-mouse, goat anti-rabbit, and goat anti-rat antibodies from Cell Signaling (Cat# 7076, 7074 and 7077) were used as secondary antibodies. SuperSignal West Femto Maximum Sensitivity Substrate (Thermo Scientific, Cat# 34096) was used for detection. All western blots shown are representative of at least two independent experiments.

Viability assays:

For cell lines, 5000 cells were plated in 50 µL in 384-well plates (Greiner, Cat#781090), treated in triplicate as indicated the following day, and incubated for 48 h. Viability was assessed using CCK-8 viability assay. In brief, 5 µL of CCK-8 reagent (Dojindo Laboratories, Cat# CK04-13) were added per well, and absorbance was measured with a Synergy HT Microplate Reader (BioTek) after 1 hour of incubation. The absorbance at 640 nm was subtracted from that at 450 nm. The resulting values were corrected by the background signal from medium alone. The experiments were performed three times.

For patient-derived ALL cells, 2500 hTERT-MSC were plated in 384-well plates in 50 µL serum-free medium (AIM-V, Life Technologies, Cat# 12055-091). After 24 hours of incubation, 25000 ALL cells were added in 7.5 µL medium. The cells were treated the following day with birinapant (0.5, 5, 50, or 500 nM), Z-VAD-FMK (25 µM), and/or necrostatin-1 (25 µM) as indicated in duplicate using an epMotion 5070 robot (Eppendorf) and pretreated for 2 h with TNFα neutralizing antibody (1

μg/mL) when indicated. After 48 hours of treatment, live cells were stained with CyQUANT (Life Technologies, Cat# C35012) and quantified using microscopy and multi-parametric image analysis as described previously (*21*). All tested primary samples were included.

TUNEL assay and active caspase-3 assay for flow cytometry:

For primary cells, 4 x 10^5 hTERT-MSCs were plated per well in 2 mL AIM-V in a 6-well plate (Sarstedt, Cat# 83.3920). ALL cells were added the following day at a concentration of 3 x 10^6/well in 400 μL. For Jurkat cell line, 10^6 cells were plated in 2 mL RPMI in a 6-well plate. The cells were treated with birinapant, TNFα (10 ng/mL), Z-VAD-FMK (25 μM), and/or necrostatin-1 (25 μM) as indicated for 24 hours. The cells were then stained with 0.25 μL Fixable Viability Dye eFluor 660 (eBioscience, Cat# 65-0864) in 500 μL of PBS and incubated for 30 minutes at 4 ºC. The cells were fixed with paraformaldehyde 1% on ice for 15 minutes and permeabilized with ethanol 70% overnight at -20 ºC. TUNEL assay was performed using APO-BrdU TUNEL Assay Kit (Invitrogen, Cat# A35126 and A35127) with minor modifications (4 μL BrdUTP, 0.375 μL TdT enzyme, 2.5 μL antiBrdU antibody) to the protocol. For active caspase-3 staining, the fixed and permeabilized cells were incubated with 20 μL FITC active caspase-3 antibody (BD Pharmingen, Cat# 51-68654X) in 100 μL of perm/wash buffer 1x (BD Pharmingen, Cat# 554723) for 30 minutes at room temperature. Flow cytometry was performed on a BD FACS Canto II (BD Biosciences), and FlowJo (version 7.1.6, TreeStar) was used for data analysis.

Quantitative RT-PCR for quantification of TNFα production

RNA was extracted using the RNAeasy Mini Kit (Qiagen, Cat# 74106). Reverse transcription was performed with MultiScribe RT transcriptase (Life Technologies, Cat# 4311235). Real time PCR was performed with TaqMan Gene Expression Master Mix (Applied Biosystems, Cat# 436916) and the following probes: TNFα (Cat# Hs01113624) and GAPDH (Cat# Hs02758991) from Life Technologies. PCR reaction was performed using a 7900HT Fast Real-Time PCR System (Applied Biosystems) and SDS 2.3 software. The quantification was performed in triplicate.

Supplemental Figures

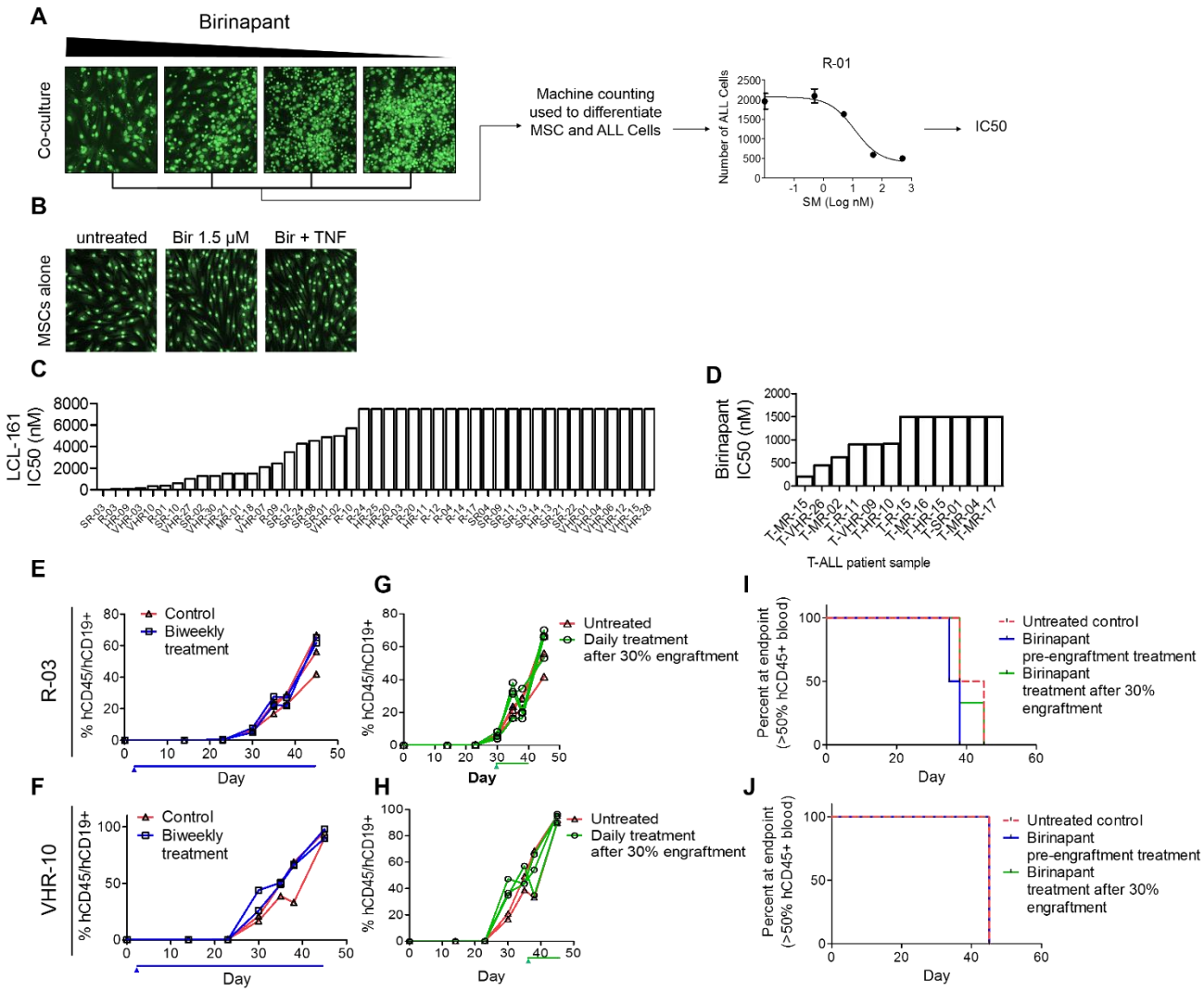

Fig. S1: **ALL patient samples are sensitive to LCL161 in vitro but not in vivo.** (**A**) Patient-derived ALL cells were co-cultured with mesenchymal stromal cells and exposed to varying doses of birinapant for 48 hours. Cells were stained with Cyquant to identify live cells. Raw image data gathered using automated microscopy of the co-culture drug screening system is shown. (**B**) Mesenchymal stromal cells were treated directly with high doses of birinapant (1.5 µM) with and without TNF. (**C**) ALL xenografts derived from B cell precursor ALL (BCP-ALL) standard risk (SR), high risk (HR), very high risk (VHR), and relapse (R) patients were treated with varying doses of LCL161. The bar graph shows the IC50 for response to LCL161 for these samples. (**D**) The IC50 of birinapant for a panel of T cell ALL patients was determined as described for BCP-ALL. **(E,F)** Mice were xenografted with SM-sensitive patient samples (R-03 and VHR10) and treated with LCL161 or vehicle control twice weekly with 50 mg/kg orally. **(G,H)** Xenografted mice were treated daily after they reached 30% engraftment with 30 mg/kg of LCL-161 intraperitoneally or vehicle control. **(I,J)** Survival curves for the above experiments (n=2-3 mice per experimental group).

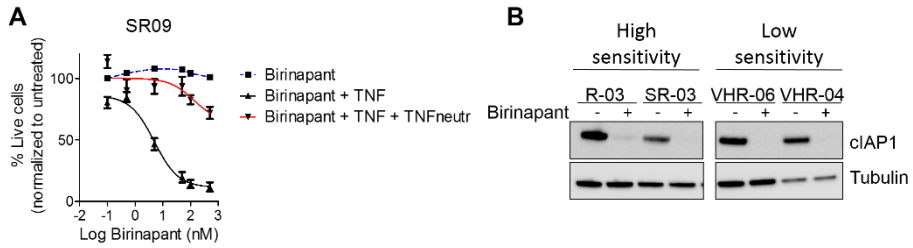

Fig. S2: **TNF blocking effectively rescues TNF-dependent response to birinapant.** (**A**) Patient-derived xenograft cells were co-cultured with MSCs and treated with varying doses of birinapant in the presence of 50 ng/mL recombinant human TNF ligand and 1 µg/mL TNF-neutralizing antibody. Cells were stained for viability and examined by automated microscopy. Graph shows the mean viability normalized to control from 3 experiments performed in duplicate. (**B**) Patient-derived xenograft cells from high and low sensitivity cases were co-cultured with MSCs, treated for 2 hours with 50 nM birinapant, and the amount of cIAP1 was assessed by western blot.

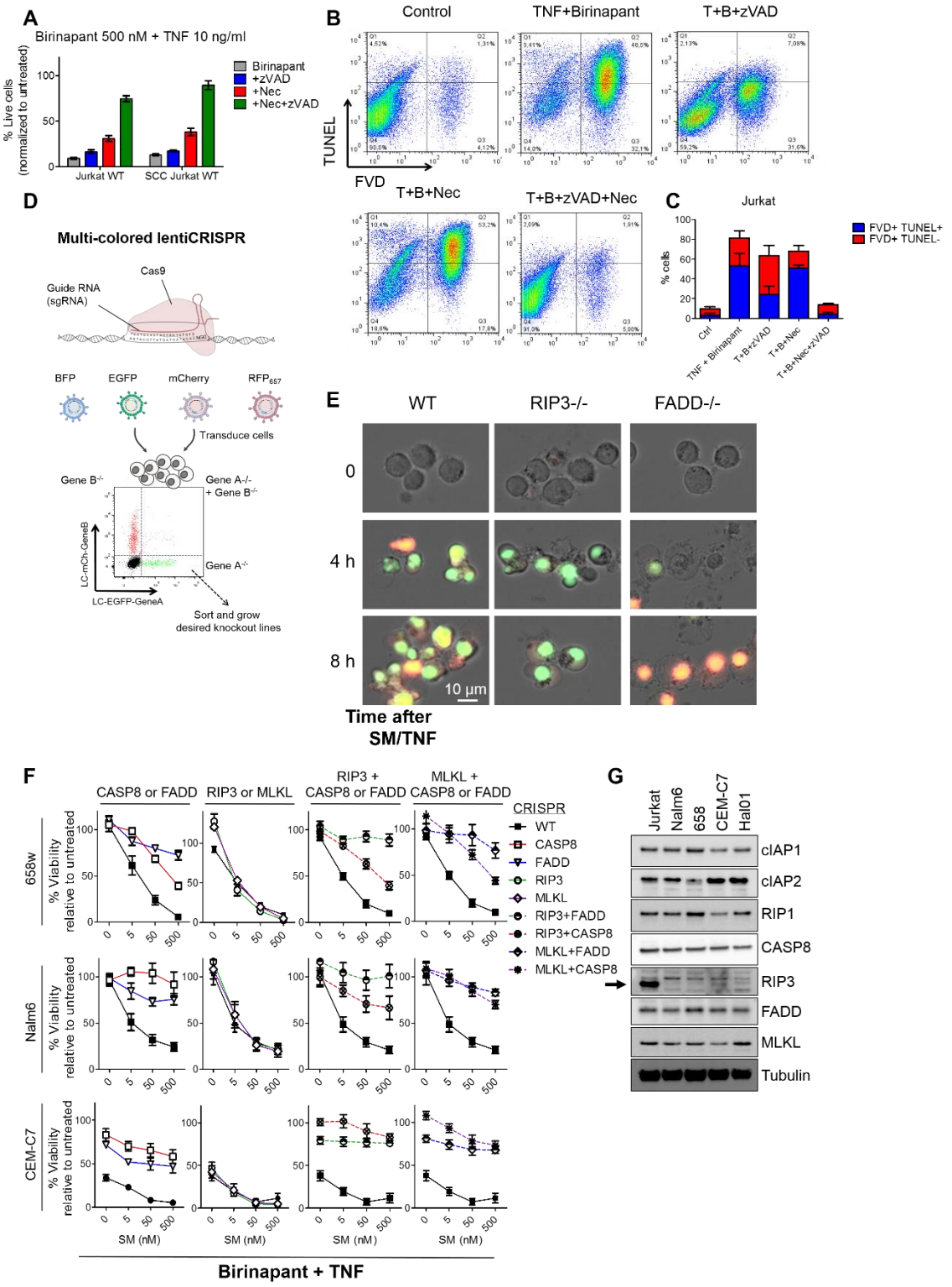

Fig. S3: **Birinapant induces dual activation of apoptosis and necroptosis in ALL cell lines.** (**A**)

Jurkat cells were grown under normal conditions and sorted into single cell clones (SCC). These cells

were treated with birinapant and TNF in the presence of apoptosis and/or necroptosis inhibitors as shown. Cell viability was determined by CCK-8 viability staining. (**B**) Jurkat cells were treated with combinations of birinapant and TNF in the presence or absence of apoptosis or necroptosis inhibitors as shown. After 24 hours, cells were stained with TUNEL and fixable viability dye and examined by FACS. (**C**) Graphs show the mean ±SD percentage of apoptotic ($TUNEL^{+}/FVD^{+}$) and necroptotic cells ($TUNEL^{dim}/FVD^{+}$) from 3 separate experiments. (**D**) Model of multi-colored LentiCRISPR gene disruption is shown. (**E**) Jurkat cells with specific disruption of RIP3 or FADD were treated for varying amounts of time with birinapant (500 nM) and TNF (50 ng/mL) as shown. Cells were stained for caspase activity (green) and propidium iodide exclusion (red, combined signal is shown as yellow), and examined via fluorescence microscopy. (**F**) Various ALL cell lines with the targeted genetic disruptions shown were treated with varying doses of birinapant in the presence of TNFα (50 ng/mL). Cell viability was examined by CCK-8 staining. Graphs show the mean viability normalized to untreated controls ±SEM from 3 experiments performed in duplicate. (**G**) The amounts of cIAP1, cIAP2, RIP1, and apoptotic and necroptotic mediators as indicated were assessed by western blotting in various ALL cell lines.

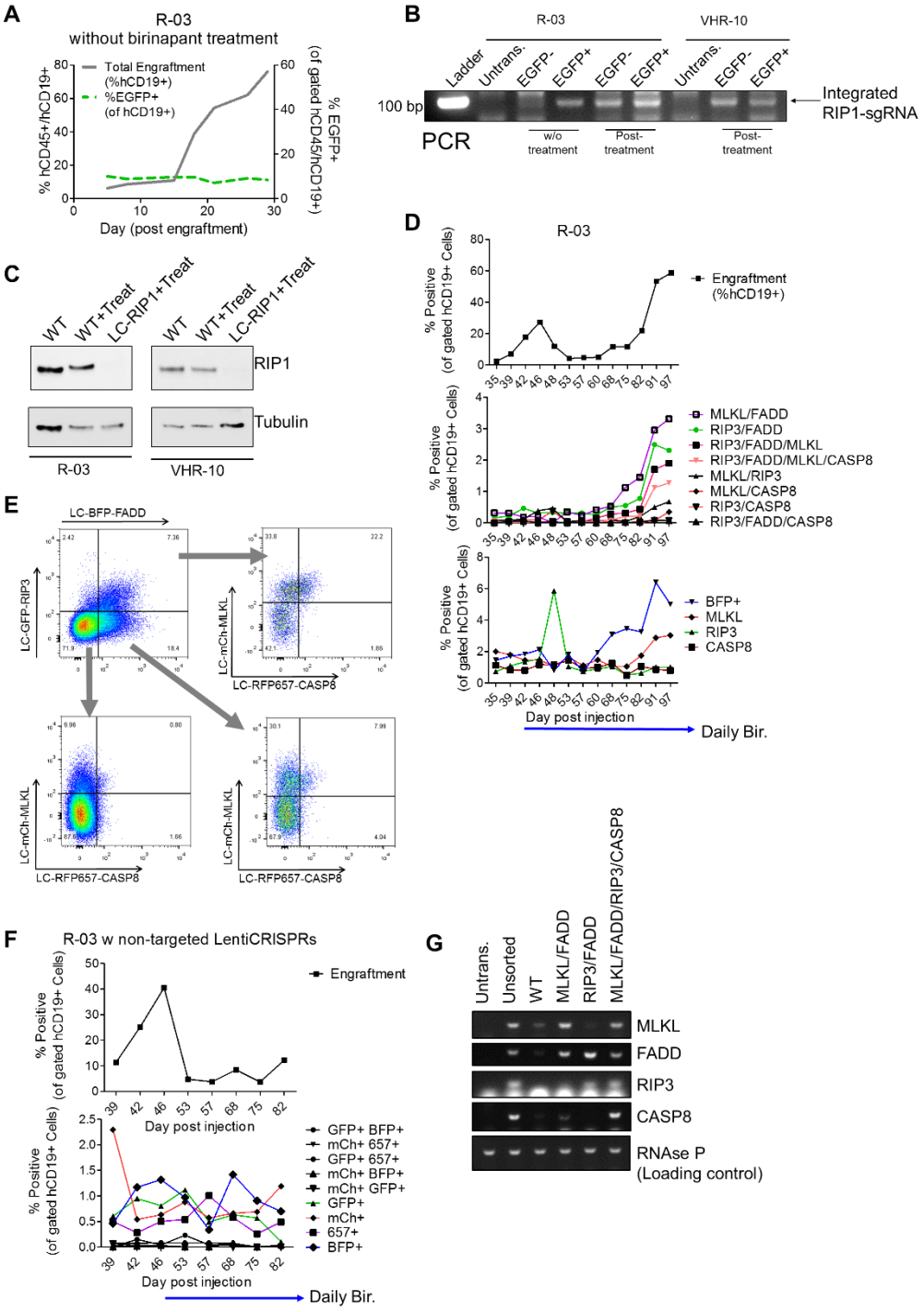
A
R-03
without birinapant treatment
Total Engraftment (%hCD19+)
%EGFP+ (of hCD19+)
% hCD45+/hCD19+
% EGFP+ (of gated hCD45/hCD19+)
Day (post engraftment)
B
R-03
VHR-10
Ladder
Untrans.
EGFP-
EGFP+
100 bp
Integrated RIP1-sgRNA
PCR
w/o treatment
Post-treatment
C
WT
WT+Treat
LC-RIP1+Treat
RIP1
Tubulin
R-03
VHR-10
D
R-03
% Positive (of gated hCD19+ Cells)
Engraftment (%hCD19+)
MLKL/FADD
RIP3/FADD
RIP3/FADD/MLKL
RIP3/FADD/MLKL/CASP8
MLKL/RIP3
MLKL/CASP8
RIP3/CASP8
RIP3/FADD/CASP8
BFP+
MLKL
RIP3
CASP8
Day post injection
Daily Bir.
E
LC-BFP-FADD
LC-GFP-RIP3
LC-mCh-MLKL
LC-RFP657-CASP8
F
R-03 w non-targeted LentiCRISPRs
Engraftment
Day post injection
GFP+ BFP+
mCh+ 657+
GFP+ 657+
mCh+ BFP+
mCh+ GFP+
GFP+
mCh+
657+
BFP+
Daily Bir.
G
Untrans.
Unsorted
WT
MLKL/FADD
RIP3/FADD
MLKL/FADD/RIP3/CASP8
MLKL
FADD
RIP3
CASP8
RNAse P
(Loading control)

Fig. S4. In vivo birinapant treatment selects CRISPR-driven RIP1-deficient cells. (**A**) Patient-derived xenograft cells were transduced with LC-EGFP-RIP1 and injected into NSG mice. Mouse blood was examined weekly for engraftment and percentage of GFP+ cells via FACS. (**B**) PCR was performed to confirm integration of the RIP1-targeting sgRNA cassette in genomes of transduced patient cells after treatment with birinapant. (**C**) Cells derived from WT untreated control, WT after birinapant treatment, and LentiCRISPR-RIP1 after birinapant treatment were examined for RIP1 expression by western blot. (**D**) Patient-derived cells from patient sample R-03 were transduced with LentiCRISPR targeted against CASP8, FADD, RIP3, and/or MLKL, transplanted into NSG mice, and treated in vivo with birinapant as described in the text. Mouse peripheral blood was examined for engraftment and the different fluorescent markers at varying time points. Graphs show the total engraftment (top), the percentage of each double, triple, and quadruple positive population (middle), and the percentage of each single positive population (bottom) among total blood lymphocytes. (**E**) Human $CD19^+$ cells were examined by hierarchical gating for expression of fluorescent tags as shown. (**F**) Cells from patient sample R-03 were transduced with non-targeted lentiCRISPRs expressing various fluorescent proteins. The experiment was performed as above. Graphs show the total engraftment (top) and the percentage of each population among total blood lymphocytes (bottom). (**G**) Sorted and re-transplanted ALL cells were examined for the presence of specific sgRNA by PCR. For all experiments shown in this figure, n = 1 mouse.

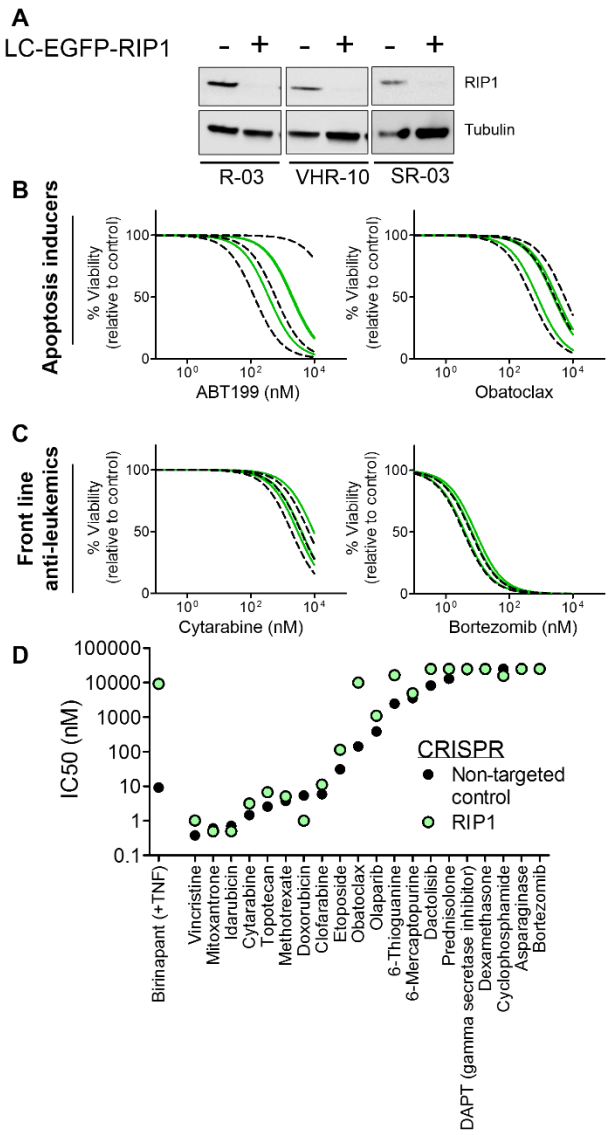

Fig. S5: **RIP1 is not required for response to a wide range of chemotherapeutic agents.** Control and RIP1-CRISPR cells derived from 3 patient samples (R-03, VHR-10, and SR-03) were examined for response to a variety of chemotherapeutic agents using in vitro co-culture with MSCs as described in the text. (**A**) Cells from LC-EGFP-RIP1 and WT cells for each patient sample were first examined for RIP1 expression via western blot. The response curves for (**B**) intrinsic apoptosis-inducing compounds and (**C**) front line anti-leukemic compounds are shown. (**D)** Non-targeted (black) and 658w-LC-EGFP-RIP1 CRISPR (green) cells were examined for response to a number of chemotherapeutic compounds.

Table S1: **Patient characteristics.**

(**A**) Patient characteristics for B cell precursor ALL samples tested

Patient-ID/ risk group	Clinical stage	Additional information (translocations)	Age (years)	Sex	Clinical prednisolone response	Outcome	Birinapant IC50 (nM)	LCL161 IC50 (nM)
SR-03	diagnosis		3.4	female	G	CCR	0.2398	4.86
HR-09	diagnosis	HHD	3.4	female	G	R	0.2519	99.9
SR-04	diagnosis	E2A-PBX1_T(1;19)	3.6	female	G	CCR	0.3636	>7500
R-03	relapse (MNR)	Hyperdiploid	5.7	female	ND	D	0.3903	52.5
VHR-10	diagnosis		14.4	female	P	CCR	0.5557	332.6
R-18	relapse (MNR)		11.2	female	ND	NA	0.7284	>1500
HR-08	diagnosis	MLL-AF4_T(4;11)	0.3	female	G	CCR	1.8	ND
SR-13	diagnosis		4.2	female	G	CCR	5.424	>7500
VHR-03	diagnosis		17.2	male	P	TD	5.918	137
R-01	relapse (MNR)	p53 mutated	9.6	female	ND	D	24.52	388
R-10	relapse (MNR)		9.7	male	ND	D	26.91	5725
VHR-30	diagnosis		9	female	P	D	41.22	1302
VHR-27	diagnosis		2.8	male	G	CCR	57.72	1011
HR-26	diagnosis	MLL-AF4_T(4;11)	12.6	female	G	NA	72.5	ND
R-14	relapse (MNR)		10.3	male	ND	D	83.31	>7500
VHR-02	diagnosis		12.8	female	P	R	100	5000
R-20	relapse		10.7	male	G	NA	204	>7500
SR-22	diagnosis	E2A-PBX1_T(1;19)	14.5	female	P	CCR	286.5	>7500
SR-02	diagnosis	Amplification AML1	12.2	male	G	CCR	378.2	1292
SR-01	diagnosis		10.5	male	G	CCR	398.2	4893
SR-10	diagnosis		7.3	male	G	CCR	424.5	597
R-12	relapse (MNR)		11.8	male	ND	NA	466.8	>7500
VHR-07	diagnosis	MLL-AF4_T(4;11)	11.7	male	P	CCR	522.4	2091
HR-03	diagnosis	BCR-ABL_T(9;22)	16.9	female	G	CCR	526.7	>7500
VHR-25	diagnosis	Trisomy 8	17.1	female	P	NA	545.7	ND
SR-08	diagnosis	E2A-PBX1_T(1;19)	12.8	female	G	CCR	552.3	4548

SR-12	diagnosis	E2A-PBX1_T(1;19)	10.4	male	G	CCR	567.3	3477
SR-24	diagnosis	E2A-PBX1_T(1;19)	15.4	female	P	CCR	601	4287
R-09	relapse (MNR)		3.3	male	ND	D	615.6	2432
SR-11	diagnosis		6.1	male	G	R	783	>7500
HR-11	diagnosis	DS-ALL , MLL-ENL_T(11;19)	16.1	female	G	CCR	917.7	>7500
SR-14	diagnosis	ETV6-RUNX1_T(12;21)	5.8	male	P	NA	1028	>7500
R-04	relapse (MNR)		9.8	male	ND	D	1090	>7500
MR-01	diagnosis	E2A-PBX1_T(1;19)	14.5	female	P	CCR	1352	>7500
HR-21	diagnosis	E2A-HLF_T(17;19)	15.5	female	G	TD	1404	>1500
VHR-28	diagnosis	BRC-ABL_T(9;22), HHD	16.9	female	G	CCR	≥1500	>7500
SR-09	diagnosis		5.5	female	G	R	≥1500	>7500
R-24	diagnosis	E2A-HLF_T(17;19)	15.5	male	G	D	≥1500	>7500
HR-25	diagnosis	E2A-HLF_T(17;19)	14.7	male	G	D	≥1500	>7500
VHR-06	diagnosis	E2A-PBX1_T(1;19), ETV6-RUNX1_T(12;21), complex karyotype	17.6	male	G	D	≥1500	>7500
VHR-12	diagnosis		15.3	female	G	R	≥1500	>7500
HR-20	diagnosis	E2A-HLF_T(17;19)	16.6	male	G	TD	≥1500	>7500
VHR-04	diagnosis		5.7	female	G	CCR	≥1500	>7500
VHR-01	diagnosis	E2A-HLF_T(17;19)	14.1	male	P	R	≥1500	>7500
R-19	relapse (MNR)		9.8	female	ND	NA	≥1500	ND
R-17	relapse (MNR)	p53 mutated	15.2	male	ND	NA	≥1500	>7500
HR-13	diagnosis	BRC-ABL_T(9;22)	9.1	male	G	CCR	≥1500	>7500
SR-21	diagnosis	E2A-PBX1_T(1;19)	14.6	male	G	CCR	≥1500	>7500
HR-10	diagnosis	MLL-AF4_T(4;11)	0.08	male	P		≥1500	>7500
R-07	relapse of HR-26 (MNR)	MLL-AF4_T(4;11)	12.6	female	ND	D	≥1500	ND
VHR-15	diagnosis	Deletion 9p	13.2	male	P	CCR	≥1500	>7500

(**B**) Patient characteristics for T cell ALL samples tested

Patient-ID/ risk group	Clinical stage	Additional information (translocations)	Age (years)	sex	prednisolone response	Outcome	Birinapant IC50 (nM)
T-MR-15	diagnosis		5.4	male	G	R	203.5
T-VHR-26	diagnosis		3.8	female	P	R	450.6
T-MR-02	diagnosis		4.6	female	G	TD	622.5
T-R-11	relapse		18.8	male	NA	D	901
T-VHR-09	diagnosis		2.3	male	P	TD	908.7
T-HR-10	diagnosis		2.2	male	P	R	914.7
T-R-15	relapse		3.1	male	NA	D	≥1500
T-MR-16	diagnosis	T(4;7)	11	male	G	R	≥1500
T-HR-15	diagnosis		18	male	P	R	≥1500
T-SR-01	diagnosis		2	male	P	CCR	≥1500
T-MR-04	diagnosis		14.3	male	G	CCR	≥1500
T-MR-17	diagnosis		9	male	G	CCR	≥1500

SR – standard risk*
MR – medium risk*
HR – high risk*
VHR – very high risk*
R – relapse
G – good
P – poor
MNR – morphological non-responder (did not reach a bone marrow remission after induction and intensification chemotherapy at relapse)
CCR – complete responder
R – relapse
TD – toxic death before CCR
D – death

HHD – high hyperdiploid
DS-ALL – down syndrome ALL
ND: not determined
NA: not available

* according to ALL-BFM 2000 risk stratification criteria

Table S2: sgRNA targeting sequences used for gene disruptions.

Gene	sgRNA targeting sequence
RIP1	GCTCTGCTGGGAAGCGAATC
RIP3	TACACGAGTGATGGTTCGGT
MLKL	ATCCCCGTGGATTCTGCTAA
FADD	ACTCCCGCACACGCTCTGTC
CASP8	GCCTGGACTACATTCCGCAA

Title: TNFR2 is essential for RIP1-dependent cell death in refractory ALL

Authors: Júlia Aguadé-Gorgorió[1], Scott McComb[1], Maria Pamela Dobay[2], Lena Harder[1], Blerim Marovca[1], Silvia Jenni[1], Gunnar Cario[3], Cornelia Eckert[4], Jean-Pierre Bourquin[1], Beat C. Bornhauser[1,*].

Affiliations:

[1]Department of Oncology and Children's Research Centre, University Children's Hospital Zürich, 8032 Zürich, Switzerland.

[2] SIB Swiss Institute of Bioinformatics, 1050 Lausanne, Switzerland.

[3]Department of General Pediatrics, University Hospital Schleswig-Holstein, 24105 Kiel, Germany.

[4]Department of Pediatric Oncology/Hematology, Charité Medical University Berlin, 13353 Berlin, Germany.

*Correspondence to: Beat Bornhauser, University Children's Hospital Zurich, August-Forelstrasse 1, CH-8008 Zurich, beat.bornhauser@kispi.uzh.ch, Phone, +41 44 634 8817; Fax, +41 44 634 88 59.

Abstract (150)

The identification of molecular determinants that regulate sensitivity to specific agents is essential for the development of new therapeutic approaches in cancer. We have earlier shown that a subset of refractory acute lymphoblastic leukaemia (ALL) samples respond to SMAC-mimetic induced IAP depletion by concurrently inducing RIP1-dependent apoptosis and necroptosis. Herein we show that this response correlates with the expression of TNF receptor 2 (TNFR2) in primary ALL. Using CRISPR/Cas9-mediated knockout of TNFR1 and 2 and in vivo selection with SMAC mimetics we show that TNFR1 and 2 are both functionally required for cell death. SMAC mimetics induced recruitment of RIP1 to TNFR1, which was abolished in cells deficient for TNFR2. Our data indicate that TNFR2 predicts sensitivity to SMAC mimetics and plays a key role in modulating a switch from RIP1-controlled cell survival to cell death.

Main text

Introduction

Refractory and relapsed disease are major clinical challenges in the treatment of acute lymphoblastic leukaemia (ALL), the most common paediatric malignancy[1,2]. Deficient apoptosis induction in response to standard chemotherapies and even in response to novel targeted therapies is one of the leading causes of relapse in ALL[3,4]. Therefore, drugs that activate alternative cell death mechanisms independently of apoptosis, such as necroptosis, may serve as strategies for the treatment of high risk malignancies.

Necroptosis is a recently discovered form of program cell death which exhibits morphological features distinct from apoptosis and is governed by independent molecular pathways[5]. RIP1 (receptor interacting protein kinase 1) is a central protein involved in the regulation of cell death by both apoptosis and necroptosis, as well as in survival and inflammation through the activation of NF-κB (nuclear factor kappa B) signalling[6]. After TNFα ligation, RIP1 is recruited to TNF receptor 1 (TNFR1) together with the inhibitor of apoptosis proteins (IAPs) cIAP1 and 2 among others. When ubiquitinated by cIAP1 and 2, RIP1 maintains survival[7]. IAPs can be targeted using compounds called SMAC (second mitochondria derived activator of caspases) mimetics (SM), leading to the deubiquitination of RIP1 and the subsequent switch from pro-survival to pro-death signalling. Consequently, RIP1 has been shown to form different complexes and induce apoptosis or necroptosis depending on the cellular context[8–11]. TNFR2, a member from the same TNFR superfamily, is not considered a death receptor because it lacks a death domain, a feature required for the recruitment of key proteins involved in the initiation of death signalling such as FADD (Fas associated death domain) or RIP1[12]. However, TNFR2 has been shown to crosstalk with TNFR1 and potentiate cell death under certain conditions[12–15], mostly through the degradation of TRAF2 (TNF receptor associated factor 2) and the consequent abrogation of pro-survival NF-κB signalling[13,16–18].

We previously described that the SM birinapant potently induces RIP1-dependent cell death in a subset of B-ALL patient-derived samples by concurrent apoptosis and necroptosis[11]. However, the identification of molecular markers to preselect those patients with high likelihood to respond to SM still remains elusive. Here we show that the expression of *TNFR2* correlates with and predicts the response of primary B-ALL to birinapant, and could be used to preselect responsive patients. We also show that TNFR2 can sensitize to TNFR1- and RIP1-mediated cell death. Furthermore, we used clustered regularly interspaced short palindromic repeats (CRISPR) to show that both TNFR1 and TNFR2 are required for SM sensitivity, and TNFR2 facilitates the recruitment of RIP1 to TNFR1 in response to birinapant. This represents a new role for TNFR2 in the regulation of RIP1-dependent cell death pathways including apoptosis and necroptosis.

Results

TNFR2 expression correlates with the response to birinapant in B-ALL patient-derived cells

We previously showed that the SM birinapant potently induces cell death by RIP1-dependent apoptosis and necroptosis in a significant proportion of patient-derived B-ALL samples, both *in vitro* and *in vivo*. However, the response to birinapant does not correlate with the protein levels of the molecular targets of birinapant (cIAP1, cIAP2 and XIAP), with RIP1, nor with its downstream apoptotic and necroptotic mediators (FADD, Caspase-8, RIP3, and MLKL (mixed lineage kinase domain like)). Additionally, the differences between responders and non-responders could not be explained by a differential expression of TNFα[11].

To find a molecular marker associated with the response to SM, we compared gene expression profiles of 6 samples with high (IC50≤100nM) and 11 with low sensitivity (IC50>100nM) to SM[19] (Supplementary Table 1). The correlation of gene expression with the sensitivity to SM using IC50 values for two SM, birinapant and LCL161, revealed *TNFRSF1B*, encoding TNFR2, and *TNFRSF1A*, encoding TNFR1, among the highest scoring genes (Fig. 1a,b and Supplementary Fig. 1a,g). Among the genes associated with low sensitivity to SM we identified *TRAF6* (TNF receptor associated factor 6), and *ADAM17*, encoding the TNF alpha converting enzyme (TACE) (Fig. 1a). As shown earlier[11], the expression of *RIPK1* (encoding RIP1), *RIPK3* (encoding RIP3), *MLKL*, *FADD*, or *TNF* did not correlate with the response to SM (Supplementary Fig. 1b-g).

To validate those results, we performed quantitative PCR (qPCR) and confirmed the significantly higher expression of *TNFR1* and *TNFR2* in responders compared to non-responders (Fig. 1c,d). Although the difference in expression of *TNFR1* in the two groups is significant, the variance is modest, making it a poor discriminatory marker (Fig. 1c and Supplementary Fig. 1a,g). Birinapant treatment *in vitro* had no significant effect on the expression of *TNFR1* or *TNFR2* (Fig. 1e). In contrast to *TNFR1*, *TNFR2* expression showed a good correlation with SM response, with a wide variance in expression, which was confirmed by flow cytometry although the general levels are low (Fig. 1f,g and Supplementary Fig. 1g). These data show that the expression of *TNFR2* correlates with the response to SM in a molecularly heterogeneous cohort of B-ALL patient-derived xenografts.

TNFR2 expression predicts the response of primary B-ALL to birinapant

We tested the predictive value of *TNFR2* expression using an independent cohort of relapsed primary samples obtained from the BFM ALL-REZ trial. *TNFR1* and *TNFR2* expression were quantified by qPCR from peripheral blood samples of 96 B- and T-ALL cases with only samples with at least 85% of leukemic blasts in peripheral blood being included (44 B- and 7 T-ALL, Supplementary Table 2). From those, 10 B-ALL samples were selected according to their *TNFR2* expression (Fig. 2a, 5 with the highest expression in blue and 5 with the lowest in red). The selected primary samples were then

blinded and screened for their response to increasing concentrations of birinapant using a co-culture model of the bone marrow microenvironment and automated quantification of live cells[11,20]. The primary samples with high *TNFR2* expression showed significantly higher sensitivity to birinapant compared to samples with low *TNFR2* expression (median IC50 of 37.4 nM vs 1310 nM, Fig. 2b,c). Corroborating these results, we could also observe a significant correlation between *TNFR2* expression and IC50 for this independent cohort (Pearson r -0.7071, p=0.0111) (Fig. 2d). To determine the cell death phenotype (i.e. apoptosis and/or necroptosis) induced by birinapant in these primary samples, we analysed the rescue in cell viability achieved by an apoptosis inhibitor (the pan-caspase inhibitor zVAD-fmk), an inhibitor of RIP1 kinase activity (necrostatin-1, short Nec) or the combination of both. 3 out of 5 samples were rescued only with the combination of zVAD and Nec, indicating a mostly mixed phenotype of apoptosis and necroptosis upon birinapant treatment, one sample was mostly necroptotic and another one was sensitive to Nec (Fig. 2e). This mirrors a similar distribution to what we previously described[11]. Using these samples, we also confirmed the stability of *TNFR2* expression after xenografting the primary blood samples (Supplementary Fig. 2a). These results indicate that the quantification of *TNFR2* expression from leukemic blasts in B-ALL patients or derived xenografts could be used to predict the response to birinapant *in vitro*, suggesting a methodology to preselect responsive patients.

TNFR2 expression sensitizes leukaemia cell lines to TNFα in a TNFR1- and RIP1-dependent manner

TNFR2 has not classically been described as a death receptor, as it does not contain a death domain at its cytoplasmic part[12]. To understand the role of TNFR2 in birinapant-induced cell death we overexpressed either full length human TNFR2 (+TNFR2) (Fig. 3a) or the extracellular domain of TNFR2 (aa 1-257) fused to the intracellular domain of the human TRAILR3 (aa 157-269), which is not involved in cell death signalling (TNFR2-ED) (Fig. 3b) using lentiviral constructs[21]. The transduction of the leukaemia cell lines with these constructs resulted in a stable overexpression of TNFR2 or TNFR-ED and had no effect on the levels of TNFR1 as determined by flow cytometry (Fig. 3c,d and Supplementary Fig. 3a). As has previously been observed[15,16,22], the overexpression of TNFR2 rendered ALL cells strikingly sensitive to TNFα, both in originally mildly TNFα-sensitive (Jurkat) or originally TNFα-resistant (Nalm6, 658) cell lines (Fig. 3e). Of note, +TNFR2 cells were not sensitized to birinapant treatment alone (Supplementary Fig. 3b). The sensitization to TNFα was dependent on the expression of TNFR1, since overexpression of TNFR2 in TNFR1 knockout cells (LC.TNFR1) generated by CRISPR-mediated genome editing did not sensitize to TNFα (Fig. 3f,g and Supplementary Fig. 3c,d).

It has been previously reported that TNFR2 can increase TNFR1-mediated signalling by accumulating TNFα at the membrane and facilitating its binding to TNFR1 (ligand passing effect)[23]. To test this

hypothesis we overexpressed TNFR2-ED (Fig. 3b) and analysed the cell viability in response to TNFα (Fig. 3h). We could not observe any sensitization, indicating that the external domain of TNFR2 is not sufficient to mediate TNFR1-dependent TNFα-induced cell death, discarding thus the hypothesis of a ligand passing effect.

We have previously described that Jurkat cells undergo concurrent apoptosis and necroptosis in response to birinapant with TNFα (Bir+TNF), modelling the response of patient-derived B-ALL cells to birinapant[11]. To determine the death phenotype of +TNFR2 cells in response to TNFα, we co-treated the cells with zVAD, Nec, or the combination of both. In agreement with the response to Bir+TNF described previously, Jurkat +TNFR2 cells showed a mixed death phenotype, while Nalm6 and 658 were purely apoptotic (Fig. 3i). The induction of concurrent apoptosis and necroptosis in Jurkat cells suggests a potential role of RIP1 in the TNFR2-mediated response to TNFα. Indeed, knocking out RIP1 by CRISPR-mediated genome editing (LC.RIP1) rescued Jurkat, as well as Nalm6 cells from TNFR2-mediated sensitization to TNFα, while 658 cells remained unaffected (Fig. 3j,k and Supplementary Fig. 3e). Taken together, these results support a role for TNFR2 in TNFR1- and RIP1-dependent cell death and provide evidence for a functional role of *TNFR2* expression in primary ALL samples for the sensitivity to SM.

The TNFR2-mediated response to TNFα or birinapant is not due to differential NF-κB activation

TNFR2 signalling can lead to the activation of the canonical and non-canonical NF-κB pathways, as well as to the inhibition of the canonical form through the degradation of TRAF2[13,14,24–26]. In order to investigate if alterations in NF-κB activation underlie TNFR2-mediated death signalling, we performed time course experiments in WT and +TNFR2 cells and evaluated the activation of the non-canonical (p100-p52) and canonical (phosphorylated p65) NF-κB markers. As expected, TNFα treatment lead to an increased degradation of TRAF2 in +TNFR2 cells compared to wild type. However, this had no major effect on the activation of p100 to p52 nor on the phosphorylation of p65. In contrast, treatment with the SM birinapant did not induce TRAF2 degradation in TNFR2+ cells, and only marginally activated non-canonical NF-kB signalling (Fig. 4a and Supplementary Fig. 4a). To confirm these findings in patient-derived cells, we performed time course experiments in SM-responding and non-responding cases. We previously reported that the activation of the canonical NF-κB does not correlate with the response to birinapant[11]. We now observed that there are no consistent differences in non-canonical NF-κB activation that could explain the differential sensitivity to birinapant (Fig. 4b). We also confirmed this by quantifying the expression levels of *cIAP2*, a known target gene of NF-κB, after birinapant treatment. We could not observe consistent differences between responders and non-responders (Supplementary Fig. 4b). Additionally, TRAF2 levels remained stable

after treatment with birinapant in all 6 cases (Fig. 4b). These data show that the sensitizing role of TNFR2 to TNFα or birinapant cannot be explained by differential activation of NF-κB signalling.

Birinapant treatment leads to the recruitment of RIP1 to TNFR1

Since birinapant induces RIP1-dependent cell death and TNFR2 can sensitize to cell death through the TNFR1/RIP1 axis, we hypothesized that the recruitment of RIP1 to TNFR1 might be influenced by the different levels of TNFR2 in responders and non-responders. In order to study this, we overexpressed 3xFlag RIP1 (RIP1-Flag) (Supplementary Fig. 5a) in Jurkat RIP1-/- cells. Reconstitution of RIP1 expression in Jurkat RIP1-/- cells restored sensitivity to Bir+TNF (Supplementary Fig. 5b,c). Flag-directed immunoprecipitations (IP) revealed a strong interaction between TNFR1 and RIP1 after 10 minutes of treatment with Bir+TNF (Fig. 5a). We analysed this interaction in birinapant-responder patient-derived cells (R-03) by immunoprecipitating the endogenous TNFR1 at different time points after birinapant treatment. We observed a strong recruitment of RIP1 after 2 and 6 hours of treatment. Also, the cleaved fragment of RIP1, produced by the proteolytic activity of caspase-8[27], was present in this TNFR1-associated complex (Fig. 5b). Interestingly, we observed a decrease of the total TNFR1 after treatment, which could be rescued by the inhibitor of the TNF alpha converting enzyme (TACE) TAPI-0, indicating that the decrease was due to TNFR1 shedding (Supplementary Fig. 5d). We confirmed recruitment of RIP1 to TNFR1 upon birinapant treatment in two more SM-sensitive patient samples (Fig. 5d). In contrast, no recruitment of RIP1 to TNFR1 was detected in samples that did not respond to birinapant (Fig. 5c,d). Finally, we wanted to demonstrate the functional relevance of this recruitment and exclude that this was not simply a consequence of the differential cell death induced in responders and non-responders. Therefore, we used cells derived from R-03 (responder) with a quadruple knockout for the apoptotic and necroptotic genes FADD, Caspase-8, RIP3 and MLKL (QUADko), which are resistant to birinapant[11]. Birinapant induced RIP1 recruitment to TNFR1 in the QUADko similarly to the WT, indicating that this interaction is upstream of cell death. In contrast to this, TNFR1 shedding did not occur in QUADko, indicating this is a downstream consequence of cell death (Fig. 5e).

Taken together, these data show that birinapant induces RIP1 recruitment to TNFR1 in SM-sensitive but not in SM-insensitive samples, and that this recruitment is not a consequence of cell death, but likely a cause.

TNFR2 is necessary for the response to birinapant

Considering the previous results, we wanted to definitively elucidate the functional importance of TNFR2 for the response to birinapant in patient-derived samples. For this we used a CRISPR-based *in vivo* selection approach as previously described[11]. In short, patient-derived ALL cells were transduced with lentiCRISPR targeting either *TNFR1* (LC.TNFR1) or *TNFR2* (LC.TNFR2) and expressing the fluorescent marker mCherry and BFP respectively, and subsequently xenotransplanted into

immunodeficient NSG mice. The total engraftment (human CD45/CD19 double positive cells), as well as the percentage of mCherry or BPF positive cells were monitored weekly in the peripheral blood. After 30% human cells were detected, the mice were treated with birinapant daily. We could observe a selective outgrowth of the *TNFR1* (Fig. 6a) and *TNFR2* knockout cells (Fig. 6b and Supplementary Fig. 6a) under birinapant treatment, indicating that both TNFR1 and TNFR2 are necessary for the response to birinapant. Interestingly, both *TNFR1* and *TNFR2* knockout patient-derived cells showed a steady engraftment in the absence of birinapant, indicating that B-ALL patient-derived cells don't depend on their signalling for proliferation (Fig. 6a,b). We collected *TNFR1*- and *TNFR2*-deficient cells after *in vivo* selection, expanded them in secondary xenografts without any further selection. Further corroborating a functional role for TNFR1 and 2 in the response to SM, both *TNFR1*- and *TNFR2*-deficient ALL cells did not respond to birinapant *ex vivo* (Fig. 6c). We could demonstrate the loss of both receptors in the respective xenografts by western blot (Fig. 6d). Similarly, we could confirm this functional importance of TNFR1 and TNFR2 for the response to SM in two more primary ALL samples (Fig. 6e-h and 6i-k). Of note, we could not detect any effect of *TNFR2* knockout on the activation of the canonical and the non-canonical NF-κB pathways (Supplementary Fig. 6b-c). These results support a functionally relevant role for TNFR2, next to its predictive capacity, for the response to the SM birinapant.

TNFR2 is necessary for RIP1 recruitment to TNFR1 in response to birinapant

Based on the requirement of TNFR1, TNFR2 and RIP1 for the response to birinapant, and on increased recruitment of RIP1 to TNFR1 in responders compared to non-responders, we wanted to know if this effect was directly caused by TNFR2. We interrogated TNFR1 immunoprecipitates WT and +TNFR2 Jurkat cells at different time points after TNFα treatment. +TNFR2 Jurkat cells showed a faster and increased association of RIP1 and TNFR1 in response to TNFα treatment than WT (Fig. 7a). Likewise, the recruitment of RIP1 to TNFR1 after birinapant treatment in SM-responsive patient-derived cells was completely abolished in TNFR2ko cells, indicating that the presence of TNFR2 determines the response to birinapant by modulating RIP1 recruitment to TNFR1 (Fig. 7b). In conclusion, we propose a model in which TNFR2 sensitizes to RIP1-dependent cell death by promoting its interaction with TNFR1, as underlying cause for its predictive value for the response to birinapant in primary B-ALL samples (Fig. 7c).

Discussion

The successful application of novel targeted therapies for cancer treatment requires the parallel discovery of predictive biomarkers in order to preselect the patients with the highest chance to benefit. Compounds from the SM family showed promising preclinical results against hematologic malignancies[11,28–32]. However, only subsets of patient samples responded, which remain still to be fully characterized. Here we describe that *TNFR2* expression is higher in SM-responders, and predicts

the response of primary cases *in vitro*. TNFR2 expression in ALL cell lines sensitizes to TNFα in a TNFR1- and RIP1-dependent manner. Furthermore, we used CRISPR/Cas9 gene editing in patient-derived cells to show that both TNFR1 and TNFR2 are required for the response to SM. By immunoprecipitating the endogenous TNFR1 in patient-derived B-ALL we show that RIP1 is recruited to TNFR1 in response to SM only in SM-responders, and this recruitment is abolished in TNFR2ko as well as in non-responders.

Quantification of *TNFR2* expression could be used to pre-select patients for clinical trials and might improve their outcome. However, the detection of TNFR2 by FACS, a methodology easily applicable to routine ALL diagnostics, is low and establishing a threshold criteria to assign patients to TNFR2–high or –low groups is difficult. Better antibodies or alternative detection methods would need to be established.

While TNFR1 is expressed pleiotropically in all cells, the expression of TNFR2 is restricted to specific cell types, including immune cells such as B- and T-cell subsets[33]. This might explain the low single agent activity of SM against many solid tumours compared to hematologic malignancies. However, the correlation of TNFR2 expression with the response to SM, as well as its contribution to TNFR1- and RIP1-mediated cell death have yet to be explored in other cancer entities.

Despite not being classified as a death receptor, TNFR2 has been implicated in the regulation of TNFα-induced cell death. Previous reports described a ligand passing effect, according to which TNFR2 could increase the concentration of TNFα at the cell surface and facilitate its interaction with TNFR1[23]. Others also described a sensitizing effect of TNFR2 caused by its degradation of TRAF2 and the inhibition of the TNFR1-induced canonical NF-κB pathway, which in turn lead to decreased transcription of anti-apoptotic proteins and increased TNFα-induced cell death[13,16,17,34]. Additionally, TNFR2 stimulation has been shown to increase TNFα production, leading to autocrine TNFα signalling and cell death[15,18,35]. We ruled out the possibility of a ligand passing effect in our system by overexpressing TNFR2-ED, and we did not observe any consistent differences in the activation of NF-κB that could explain the different sensitivity. Furthermore, we could not detect any differences in TNFα expression between responders and non-responders[11].

The use of CRISPR/Cas9 in patient-derived cells represents an exceptional tool to study signalling pathways in a clinically relevant model, and coupled with an *in vivo* selection approach it allows the discovery of molecules that are key for the response to a particular drug. Here we show that the presence of TNFR2 is required for the recruitment of RIP1 to TNFR1 upon birinapant treatment and is the cause for the differential response among patient-derived B-ALL samples. The effect of TNFR2 on the recruitment of RIP1 to TNFR1 was also described by Chan et al., who observed that TNFR2 pre-stimulation increased TNFR1-mediated necroptosis in Jurkat cells through an enhanced

recruitment of RIP1 to TNFR1[36]. However, TNFR2 had not been implicated in the response to SM to date, indicating a novel role of TNFR2 in the regulation of cell death.

The exact mechanism by which TNFR2 mediates the recruitment of RIP1 to TNFR1, and the mechanism by which the two receptors cooperate in the induction of cell death in response to SM still remain elusive and need to be further investigated. Understanding the detailed mechanism by which TNFR2 sensitizes to SM could provide insight into effective drug-combination strategies for high risk patients and could help establish biomarkers of SM response.

Materials and Methods

Gene expression profiles

Gene expression profiles of patient-derived B-ALL samples were previously published[19]. In short, bone marrow or peripheral blood samples with more than 80% blasts were used. After RNA extraction and cDNA synthesis, spotted cDNA microarrays containing more than 43,000 features and representing around 30,000 genes were used (Stanford Functional Genomics Facility, Stanford, CA, USA). Gene expression profiles were correlated with responses (IC50) to Birinapant and LCL161 using Pearson correlation. Joint correlation coefficients (JCC) were calculated from the sum of the Pearson coefficients; genes with significant ($p < 0.05$) correlation to IC50 were arranged as a function of decreasing JCC (top to bottom) and drug response IC50 values (left to right). All gene expression values are shown in a mean-centered and scaled heatmap (R package NMF_0.20.6).

Quantitative real time PCR (qPCR)

RNA was extracted using the RNAeasy® Mini Kit (Quiagen, Cat# 74106). Reverse transcription was performed with MultiScribe RT transcriptase (Life Technologies, Cat# 4311235). Real time PCR was performed with TaqMan® Gene Expression Master Mix (Applied Biosystems, Cat# 436916) and the following probes: TNFRSF1A (Cat# Hs01042313), TNFRSF1B (Cat# Hs00961749), MLKL (Cat# Hs04188508) and GAPDH (Cat# Hs02758991) from Life Technologies. PCR reaction was performed using a 7900HT Fast Real-Time PCR System (Applied Biosystems) and SDS 2.3 software. The quantification was performed in triplicates.

Reagents and antibodies

The following antibodies were used for western blot and/or IP: rabbit anti-TNFR1 (Cat# 3736), rabbit anti-TNFR2 (Cat# 3727), rabbit anti-cIAP2 (Cat# 3130), rabbit anti-TRAF2 (Cat# 4712), rabbit anti-p100/p52 (Cat# 4842), rabbit anti-p65 (Cat# 4764), and rabbit anti-phospho-p65 (Cat#3033) were obtained from cell signaling. Mouse anti-RIP1 (Cat#51-6559) was from BD Biosciences, mouse anti-

cIAP1 (Cat# MAB818) from R&D, mouse anti-Flag (Cat# F1804, M2 clone) form Sigma-Aldrich, goat anti-TNFR2 (Cat# AB-226-PB) from R&D, and mouse anti-tubulin (Cat#081M4861) from Sigma-Aldrich. Goat anti-mouse and goat anti-rabbit from Cell Signaling (Cat# 7076 and 7074), donkey anti-goat (Cat# sc-2020) from Santa Cruz, and easy Blot anti-Rabbit and anti-mouse (Cat# GTX221666-01, GTX221667-01) conjugated to horseradish peroxidase were used as secondary antibodies. SuperSignal® West Femto Maximum Sensitivity Substrate (Thermo Scientific, Cat# 34096) was used for detection. For flow cytometry, TNFR1-APC (Cat# FAB225A) and TNFR2-PE (Cat# FAB226P) antibodies from R&D were used.

Recombinant human TNFα was purchased from Gibco/Life Technologies (Cat# PHC3011), birinapant (TL32711) for *in vitro* studies was purchased from Selleckchem (Cat# S7015) and from ChemieTek, (Cat# CT-Biri) for *in vivo* studies , Z-VAD-FMK was purchased from APExBIO (Cat# A1902, used at a final concentration of 25 µM), Necrostatin-1s was purchased from BioVision (Cat# 2263-1, used at a final concentration of 25 µM) and TAPI-0 (Cat# Ab141497) from Abcam.

Cell culture

Jurkat, Nalm6, patient-derived 658w cell lines and hTERT-immortalized primary bone marrow mesenchymal stromal cells (hTERT-MSC) were cultured in RPMI-1640 (Sigma-Aldrich, Cat# R0883) supplemented with 10% fetal bovine serum (Sigma-Aldrich), 0.5% L-glutamine (Bioconcept) and 0.5% penicillin-streptomycin (Life Technologies). The medium was also supplemented with 1 µM Hydrocortisone (Sigma-Aldrich, Cat# H0888) for hTERT-MSCs. Cells were incubated at 37 ºC and 5% CO2. Co-culture experiments with xenograft-derived primary cells were performed serum-free conditions in AIM-V® (Life Technologies, Cat# 12055-091).

Viability assays

Viability assays were performed as described previously[11]. For cell lines, 5000 cells were plated per well in 384-well plates and treated the following day as indicated. Cell viability was measured 48 hours after treatment using CCK-8 viability assay (Cat# CK04-11, from Dojindo molecular technologies) and a Synergy HT microplate Reader (BioTek). For patient-derived ALL cells, 2500 hTERT-MSC were plated in serum-free AIM-V medium (Cat# 12055-091, form Life Technologies). After 24 hours of incubation, 25000 ALL cells were added. The cells were treated the following day as indicated using HP D300 Digital Dispenser (Tecan). After 48 hours of treatment, live cells were stained with CyQUANT (Cat# C35012, from Life Technologies) and quantified using automated microscopy and multi-parametric image analysis as described previously[11,37].

Immunoprecipitations and immunoblotting

25 to 30 million cells were plated and treated as indicated in each case. The cells were collected, washed with cold PBS and lysed in RIPA buffer (150 mM NaCl, 20 mM Tris pH 7.5, 1% NP-40, 1 mM EDTA pH 8.0, 0.1% SDS) containing protease inhibitors (Roche Cat# 11836153001). For TNFR1 IPs, 20 µl of lysate were kept for input control and 5ul of anti-TNFR1 antibody (cell signaling, Cat# 3736) were added to the rest. The lysates were incubated with the antibody at 4ºC overnight and afterwards incubated with Dynabeads protein G (Cat# 1004D, from Life Technologies) at room temperature for 4h. The beads were washed 3 times with RIPA buffer and the complex was eluted by adding 1x SDS loading buffer (62.5nM Trips pH 6.8, 1%SDS, 0.005% Bromophenol Blue, 4% glycerol, 1% ß-mercaptoethanol) and boiling at 95ºC for 5 minutes.

For the 3xFlag IPs, 50 µl of Dynabeads protein G were incubated with 8 µg of anti-Flag antibody in 200ul PBS/0.02% tween for 20 min at room temperature. The lysates were then added to the beads and incubated for 4 hours at room temperature. The beads were washed 3 times with RIPA and eluted with 20 µl of 3xFlag peptide (Cat# F4799, Sigma-Aldrich) after incubating 20 minutes at room temperature. 10µ of 4xSDS were added and the samples were boiled at 95ºC for 5 minutes.

For western blot, $3x10^5$ cells were lysed in 1x SDS loading buffer. Cell lysates were separated by SDS-PAGE (Criterion™ XT Precast Gels, BIO-RAD, 4-12% Bis-Tris, Cat# 345-0125) and transferred onto nitrocellulose membranes (Trans-Blot Turbo transfer pack, BIO-RAD, Cat# 170-4159). Membranes were blocked with 5% non-fat milk or 5% BSA in the case of cIAP2.

Plasmids, constructs

Multicolor lentiCRISPR constructs were generated as previously published[11]. Various sgRNA sequences were tested and the most efficient as determined by western blotting were used for further experiments. The sgRNAs used for TNFR1 and TNFR2 are listed below. The sgRNAs used for RIP1, RIP3, MLKL, caspase-8 and FADD are published[11].

TNFR1	CACTCCAATAATGCCGGTAC
TNFR2	ACACACGGTGTCCGAGGTCT
TNFR2 (alternative sgRNA)	GGCATTTACACCCTACGCCC

The overexpression plasmids for TNFR2, TNFR2-ED, RIP1-Flag and RIP1m-Flag were generated on the pRCDRMB-EF1-MCS-2A-Bleo backbone plasmid (a gift from Dr. Laura Lopez Garcia). IRES-GFP was cloned into the EcoRI site using IRES-GFP fwd and rev primers and In-Fusion HD cloning (Cat# 639648, Clontech).

To generate the TNFR2 plasmid, the sequence for Ig-Flag-TNFR2 was cloned from the Ps520 plasmid obtained from Pascal Schneider[21] into the NheI site in the MCS by In-Fusion HD cloning using Ig-Flag-TNFR2 fwd and rev primers. A similar strategy was used to clone the sequence for Ig-TNFR2ED (1-257)-TRAILR3 (157-269) from the Ps1586 Plasmid obtained from Pascal Schneider[21]. In this case the primers used for infusion cloning were TNFR2-ED fwd and TRAILR3 rev.

To generate the RIP1-Flag plasmid, the 3xFlag tag was introduced into the NheI site using Flag fwd and Flag rev primers and In-Fusion cloning. The RIP1 coding sequence was cloned by PCR from cDNA from a patient-derived sample (SR-21) using specific In-Fusion primers RIP1 fwd and RIP1 rev. The PCR product was introduced into the XbaI site in the MCS by In-Fusion HD cloning.

To generate the RIP1m-Flag plasmid, the IRES-GFP sequence from the RIP1-Flag plasmid was first switched for an IRES-BFP sequence. For this, the IRES-BFP sequence was cloned from the plasmid pCVL.SFFV.Kozak.HA.NLS.Y2Ani.IRES.BFP (gift from Andrew Scharenberg, Addgene plasmid # 45578[38]) using specific In-Fusion primers IRES-BFP fwd and rev. The PCR product was then introduced into the RIP1-Flag plasmid after digestion with EcoRI (Cat# R0101S, New England Biolabs) by In-Fusion HD cloning. To generate the silent mutation in the PAM site of RIP1 targeted by the lentiCRISPR construct used, oligonucleotide-directed internal mutagenesis was performed with Phusion hotstart DNA polymerase (Cat# M0535S, New England Biolabs), DMSO and the primers RIP1mut fwd and rev. DpnI (Cat# R0176S, New England Biolabs) was added to the PCR product and incubated for 3h at 37ºC. The mutation was confirmed by sequencing.

Primer	Sequence
IRES-GFP fwd	TAGAGCTAGCGAATTCCCCCTCTCCCTCCCCCCC
IRES-GFP rev	ATTTAAATTCGAATTCTTACTTGTACAGCTCGTCCATGCCG
Flag fwd	CTACTCTAGAGCTAGCATGGACTACAAAGACCATGACGGTG
Flag rev	GGGGGAATTCGCTAGCTACTTGTCATCGTCATCCTTGTAATCG
Ig-Flag-TNFR2 fwd	CTACTCTAGAGCTAGCATGAACTTCGGGTTCAGCTTGA
Ig-Flag-TNFR2 rev	ATTCGAATTCGCTAGCTTAACTGGGCTTCATCCCAGCA
TNFR2-ED fwd	CTACTCTAGAGCTAGCATGGCGCCCGTCGCCGTCT
TRAILR3 rev	ATTCGAATTCGCTAGCTCAAACAAACACAATCAGAAGCAC
RIP1 fwd	CGGCGCCTACTCTAGAATGCAACCAGACATGTCCTTGA
RIP1 rev	CCATGCTAGCTCTAGAGTTCTGGCTGACGTAAATCAAGC
IRES-BFP fwd	TAGAGCTAGCGAATTCCCCCTCTCCCTCCCCCCC
IRES-BFP rev	ATTTAAATTCGAATTCTCAATTAAGCTTGTGCCCCAGT
RIP1mut fwd	TCTGCTGGGAAGCGAATCCAGAAGCTCGGCCGACATTTCC
RIP1mut rev	GAAATGTCGGCCGAGCTTCTGGATTCGCTTCCCAGCAGA G

Transduction and *in vivo* CRISPR selection studies

Lentivirus was produced transfecting 293T cells with psPAX2 (Addgene, #12260), p.CMV.VSV.G plasmid (Addgene, #8454), and each construct (lentiCRISPR, or the various overexpression constructs) using Polyethylenimin (PEI) transfection reagent (Sigma Aldrich, Cat# 408727). The cell supernatant was collected after 24h and added to the cells together with polybrene 8 µg/ml final concentration (Cat# H9268, Sigma Aldrich). For patient-derived cells, the supernatant containing the virus was concentrated 20x using PEG 6000 (Cat# 81253, Sigma Aldrich). 10^6 patient-derived ALL cells were incubated with the virus for 24 hours and washed 3 times with PBS before transplanting them intravenously into immunodeficient NOD/SCID/IL2rγnull (NSG) mice. Mice were bled weekly after xenotransplantation. After red blood cell lysis, the blood was stained with hCD19-PE-Cy7 (Biolegend, Cat# 302208), hCD45-Alexa Fluor 647 (Biolegend, Cat# 304018) and mCD45-eFluor 450 (eBioscience, Cat# 48-0451-82) and analysed by flow cytometry (performed in a FACS Canto II flow cytometer, BD Biosciences). For in vivo experiments birinapant was dissolved in 12% Captisol (Ligand Pharmaceuticals) with 0.1% Tris at pH 6.8. Birinapant was given daily by intraperitoneal injection at 30 mg/kg during the indicated periods. Animal samples sizes were chosen to minimize the number of animals used as inter-animal variation in leukemic engraftment was generally low. No animals were excluded from analysis. In vivo experiments were approved by the veterinary office of the Canton of Zurich.

Human samples

Xenografts were obtained from primary human ALL samples recovered from cryopreserved bone marrow aspirates or peripheral blood samples of patients enrolled in the ALL-BFM 2000, ALL-BFM 2009, and ALL-REZ-BFM 2002 studies. Informed consent was given in accordance with the Declaration of Helsinki, and approval was granted by the Ethics Commission of the Kanton Zürich (approval no. 2014-0383). Samples were classified as standard risk, medium risk, high risk, very high risk, morphological non-responders, or relapse samples according to the clinical criteria used in the ALL-BFM 2000 and ALL-REZ 2002 studies[39,40].

References

1. Hunger, S. P. & Mullighan, C. G. Acute Lymphoblastic Leukemia in Children. *New England Journal of Medicine* **373,** 1541–1552 (2015).
2. Locatelli, F., Schrappe, M., Bernardo, M. E. & Rutella, S. How I treat relapsed childhood acute lymphoblastic leukemia. *Blood* **120,** 2807–2816 (2012).
3. Holleman, A., den Boer, M. L., Kazemier, K. M., Janka-Schaub, G. E. & Pieters, R. Resistance to different classes of drugs is associated with impaired apoptosis in childhood acute lymphoblastic leukemia. *Blood* **102,** 4541–4546 (2003).
4. Holleman, A. The expression of 70 apoptosis genes in relation to lineage, genetic subtype, cellular drug resistance, and outcome in childhood acute lymphoblastic leukemia. *Blood* **107,** 769–776 (2006).
5. Vandenabeele, P., Galluzzi, L., Vanden Berghe, T. & Kroemer, G. Molecular mechanisms of necroptosis: an ordered cellular explosion. *Nature Reviews Molecular Cell Biology* **11,** 700–714 (2010).
6. Christofferson, D. E., Li, Y. & Yuan, J. Control of Life-or-Death Decisions by RIP1 Kinase. *Annual Review of Physiology* **76,** 129–150 (2013).
7. Bertrand, M. J. M. *et al.* cIAP1 and cIAP2 Facilitate Cancer Cell Survival by Functioning as E3 Ligases that Promote RIP1 Ubiquitination. *Molecular Cell* **30,** 689–700 (2008).
8. Varfolomeev, E. *et al.* IAP Antagonists Induce Autoubiquitination of c-IAPs, NF-κB Activation, and TNFα-Dependent Apoptosis. *Cell* **131,** 669–681 (2007).
9. Bai, L., Smith, D. C. & Wang, S. Small-molecule SMAC mimetics as new cancer therapeutics. *Pharmacology & Therapeutics* **144,** 82–95 (2014).
10. Fulda, S. Smac mimetics as IAP antagonists. *Seminars in Cell & Developmental Biology* **39,** 132–138 (2014).
11. McComb, S. *et al.* Activation of concurrent apoptosis and necroptosis by SMAC mimetics for the treatment of refractory and relapsed ALL. *Science Translational Medicine* **8,** 339ra70 (2016).
12. Cabal-Hierro, L. & Lazo, P. S. Signal transduction by tumor necrosis factor receptors. *Cellular Signalling* **24,** 1297–1305 (2012).
13. Naudé, P. J. W., den Boer, J. A., Luiten, P. G. M. & Eisel, U. L. M. Tumor necrosis factor receptor cross-talk. *FEBS J.* **278,** 888–898 (2011).
14. Cabal-Hierro, L. *et al.* A TRAF2 binding independent region of TNFR2 is responsible for TRAF2 depletion and enhancement of cytotoxicity driven by TNFR1. *Oncotarget* **5,** 224–236 (2014).
15. Grell, M. *et al.* Induction of cell death by tumour necrosis factor (TNF) receptor 2, CD40 and CD30: a role for TNF-R1 activation by endogenous membrane-anchored TNF. *EMBO J.* **18,** 3034–3043 (1999).
16. Weiss, T. *et al.* Enhancement of TNF receptor p60-mediated cytotoxicity by TNF receptor p80: requirement of the TNF receptor-associated factor-2 binding site. *J Immunol* **158,** 2398–2404 (1997).
17. Weiss, T. *et al.* TNFR80-dependent enhancement of TNFR60-induced cell death is mediated by TNFR-associated factor 2 and is specific for TNFR60. *J. Immunol.* **161,** 3136–3142 (1998).
18. Siegmund, D., Kums, J., Ehrenschwender, M. & Wajant, H. Activation of TNFR2 sensitizes macrophages for TNFR1-mediated necroptosis. *Cell Death Dis* **7,** e2375 (2016).
19. Cario, G. *et al.* Initial leukemic gene expression profiles of patients with poor in vivo prednisone response are similar to those of blasts persisting under prednisone treatment in childhood acute lymphoblastic leukemia. *Ann Hematol* **87,** 709 (2008).
20. Boutter, J. *et al.* Image-based RNA interference screening reveals an individual dependence of acute lymphoblastic leukemia on stromal cysteine support. *Oncotarget* **5,** 11501–11512 (2014).
21. Bossen, C. *et al.* Interactions of Tumor Necrosis Factor (TNF) and TNF Receptor Family Members in the Mouse and Human. *J. Biol. Chem.* **281,** 13964–13971 (2006).
22. Fotin-Mleczek, M. *et al.* Apoptotic crosstalk of TNF receptors: TNF-R2-induces depletion of TRAF2 and IAP proteins and accelerates TNF-R1-dependent activation of caspase-8. *Journal of Cell Science* **115,** 2757–2770 (2002).
23. Tartaglia, L. A., Pennica, D. & Goeddel, D. V. Ligand passing: the 75-kDa tumor necrosis factor (TNF) receptor recruits TNF for signaling by the 55-kDa TNF receptor. *J. Biol. Chem.* **268,** 18542–18548 (1993).

24. Li, X., Yang, Y. & Ashwell, J. D. TNF-RII and c-IAP1 mediate ubiquitination and degradation of TRAF2. *Nature* **416,** 345–347 (2002).
25. Rauert, H. *et al.* Membrane Tumor Necrosis Factor (TNF) Induces p100 Processing via TNF Receptor-2 (TNFR2). *J. Biol. Chem.* **285,** 7394–7404 (2010).
26. Cabal-Hierro, L. *et al.* TRAF-mediated modulation of NF-kB AND JNK Activation by TNFR2. *Cellular Signalling* **26,** 2658–2666 (2014).
27. Ofengeim, D. & Yuan, J. Regulation of RIP1 kinase signalling at the crossroads of inflammation and cell death. *Nat Rev Mol Cell Biol* **14,** 727–736 (2013).
28. Chromik, J., Safferthal, C., Serve, H. & Fulda, S. Smac mimetic primes apoptosis-resistant acute myeloid leukaemia cells for cytarabine-induced cell death by triggering necroptosis. *Cancer Letters* (2013). doi:10.1016/j.canlet.2013.10.018
29. Fulda, S. Inhibitor of Apoptosis (IAP) proteins in hematological malignancies: molecular mechanisms and therapeutic opportunities. *Leukemia* **28,** 1414–1422 (2014).
30. Belz, K. *et al.* Smac mimetic and glucocorticoids synergize to induce apoptosis in childhood ALL by promoting ripoptosome assembly. *Blood* **124,** 240–250 (2014).
31. Brumatti, G. *et al.* The caspase-8 inhibitor emricasan combines with the SMAC mimetic birinapant to induce necroptosis and treat acute myeloid leukemia. *Science Translational Medicine* **8,** 339ra69–339ra69 (2016).
32. Richmond, J. *et al.* Acute sensitivity of Ph-like acute lymphoblastic leukemia to the SMAC-mimetic birinapant. *Cancer Res.* (2016). doi:10.1158/0008-5472.CAN-16-0523
33. Richter, C. *et al.* The Tumor Necrosis Factor Receptor Stalk Regions Define Responsiveness to Soluble versus Membrane-Bound Ligand. *Mol. Cell. Biol.* **32,** 2515–2529 (2012).
34. Ting, A. T. & Bertrand, M. J. M. More to Life than NF-κB in TNFR1 Signaling. *Trends in Immunology* **37,** 535–545 (2016).
35. Faustman, D. & Davis, M. TNF receptor 2 pathway: drug target for autoimmune diseases. *Nat Rev Drug Discov* **9,** 482–493 (2010).
36. Chan, F. K.-M. *et al.* A Role for Tumor Necrosis Factor Receptor-2 and Receptor-interacting Protein in Programmed Necrosis and Antiviral Responses. *J. Biol. Chem.* **278,** 51613–51621 (2003).
37. Fischer, U. *et al.* Genomics and drug profiling of fatal TCF3-HLF-positive acute lymphoblastic leukemia identifies recurrent mutation patterns and therapeutic options. *Nat Genet* **47,** 1020–1029 (2015).
38. Kuhar, R. *et al.* Novel fluorescent genome editing reporters for monitoring DNA repair pathway utilization at endonuclease-induced breaks. *Nucleic Acids Res.* **42,** e4 (2014).
39. Bonapace, L. *et al.* Induction of autophagy-dependent necroptosis is required for childhood acute lymphoblastic leukemia cells to overcome glucocorticoid resistance. *Journal of Clinical Investigation* **120,** 1310–1323 (2010).
40. Schmitz, M. *et al.* Xenografts of highly resistant leukemia recapitulate the clonal composition of the leukemogenic compartment. *Blood* **118,** 1854–1864 (2011).

Acknowledgements and funding

This work was supported by the "Stiftung Kinderkrebsforschung Schweiz", the MAM-Fonds of the Children's Research Centre of the University Children's Hospital Zurich, the Empiris foundation, the clinical research focus program "human hemato-lymphatic diseases" of the University of Zurich, the Swiss Cancer League (KFS 3609-02-2015), the Novartis Foundation for Biomedical Research, the Swiss national Science Foundation SNF (310030-133108), the Canadian institutes for health research CIHR, the Forschungskredit of the University of Zurich (FK-14-016) and the Fondation Panacée.

Author contributions: J.A.-G., S.M., MP.D, L.H., B.M., S.J. performed experiments and analyzed data, G.C., and C.E. provided samples and clinical data, J.A.-G., S.M., JP.B., and B.C.B. wrote the manuscript, JP.B. and B.C.B. conceived and supervised the study.

Competing interests: All authors declare no conflict of interest.

Figure legends

Figure 1 Identification of TNFR2 as a marker of SM-responsive B-ALL. (**a**) Gene expression profiles for 17 patient-derived B-ALL samples and joint correlation coefficients calculated from the sum of Pearson coefficients for each gene with the IC50 for birinapant and LCL161 (see Materials and Methods). Only genes with significant ($p < 0.05$) correlation are shown. All gene expression values are shown in a mean-centered and scaled heatmap. (**b**) Expression of *TNFRSF1B* (encoding TNFR2) in the 17 cases. (**c,d**) Expression of *TNFR1* and *TNFR2* in 12 responsive (IC50≤100 nM) and 22 non-responsive (IC50>100 nM) patient-derived B-ALL cases as quantified by qPCR. n=1 experiment in triplicates for the indicated number of samples. (**e**) Expression of *TNFR1* and *TNFR2* in 16 and 15 cases respectively before and after treatment with birinapant (50 nM) for 6h. n=1 experiment in triplicates for the indicated number of samples. (**f,g**) Histograms (**f**) and quantification (**g**) of TNFR2 levels by flow cytometry in 8 responders and 11 non-responders. n=1 experiment for 19 samples. For quantifications in **c**, **d**, **e**, and **g**, data representing mean±s.e.m. (standard error of the mean) were derived from the indicated number of measurements.

Figure 2 *TNFR2* expression predicts the response to birinapant in an independent cohort. (**a**) Expression of *TNFR1* and *TNFR2* was quantified by qPCR for 44 B-ALL and 7 T-ALL peripheral blood samples with ≥ 85% leukemic blasts. n=1 experiment for 51 samples. Measurements were performed at least in duplicates. (**b-d**) 5 samples with the highest (in blue) and 5 samples with lowest (in red) *TNFR2* expression were blinded and screened for the response to birinapant *in vitro*. n=1 experiments in triplicates. (**b**) Drug response curves, (**c**) calculated IC50 values, and (**d**) correlation

with the expression levels for the 10 screened cases. (**e**) Cells were co-treated with an apoptosis inhibitor (+zVAD, 25 µM), the RIPK1 kinase inhibitor necrostatin-1 (+Nec, 25 µM), and the combination (+Nec+zVAD). The cell death phenotype is determined by the rescue achieved by each inhibitor or the combination at the IC50 concentration. Necroptotic cases are rescued by Nec alone, mixed phenotype cases are rescued only by the combination of both inhibitors, and Nec sensitive cases undergo cell death in response to necrostatin alone. n=1 experiment for 5 samples in triplicate. In all cases the percentage of live cells was determined after 48 h treatment using an established drug-screening platform in co-culture conditions representative of the bone marrow microenvironment, automated microscopy, and machine learning software[20, 37]. For all quantifications, data represent mean±s.e.m. and were derived from one experiment in triplicates for 10 primary samples.

Figure 3 TNFR2 expression sensitizes to TNFα in a TNFR1- and RIPK1-dependent manner. (**a,b**) Overexpression constructs for full length TNFR2 (**a**) and TNFR2-ED (**b**). (**c**,**d**) FACS quantification of TNFR2 (**c**) and TNFR2-ED (**d**) in Jurkat, Nalm6, and 658 ALL cell lines. (**e**,**f**) % viability in response to increasing concentrations of TNFα after overexpression of TNFR2 (+TNFR2) in WT (**e**) and *TNFR1* knockout (LC.TNFR1) cell lines (**f**). n=3 independent experiments. (**g**) Western blot for LC.TNFR1±TNFR2 in Jurkat, Nalm6, and 658 cell lines. LentiCRISPR targeting TNFR1 produced a smaller non-functional protein, indicated with an arrow. Phenotypic testing of LC.TNFR1 cells is shown in Supplementary figure 3d. (**h**) % viability in response to increasing concentrations of TNFα in WT and +TNFR2-ED cell lines. n=3 independent experiments. (**i**) % viability in response to increasing concentrations of TNFα co-treated with zVAD (25 µM), Nec (25 µM), or both. n=3 independent experiments (**j**) Western blot for TNFR2 overexpression in *RIP1* knockout (LC.RIP1) ALL cell lines. (**k**) % viability in response to increasing concentrations of TNFα after expression of +TNFR2 in LC.RIP1 ALL cell lines. n=3 independent experiments. For all viability measurements the cells were treated for 48 h. For all quantifications, data representing mean±s.e.m. were derived from the indicated number of independent experiments.

Figure 4 Effect of TNFR2 in the activation of NF-κB signalling in response to TNF and birinapant. (**a**) Western blot for canonical and non-canonical NF-κB markers after 0, 0.5, 6, 10, and 25 hours of treatment with TNF (10ng/ml) or birinapant (50 nM) in Jurkat WT or +TNFR2 cells. Western blot representative of n=2 independent experiments. (**b**) Western blot for non-canonical NFkB markers after 0, 10 min, 30 min, 1 h, 2h, and 6h, of treatment with birinapant (50 nM) in responsive and non-responsive patient-derived ALL cells. n=1 for 6 patient-derived samples. * indicates non-specific background from stripping the membrane.

Figure 5 Birinapant treatment leads to recruitment of RIPK1 to TNFR1 in SM-responders. (**a**) Flag immunoprecipitation (IP) in RIP1-/- Jurkat cells reconstituted with Flag-RIP1 after different time

points of treatment with birinapant (500 nM) and TNF (10 ng/ml). The left panel shows the lysates and the right panel the IP. (**b**) IP of endogenous TNFR1 in R-03 patient-derived cells (birinapant IC50=0.39 nM) after treatment with birinapant. (**c**,**d**) IP of endogenous TNFR1 in birinapant non-responsive (VHR-01, VHR-06, VHR-15) and responsive (VHR-10, SR-13) patient-derived cells after treatment with birinapant (5 0nM). * indicates signal from IgG bands. (**f**) IP of endogenous TNFR1 in R-03 WT and QUADko (quadruple knockout for FADD, caspase-8, RIP3, and MLKL)[11]. For **b**-**f**, cells were treated with 50 nM birinapant for 0, 2, and 6 h. All data shown are from one experiment that is representative of two (**c**-**e**) or three (**a**,**b**) independent experiments.

Figure 6 CRISPR *in vivo* selection reveals that TNFR1 and 2 are necessary for the response to birinapant. (**a**,**b**) % of human engraftment (hCD45/hCD19 positive, in black), and % of LC.TNFR1 mCherry positive cells (red) (**a**,**e**,**i**) or LC.TNFR2 BFP positive cells (blue) (**b**,**f**,**j**) over the total engraftment of R-03, SR-13, and VHR-01 patient-derived cells as quantified by FACS from peripheral blood. Birinapant treatment 30 mg/kg was given intraperitoneally daily. Arrow indicates the start of treatment. n=1. (**c**,**g**,**k**) Drug response curves for LC.TNFR1 (red) and LC.TNFR2 (blue) cells after treatment with increasing concentrations of birinapant for 48 h. n=3 independent experiments. (**d**,**h**) Western blot performed with the ALL cells extracted from the spleen and re-engrafted without treatment to confirm the loss of TNFR1 and TNFR2 respectively. For all drug response curves (**c**,**g**,**k**) the percentage of live cells was determined using an established drug-screening platform in co-culture conditions representative of the bone marrow microenvironment, automated microscopy, and machine learning software[20,37]. For all quantifications, data representing mean±s.e.m. were derived from the indicated number of independent experiments.

Figure 7 TNFR2 facilitates the recruitment of RIP1 to TNFR1. (**a**) IP of endogenous TNFR1 in WT and +TNFR2 Jurkat cells after treatment with TNF (10 ng/ml) for different time points. Left panel shows the lysates and right panel the IP. Data from one experiment representative of n=3 independent experiments. (**b**) IP of endogenous TNFR1 in WT and LC.TNFR2 R-03 patient-derived cells after treatment with birinapant (50 nM) for increasing time points. Data from one experiment representative of n=3 independent experiments. (**c**) Proposed model for the role of TNFR2 in birinapant-induced TNFR1- and RIP1-dependent cell death.

Figures

Figure 1

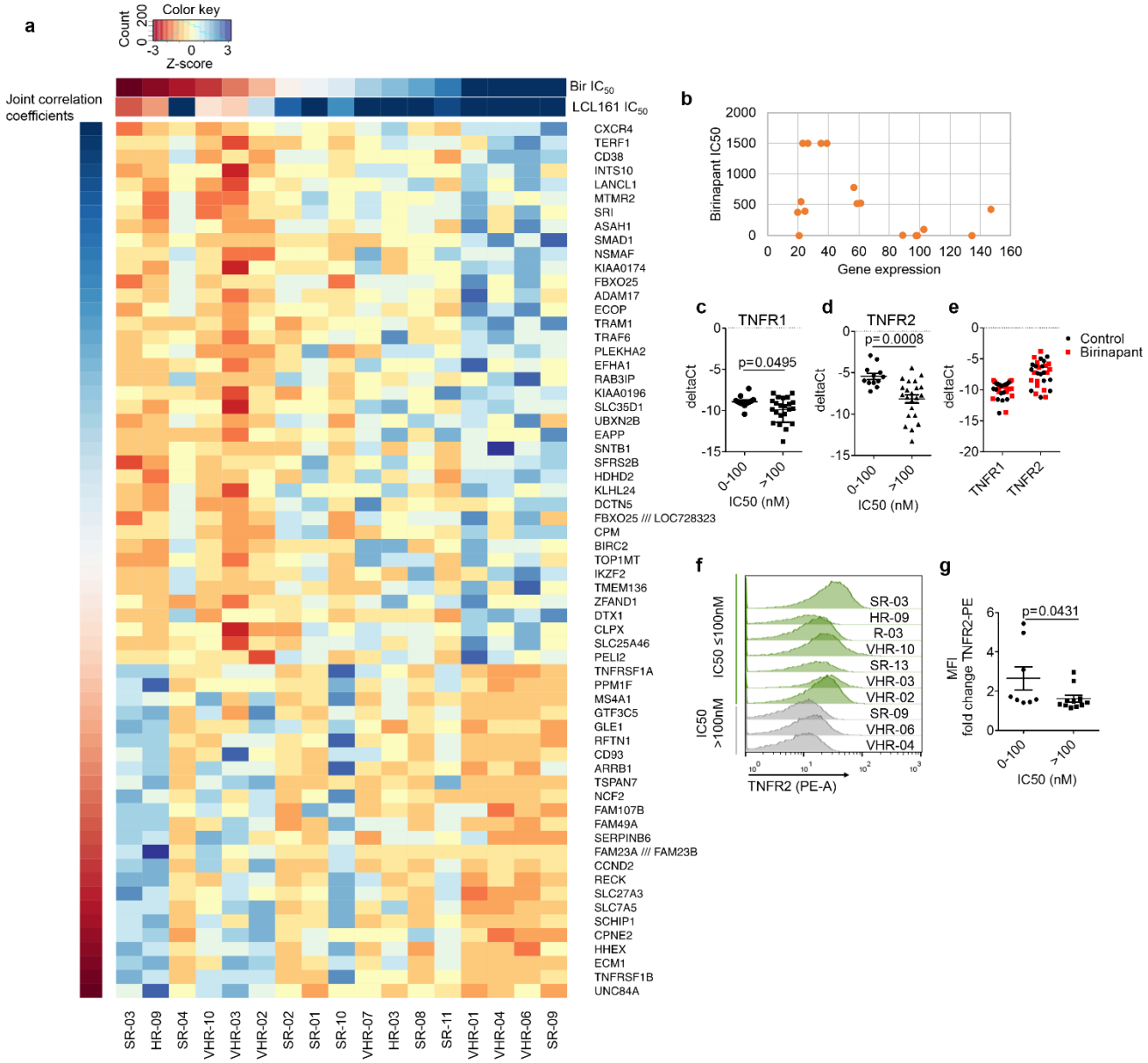

Figure 2

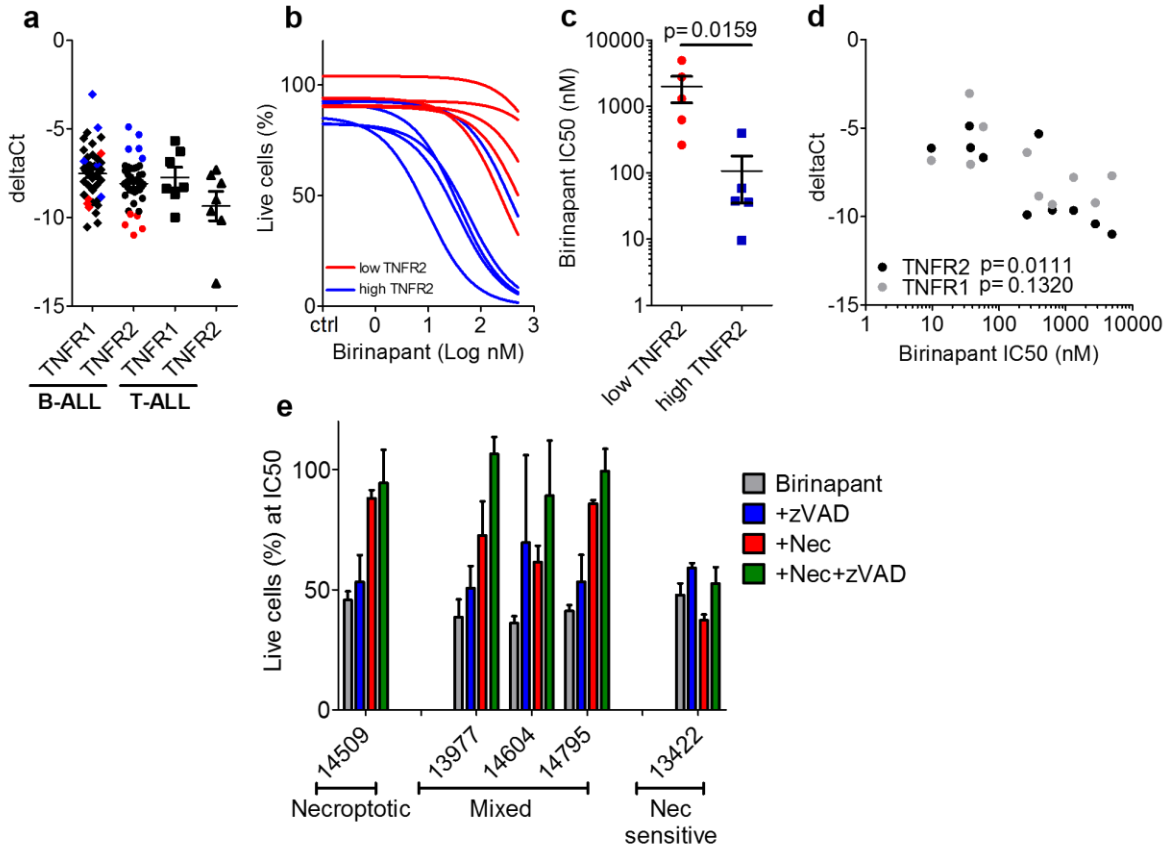
a
deltaCt
0
-5
-10
-15
TNFR1
TNFR2
TNFR1
TNFR2
B-ALL
T-ALL
b
Live cells (%)
100
50
0
low TNFR2
high TNFR2
ctrl
0
1
2
3
Birinapant (Log nM)
c
p=0.0159
Birinapant IC50 (nM)
10000
1000
100
10
1
low TNFR2
high TNFR2
d
deltaCt
0
-5
-10
-15
TNFR2 p=0.0111
TNFR1 p=0.1320
1
10
100
1000
10000
Birinapant IC50 (nM)
e
Live cells (%) at IC50
100
50
0
Birinapant
+zVAD
+Nec
+Nec+zVAD
14509
13977
14604
14795
13422
Necroptotic
Mixed
Nec sensitive

Figure 3

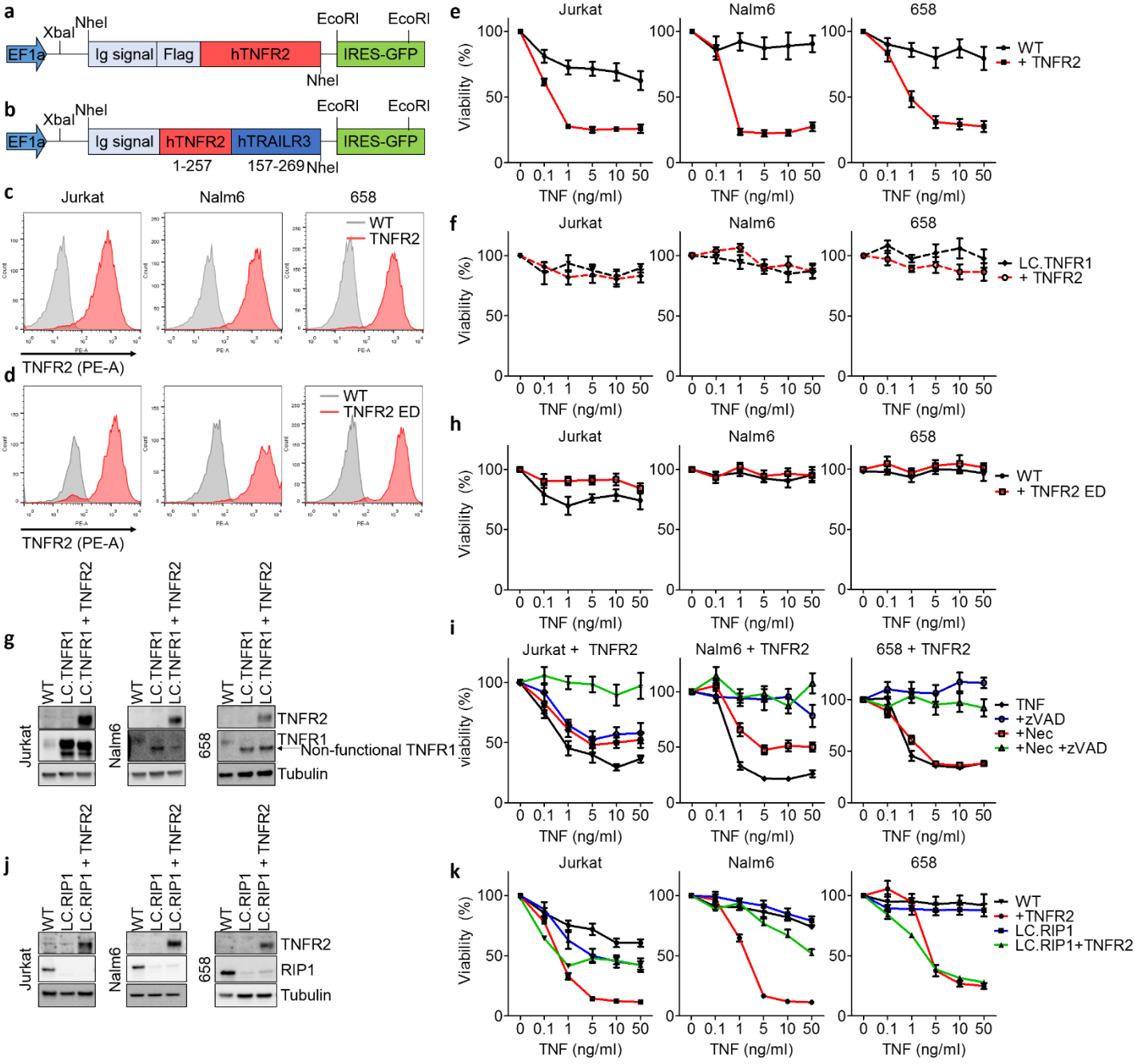
a
XbaI
NheI
EcoRI
EcoRI
EF1a
Ig signal
Flag
hTNFR2
IRES-GFP
NheI
b
XbaI
NheI
EcoRI
EcoRI
EF1a
Ig signal
hTNFR2
hTRAILR3
IRES-GFP
1-257
157-269
NheI
c
Jurkat
Nalm6
658
WT
TNFR2
TNFR2 (PE-A)
d
WT
TNFR2 ED
TNFR2 (PE-A)
e
Jurkat
Nalm6
658
Viability (%)
TNF (ng/ml)
WT
+ TNFR2
f
LC.TNFR1
+ TNFR2
h
WT
+ TNFR2 ED
i
Jurkat + TNFR2
Nalm6 + TNFR2
658 + TNFR2
viability (%)
TNF
+zVAD
+Nec
+Nec +zVAD
g
WT
LC.TNFR1
LC.TNFR1 + TNFR2
Jurkat
Nalm6
658
TNFR2
TNFR1
Non-functional TNFR1
Tubulin
j
WT
LC.RIP1
LC.RIP1 + TNFR2
Jurkat
Nalm6
658
TNFR2
RIP1
Tubulin
k
WT
+TNFR2
LC.RIP1
LC.RIP1+TNFR2

Figure 4

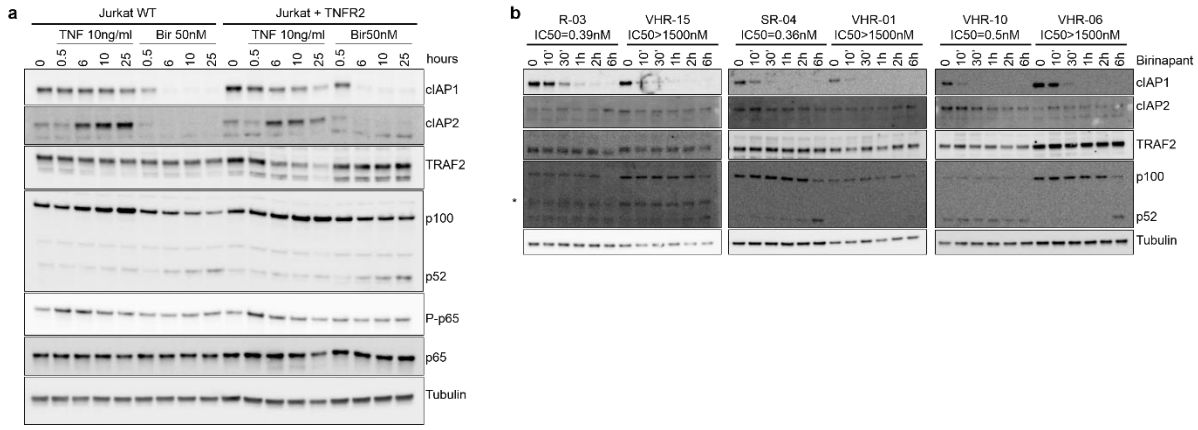

Figure 5

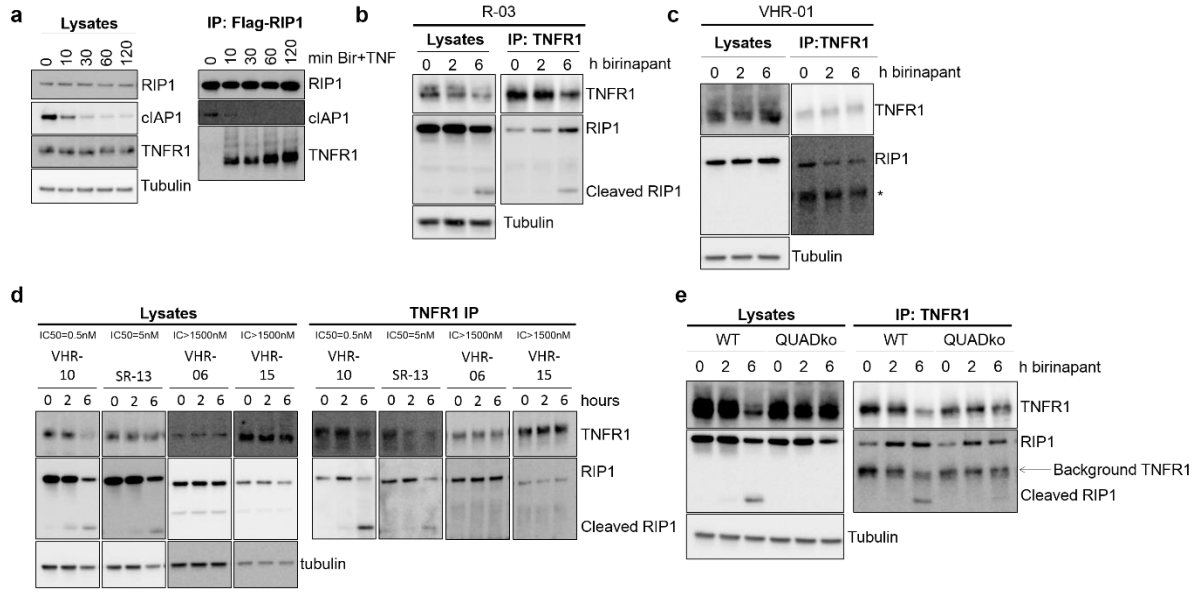

Figure 6

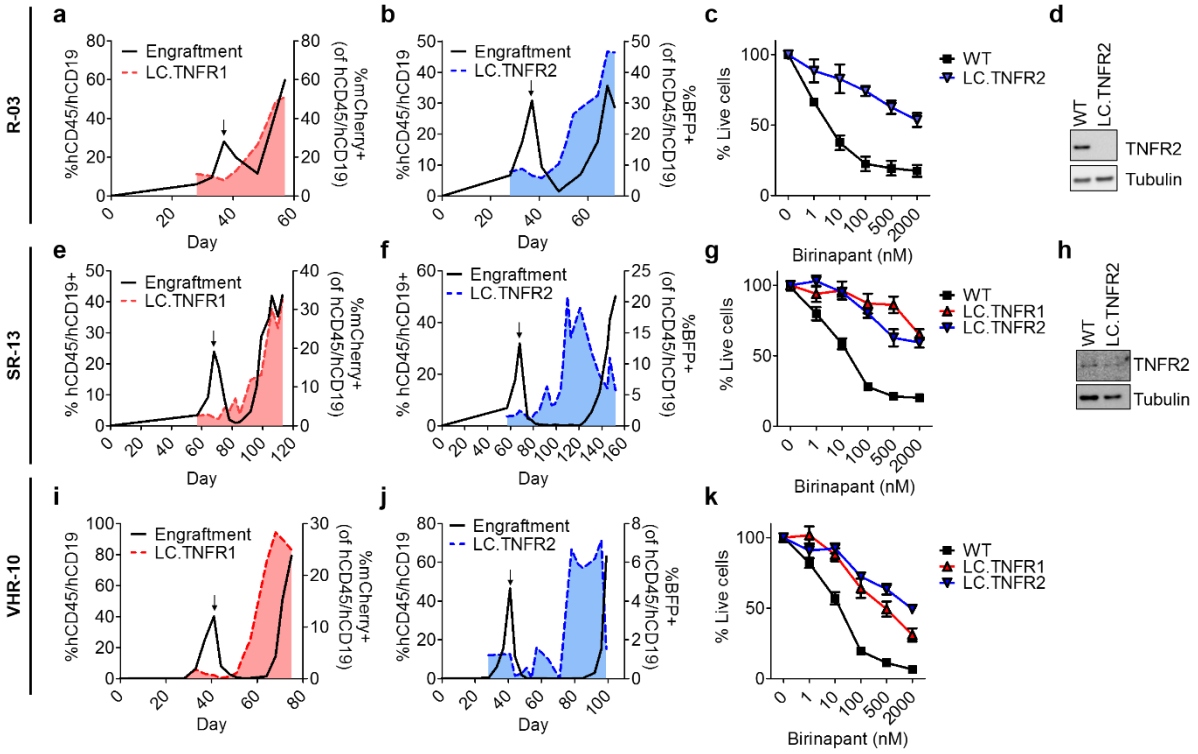
R-03
SR-13
VHR-10
a
b
c
d
e
f
g
h
i
j
k
Engraftment
LC.TNFR1
LC.TNFR2
%hCD45/hCD19
%hCD45/hCD19+
%mCherry+ (of hCD45/hCD19)
%BFP+ (of hCD45/hCD19)
Day
% Live cells
Birinapant (nM)
WT
LC.TNFR1
LC.TNFR2
TNFR2
Tubulin

Figure 7

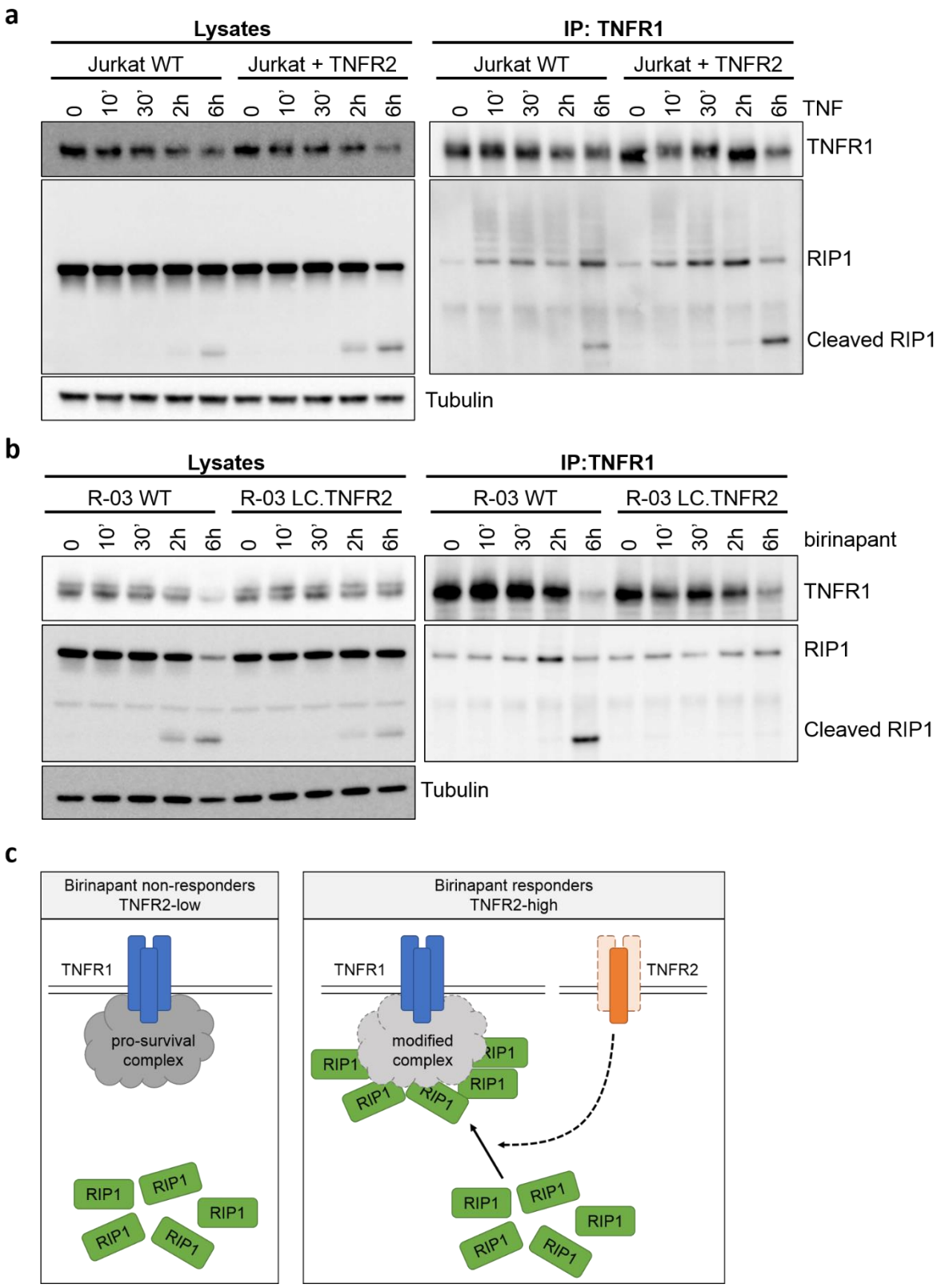
a
Lysates
IP: TNFR1
Jurkat WT
Jurkat + TNFR2
0
10'
30'
2h
6h
TNF
TNFR1
RIP1
Cleaved RIP1
Tubulin
b
Lysates
IP:TNFR1
R-03 WT
R-03 LC.TNFR2
birinapant
TNFR1
RIP1
Cleaved RIP1
Tubulin
c
Birinapant non-responders
TNFR2-low
TNFR1
pro-survival
complex
RIP1
Birinapant responders
TNFR2-high
TNFR2
modified
complex

Supplementary Figures

Supplementary Figure 1

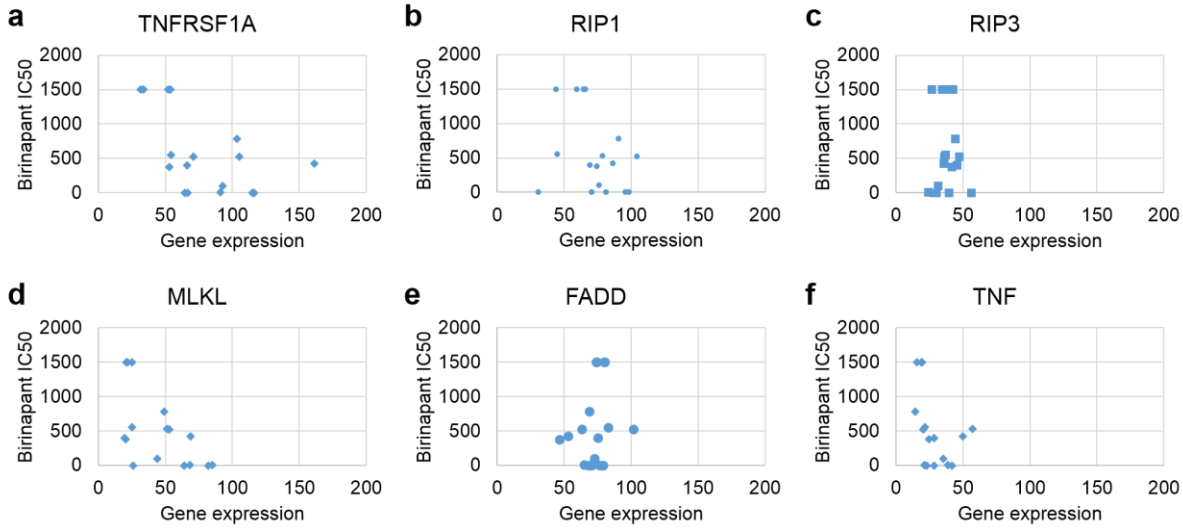

g

Gene	Pearson r with Bir IC50	Pearson r with LCL161 IC50	Variance	Total Pearson r
TNFRSF1B	-0.5299	-0.8526	2.0479	-1.3825
TNFRSF1A	-0.5486	-0.6027	1.6565	-1.1514
MLKL	-0.6229	-0.6229	1.4944	-1.2458
RIPK1	-0.3307	-0.0519	1.0101	-0.3826
RIPK3	0.0299	0.2857	0.8541	0.3155
FADD	0.2111	0.2223	0.7666	0.4334
TNF	-0.4562	-0.1729	1.5338	-0.6291

Supplementary figure 1 Genes involved in the TNFR1-RIP1 death axis don't correlate with the response to birinapant. (**a-f**) Gene expression and IC50 in response to birinapant for 17 patient-derived B-ALL. (**g**) Pearson correlation, variance, and total correlation of gene expression with IC50 in response to birinapant and/or LCL161 for 17 patient-derived B-ALL cases.

Supplementary Figure 2

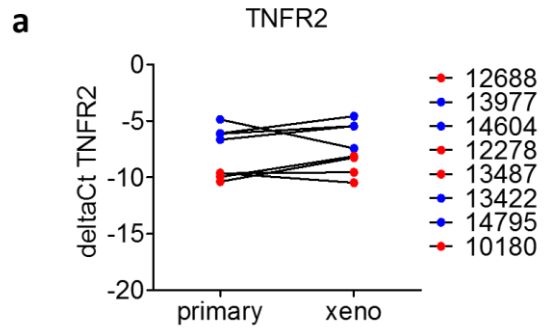

Supplementary Figure 2 *TNFR2* expression in primary B-ALL is maintained in xenografts. (**a**) 8 peripheral blood samples from B-ALL patients from the BFM ALL-REZ trial were xenografted in immunodeficient NSG mice. *TNFR2* expression was quantified by qPCR in the original primary sample and in the leukemic cells obtained after Xenografting. n=1 experiment in triplicates for 8 samples.

Supplementary figure 3

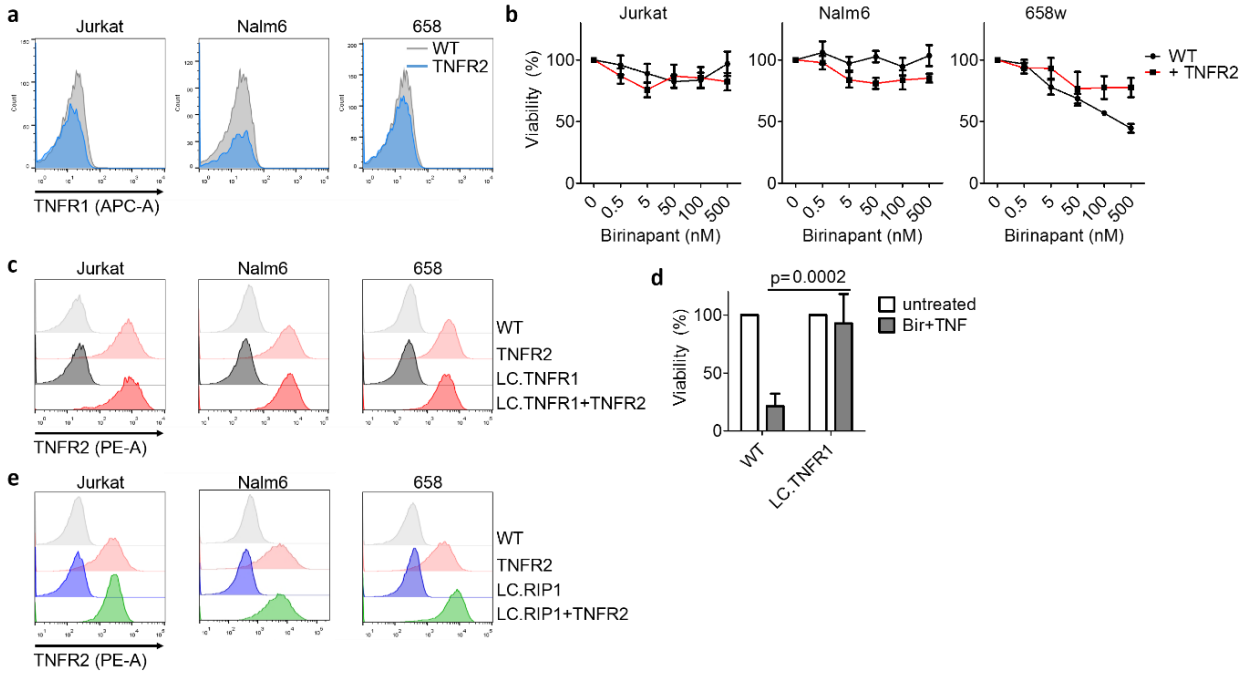

Supplementary figure 3 Expression of TNFR2 in ALL cell lines. (**a**) TNFR1levels by flow cytometry in WT and +TNFR2 cell lines. (**b**) Viability of WT and +TNFR2 cell lines in response to increasing concentrations of birinapant. n=3 independent experiments. (**c**) TNFR2 levels by flow cytometry in LC.TNFR1 ± TNFR2 cell lines compared to WT and +TNFR2. (**d**) Viability of WT and LC.TNFR1 Jurkat cells in response to birinapant (50 nM) and TNF (10 ng/ml) (Bir+TNF). n=3 independent experiments. (**e**) TNFR2 levels by flow cytometry in LC.RIP1± TNFR2 cell lines compared to WT and +TNFR2. For all quantifications, data representing mean±s.e.m. (standard error of the mean) were derived from the indicated number of measurements.

Supplementary Figure 4

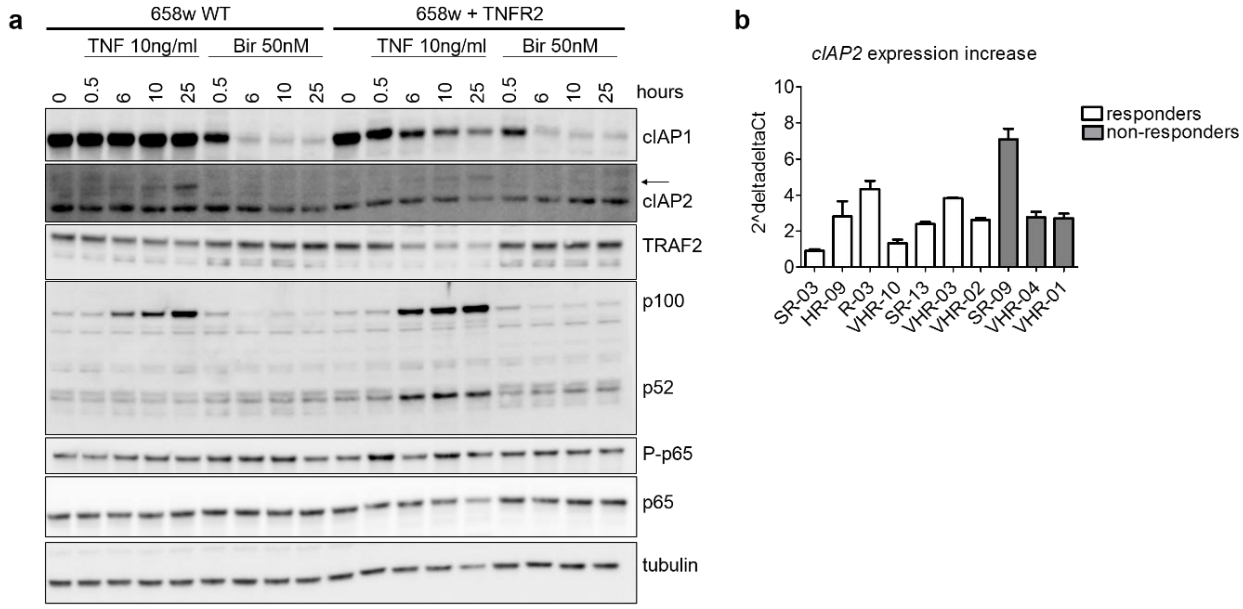

Supplementary figure 4 Effect of TNFR2 in NFkB activation. (**a**) Western blot for canonical and non-canonical NF-κB markers after 0, 0.5, 6, 10, and 25 hours of treatment with TNF (10ng/ml) or birinapant (50 nM) in 658 WT or +TNFR2 cells. n=1 Arrow indicates the specific cIAP2 band. (**b**) Increase in *cIAP2* expression in birinapant responders and non-responders after treatment with birinapant (50 nM) for 6 h. n=1 experiment in triplicates for 10 patient-derived samples. Data represent mean±s.e.m for the indicated number of measurements.

Supplementary Figure 5

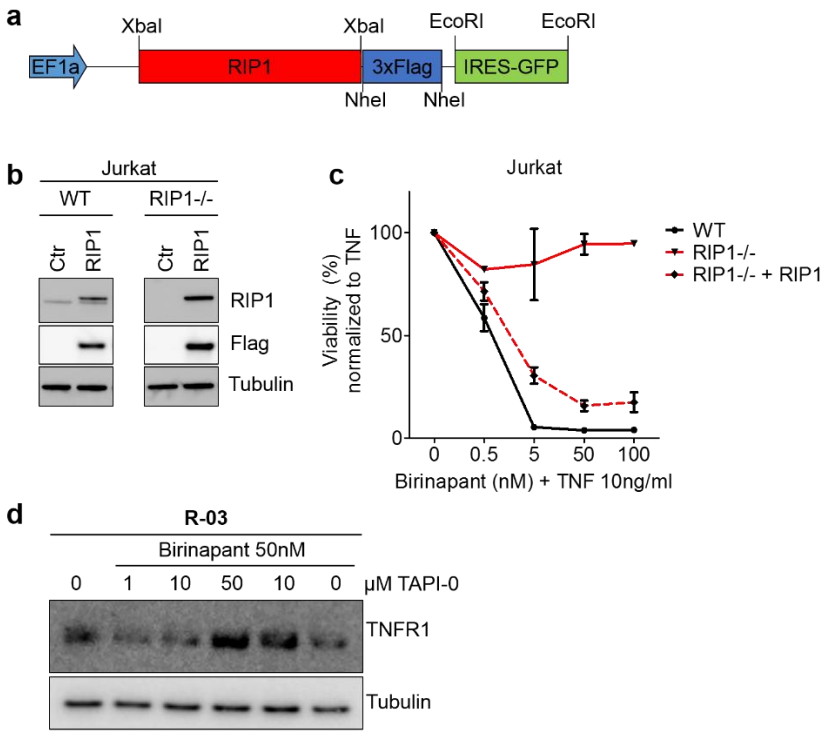

Supplementary figure 5 RIP1 reconstitution and TNFR1 shedding. (**a**) Representation of the construct to reconstitute 3x Flag-tagged RIP1 (RIP1-Flag). (**b**) Western blot of RIP1-Flag overexpression in WT and reconstitution in RIP1-/- Jurkat cells. (**c**) Viability for WT, RIP1-/-, and RIP1-/- + RIP1 (reconstituted) Jurkat cells in response to treatment with TNF (10 ng/ml) and increasing concentration of birinapant. Viability was measured after 48h treatment. n=3 independent experiments. Data indicate mean±s.e.m. (**d**) Western blot in birinapant responder R-03 patient-derived sample pre-treated for 2 h with increasing concentrations of the TACE inhibitor TAPI-0 and treated with birinapant (50 nM) for 6 h. Data shown is representative from n=3 independent experiments.

Supplementary Figure 6

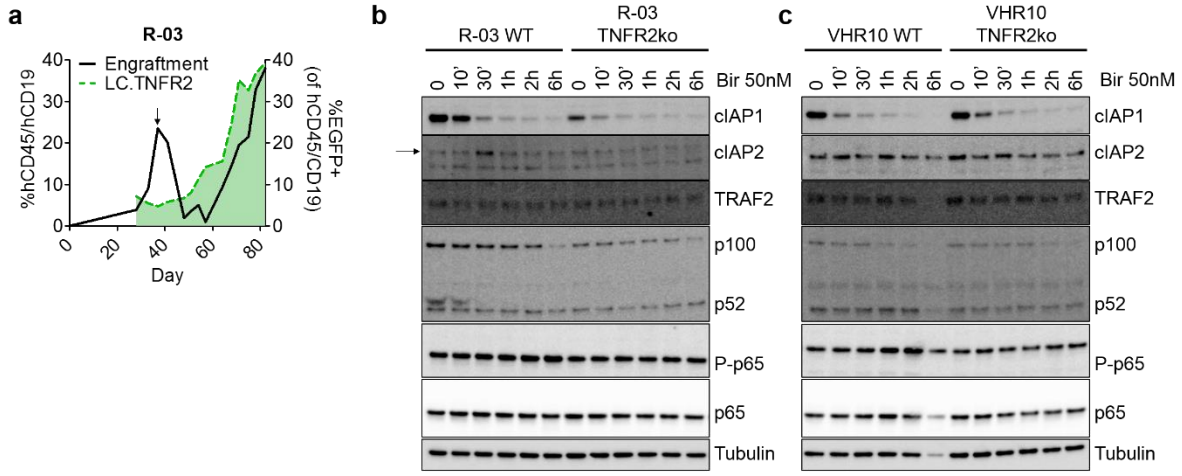

Supplementary figure 6 TNFR2 is necessary for the response to birinapant independently of NF-κB signalling. (**a**) % of human engraftment (hCD45/hCD19 positive, in black), and % of LC.TNFR2 (with an alternative sgRNA) EGFP positive cells (green) over the total engraftment of R-03 patient-derived cells as quantified by FACS from peripheral blood. Birinapant treatment 30 mg/kg was given intraperitoneally daily. Arrow indicates the start of treatment. n=1. (**b**,**c**,) Western blot for canonical and non-canonical NF-κB markers in WT and *TNFR2* knockout patient-derived cells after treatment with birinapant (50 nM) for the indicated time points. n=1 experiment for each patient-derived sample. Arrow indicates the specific cIAP2 band.

Supplementary Table 1. Primary cohort patient characteristics

	number of cases	clinical stage	TNFR1 mean (min,max)	TNFR2 mean (min,max)
BCP-ALL	36	diagnosis (28), relpase (8)	-9.54 (-13.76,-7.33)	-7.20 (-13.28,-2.91)

Supplementary Table 2. Secondary cohort patient characteristics

	Patient -ID	TNFR1	TNFR2	% BLASTS	TNFR2 xenograft	Birinapant IC50 (nM)
Selected BCP-ALL cases	12278	-6.38	-9.9	93	-8.12	262
	12286	-7.69	-10.99	93	ND	4944
	12688	-9.22	-10.41	99	-8.26	2781
	13422	-6.83	-6.13	98	-5.23	9.595
	13977	-7.05	-6.11	95	-4.58	37.4
	14509	-8.84	-5.32	96	ND	393.2
	14604	-3.04	-4.88	90	-7.42	35.95
	14795	-4.92	-6.66	93	-5.23	57.9
	10180	-9.32	-9.64	99	-9.34	628.8
	13487	-7.78	-9.65	96	-9.94	1310

		number of cases	clinical stage	TNFR1 mean (min,max)	TNFR2 mean (min, max)	%blasts mean±STD
Screened cases	T-ALL	7	relapse	-7.74 (-10.0, -5.67)	-9.35 (-13.71, -7.31)	94.00±3.21
	BCP-ALL	34	relapse	-7.64 (-10.54, -5.21)	-8.12 (-10.63, -8.08)	93.79±4.29